INTRODUÇÃO À FISICA NUCLEAR FNC404

1º semestre de 2011

ALEJANDRO SZANTO DE TOLEDO
szanto@dfn.if.usp.br
tel: 3091 6955

endereço eletrônico do curso:

PROGRAMA

1) INTRODUÇÃO: O QUE É A FÍSICA NUCLEAR- SUAS QUESTÕES - SUA FRONTEIRA – SUAS APLICAÇÕES

2) O PROGRAMA:

- BLOCO 1: INTRODUÇÃO
- BLOCO 2: GRANDEZAS MACROSCÓPICAS DO NÚCLEO
- BLOCO 3: FÍSICA NUCLEAR DE ALTAS ENERGIAS : FÍSICA HADRÔNICA
- BLOCO 4: MODELOS NUCLEARES
- BLOCO 5: REAÇÕES NUCLEARES
- BLOCO 6: ACELERADORES E INSTRUMENTAÇÃO NUCLEAR

3) PROJETO E/OU TRABALHO DE FIM DE CURSO

PROVAS

PRIMEIRA PROVA (P1): 29 MARÇO

SEGUNDA PROVA (P2): 6 MAIO

TERCEIRA PROVA (P3): 17 JUNHO

PROJETO E/OU TRABALHO DE FIM DE CURSO:
NOTA TT

MEDIA: $M = 1/3\left(P_1 + P_2 + P_3\right) + \alpha . TT$

M > 5 ➔ APROVADO
M < 3 ➔ REPROVADO
3 < M < 5 ➔ REC se $1/3\left(M + 2REC\right) > 5$ **➔ APROVADO**

Referências

Nuclear and Particle Physics
(W.S.C. Williams) - Claredon Press-Oxford

Física Nuclear
(Theo Mayer-Kuckuk) - Fundação Calouste Gulbenkian

Introductory Nuclear Physics
Kenneth S. Krane – John Wiley & Sons

Introduction to Nuclear Reactions
(G.R. Satchler) – MacMillan Education Ltd

Introdução à Física Nuclear
(K.C. Chung) – editora UERJ

BLOCO 1
INTRODUÇÃO

EVOLUÇÃO DO UNIVERSO:
BIG BANG - HADRONIZAÇÃO - FORMAÇÃO DAS ESTRELAS

A MATÉRIA NUCLEAR

A NUCLEO-SÍNTESE DOS ELEMENTOS NAS ESTRELAS:
OS CICLOS p-p , CNO, O SOL, PROCESSOS r, rp ...

O NÚCLEO E SUA ESTRUTURA : TABELA PERIÔDICA

O CAMINHO INVERSO: COLISÕES DE ÍONS PESADOS RELATIVÍSTICOS

APLICAÇÕES DA FÍSICA NUCLEAR

TECNOLOGIA NUCLEAR

Referências para o bloco 1

http://particleadventure.org/particleadventure/

http://ie.lbl.gov/education/glossary/glossaryf.htm

http://www.cpepweb.org/

http://books.nap.edu/books/0309062764/html/index.html

http://webphysics.ph.msstate.edu/jc/library/

http://WWW.PHYS.VIRGINIA.EDU/CLASSES/252/home.html
http://WWW.PHYS.VIRGINIA.EDU/CLASSES/252/Nuclear_Notes/nuclear_notes.html

http://www.overture.com/d/search/p/netscape/?Keywords=rutherford+scattering+applets

http://www2.slac.stanford.edu/vvc/Default.htm

http://www2.slac.stanford.edu/vvc/Default.htm
http://home.a-city.de/walter.fendt/phe/decayseries.htm
http://www.phys.virginia.edu/classes/109N/more_stuff/Applets/rutherford/rutherford2.html
http://www.phys.virginia.edu/classes/109N/more_stuff/Applets/rutherford/rutherford.html

Expansion of the Universe

After the Big Bang, the universe expanded and cooled. At about 10^{-6} second, the universe consisted of a soup of quarks, gluons, electrons, and neutrinos. When the temperature of the Universe, $T_{universe}$, cooled to about 10^{12} K, this soup coalesced into protons, neutrons, and electrons. As time progressed, some of the protons and neutrons formed deuterium, helium, and lithium nuclei. Still later, electrons combined with protons and these low-mass nuclei to form neutral atoms. Due to gravity, clouds of atoms contracted into stars, where hydrogen and helium fused into more massive chemical elements. Exploding stars (supernovae) form the most massive elements and disperse them into space. Our earth was formed from supernova debris.

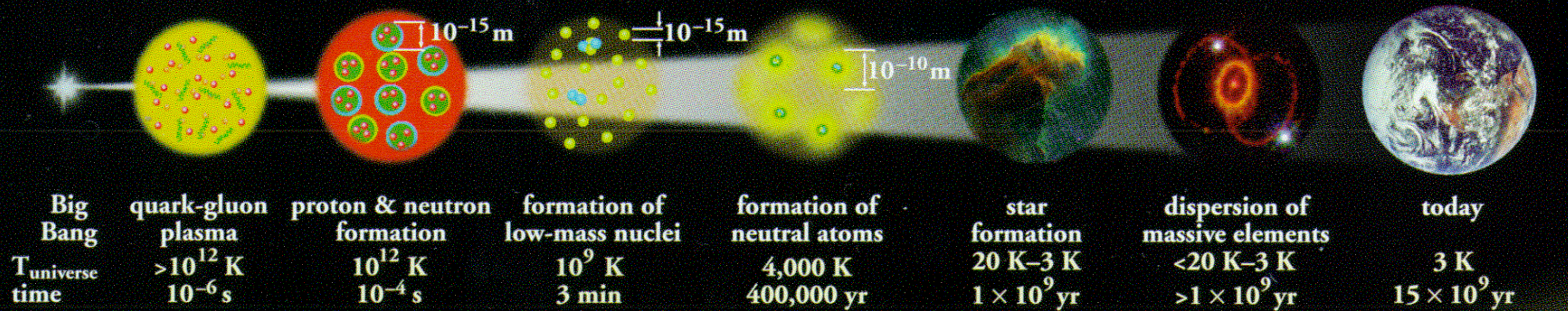

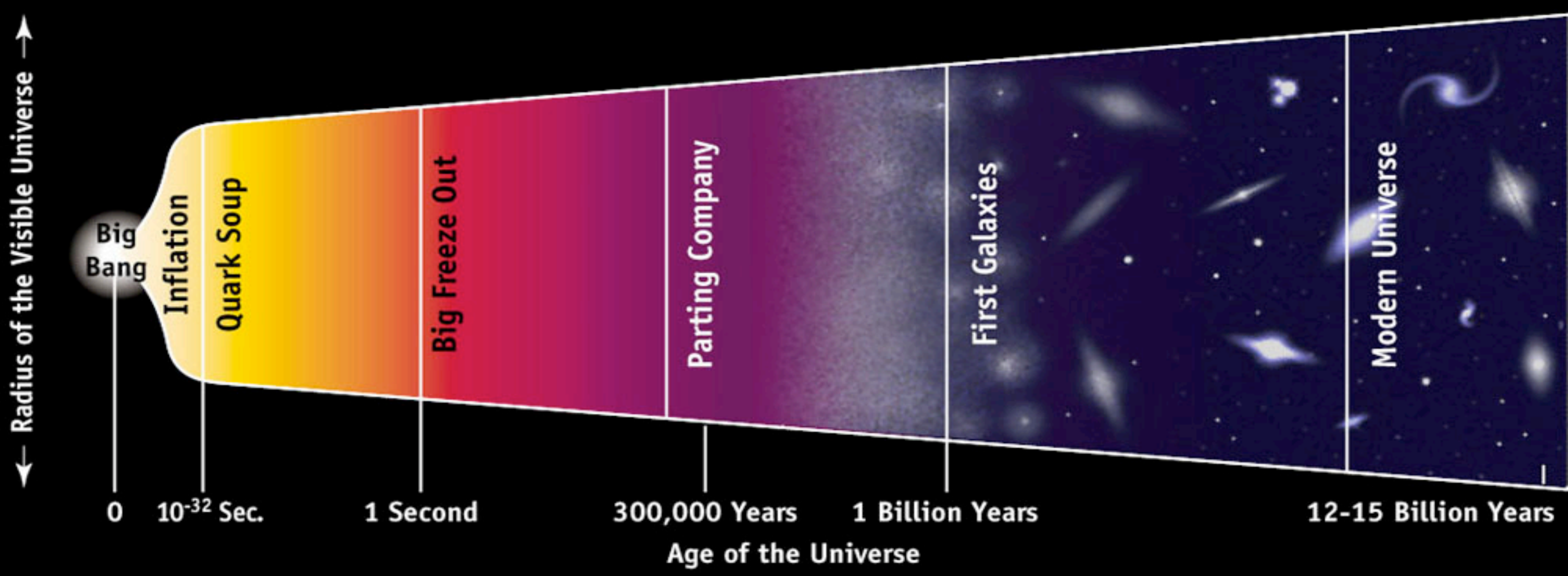

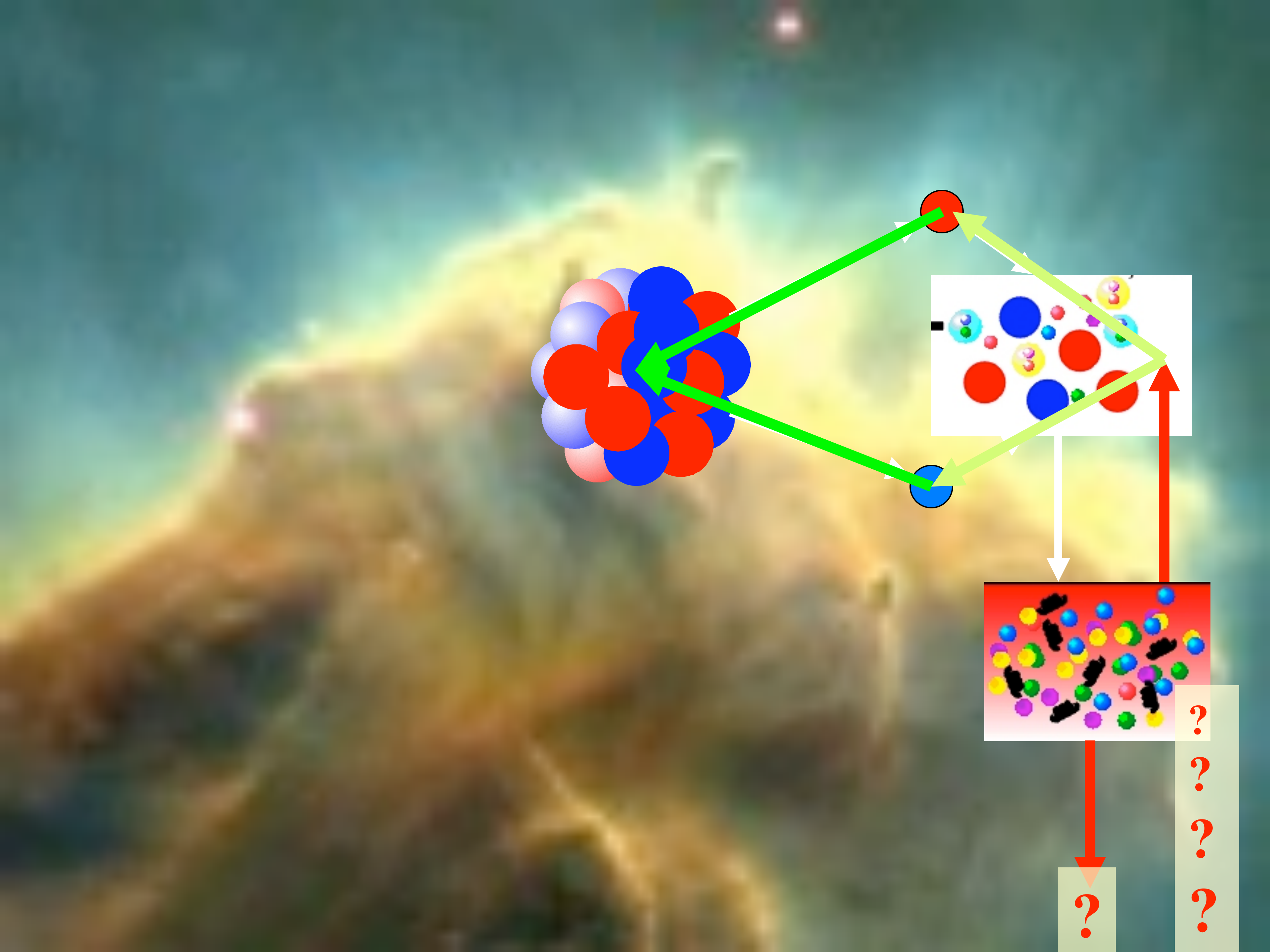

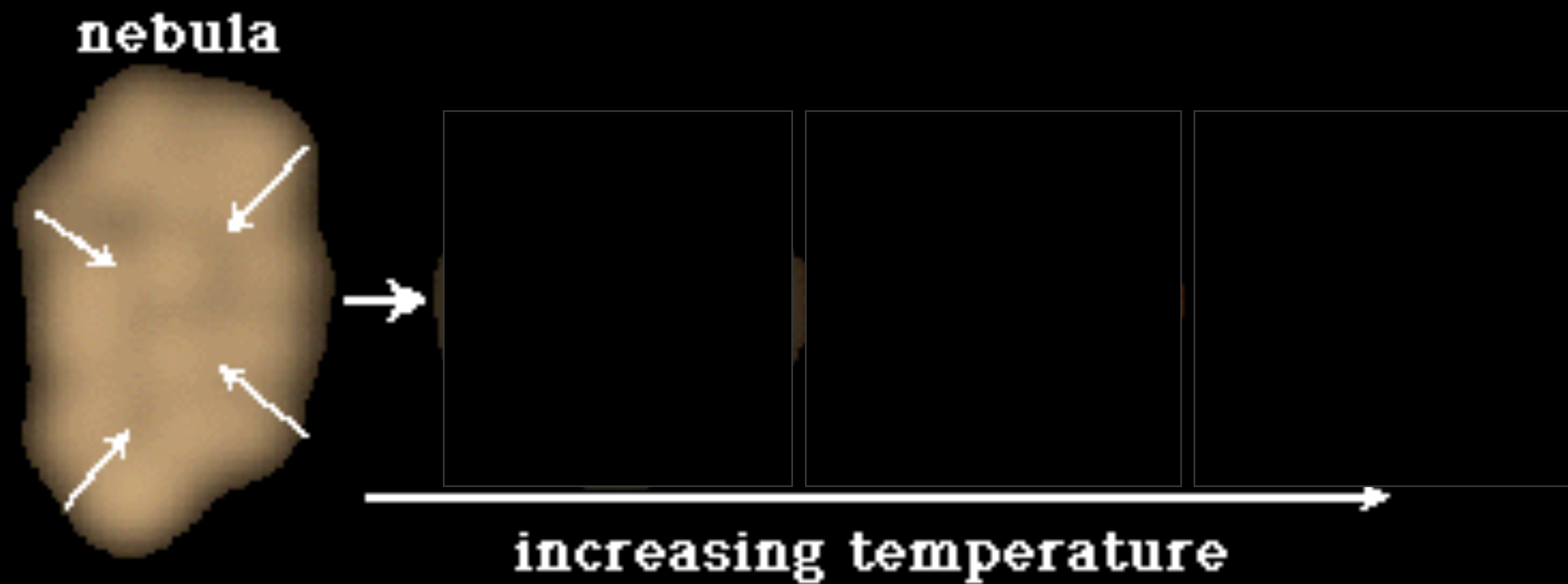
nebula
increasing temperature

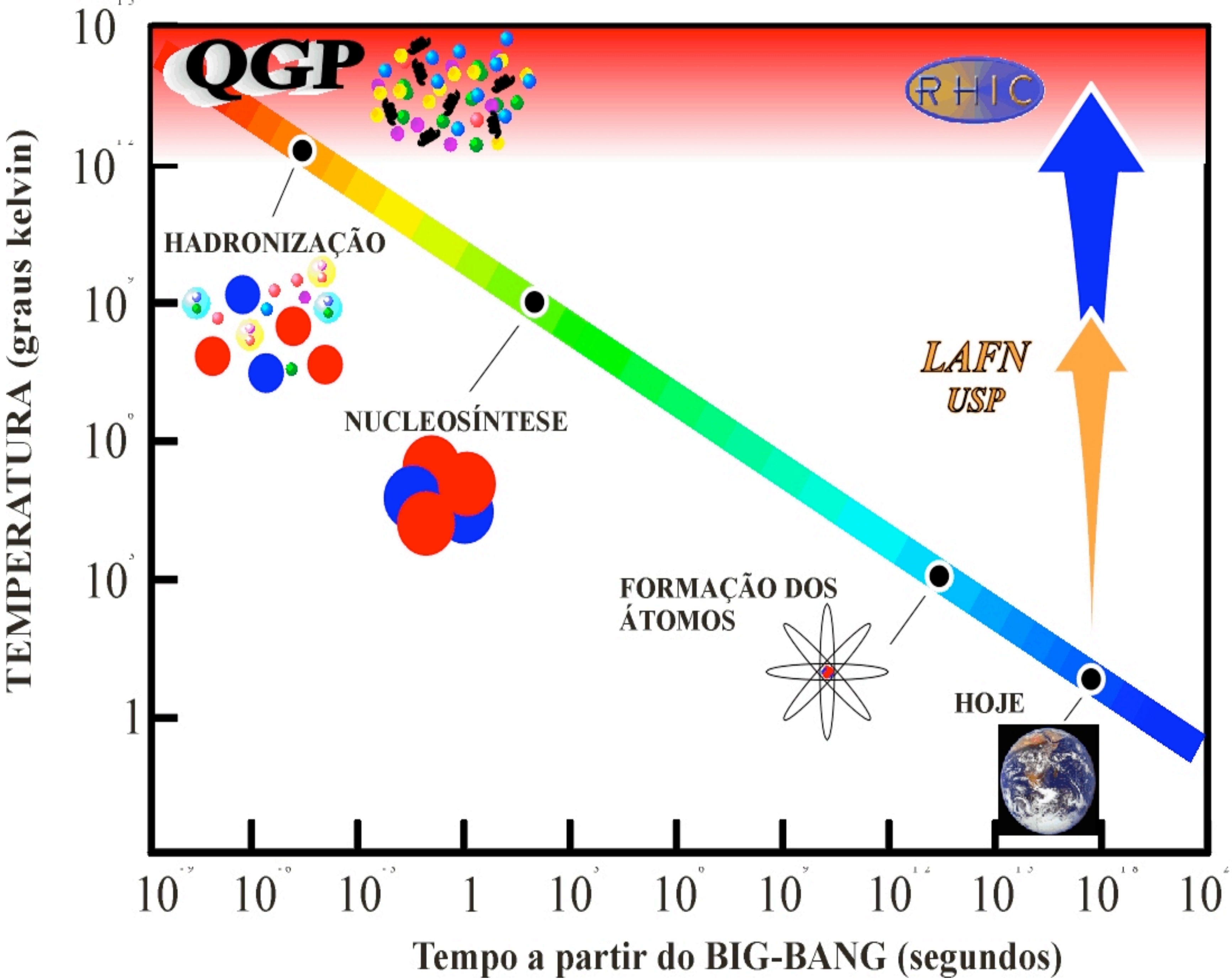

QGP
RHIC
HADRONIZAÇÃO
NUCLEOSÍNTESE
LAFN
USP
FORMAÇÃO DOS
ÁTOMOS
HOJE
TEMPERATURA (graus kelvin)
10^{15}
10^{12}
10^{9}
10^{6}
10^{3}
1
10^{-9} 10^{-6} 10^{-3} 1 10^{3} 10^{6} 10^{9} 10^{12} 10^{15} 10^{18} 10^{21}
Tempo a partir do BIG-BANG (segundos)

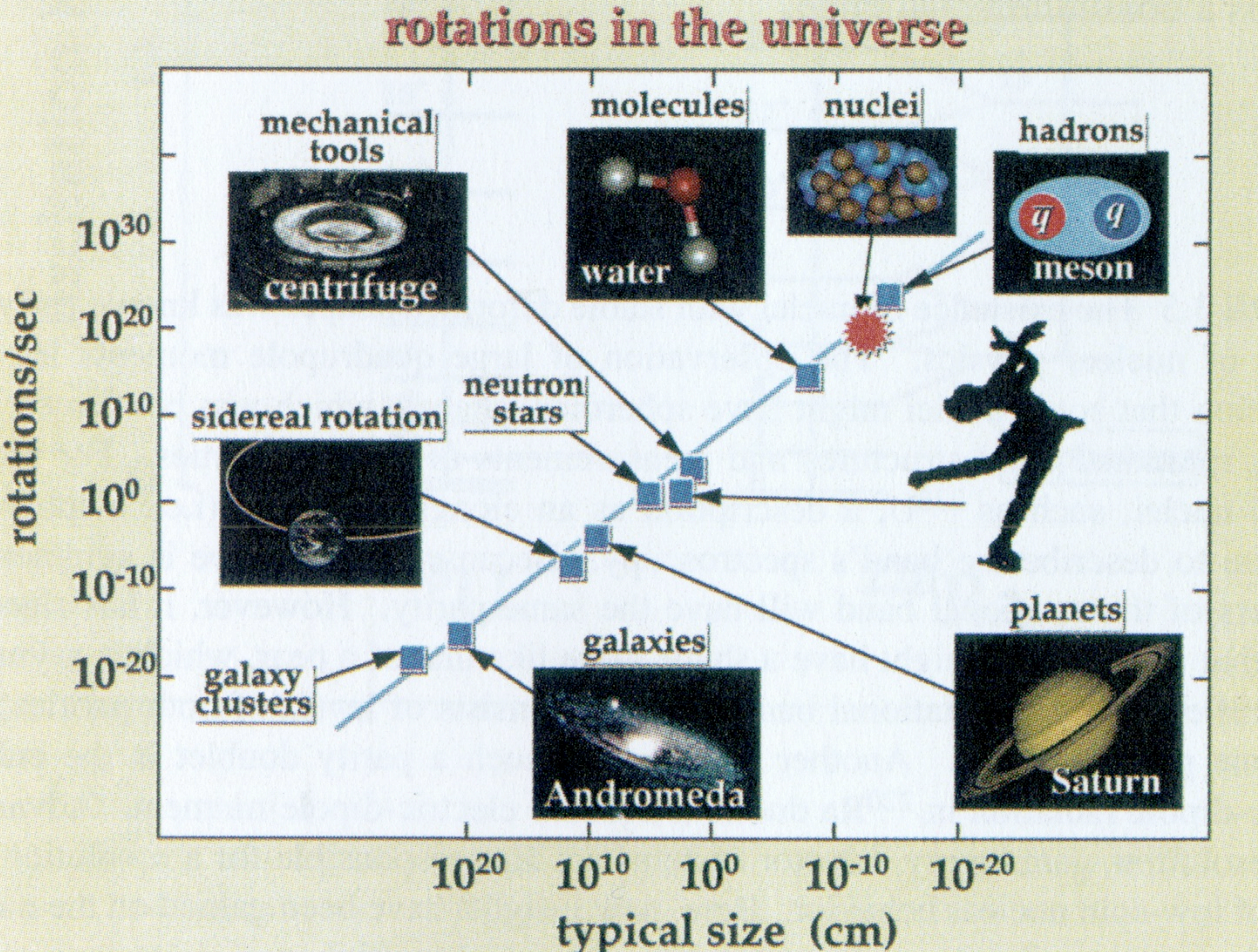
rotations in the universe
rotations/sec
10^{30}
10^{20}
10^{10}
10^{0}
10^{-10}
10^{-20}
mechanical tools
centrifuge
molecules
water
nuclei
hadrons
q̄
q
meson
neutron stars
sidereal rotation
planets
Saturn
galaxies
Andromeda
galaxy clusters
10^{20}
10^{10}
10^{0}
10^{-10}
10^{-20}
typical size (cm)

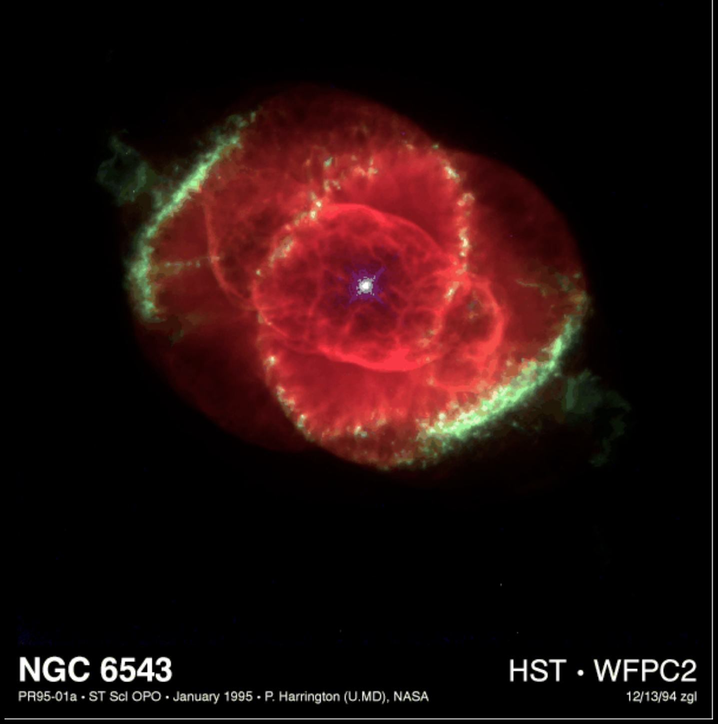

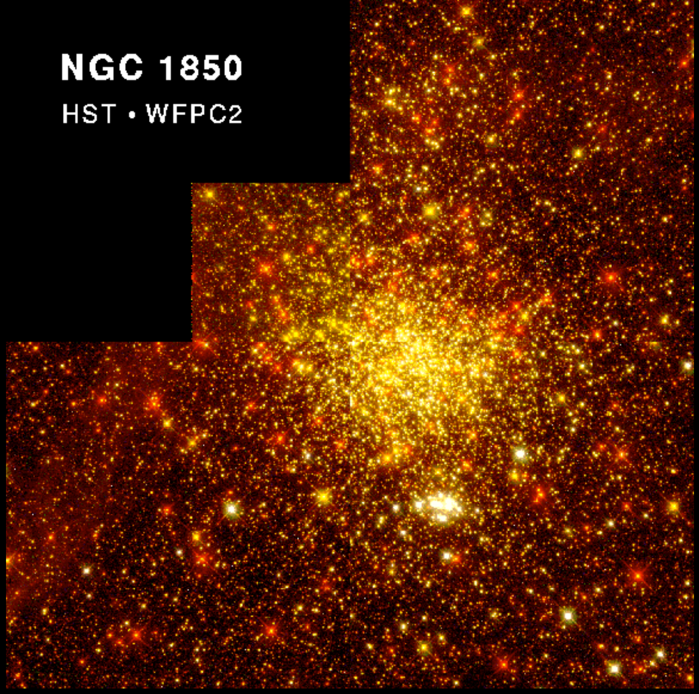

Supernova 1987A Rings

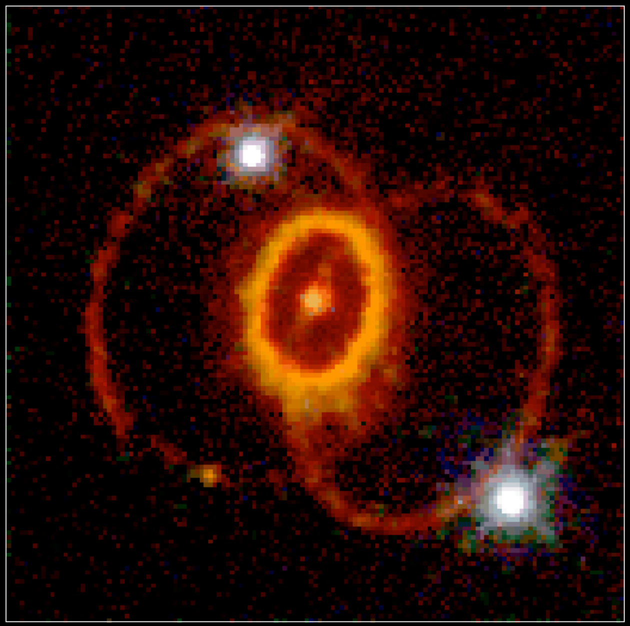

Hubble Space Telescope

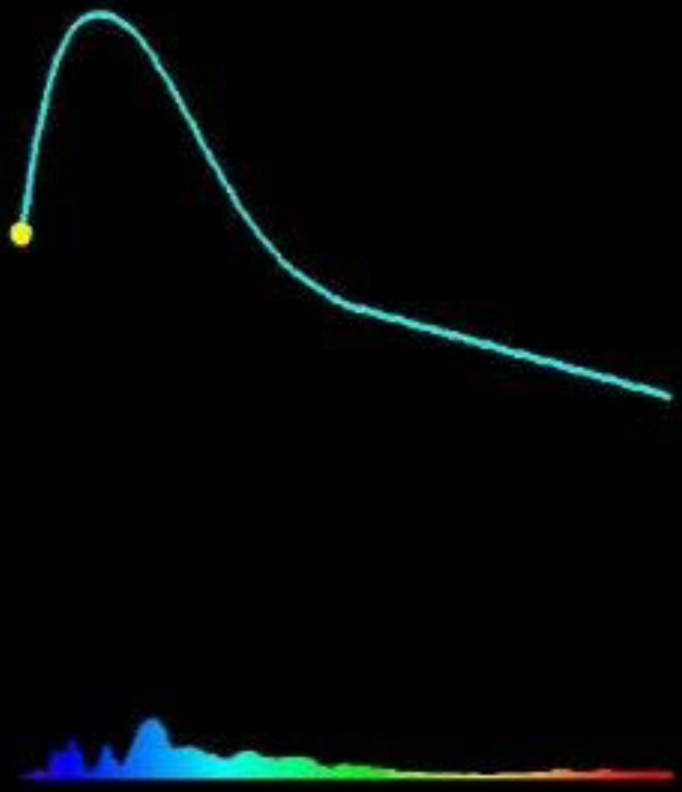

COMO SE FAZ FÍSICA NUCLEAR

DO PONTO DE VISTA EXPERIMENTAL

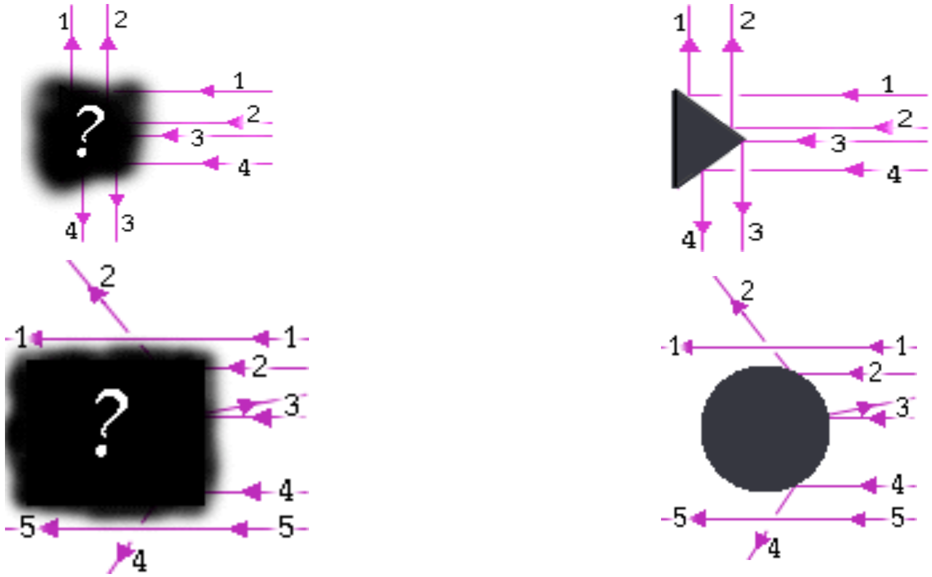

COMO SE FAZ FÍSICA NUCLEAR
DO PONTO DE VISTA EXPERIMENTAL

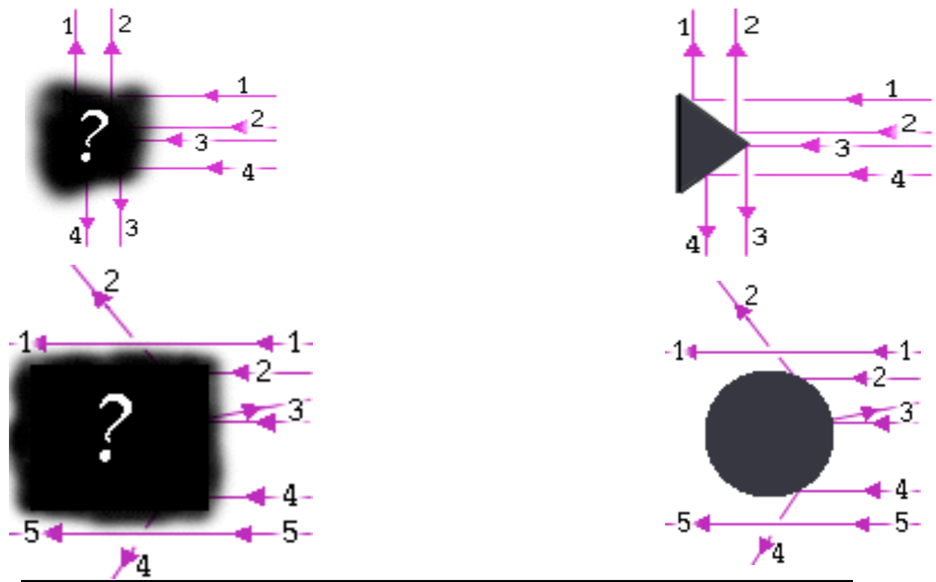

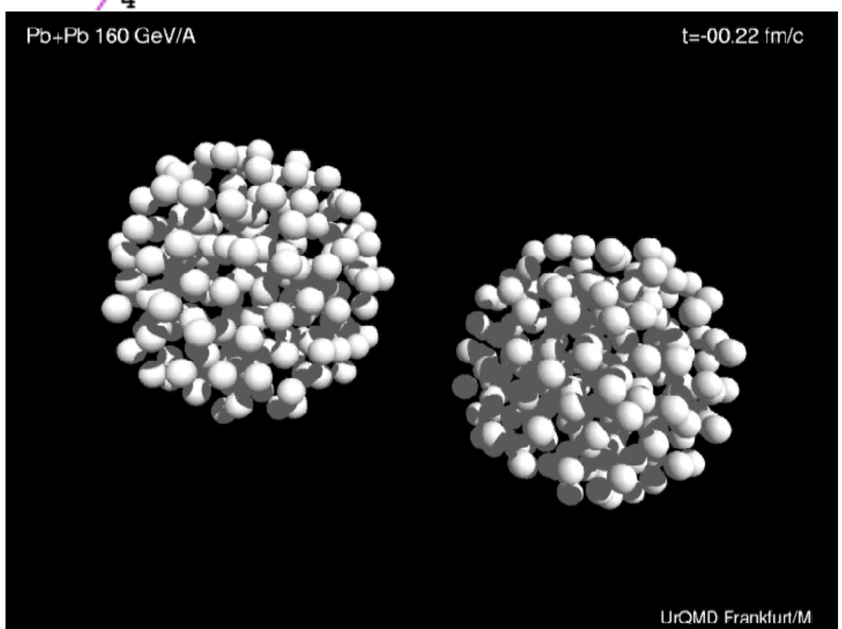

NUCLEO DE THOMSON

→ ***ANIMAÇÃO***

http://galileoandeinstein.physics.virginia.edu/more_stuff/Applets/rutherford/rutherford2.html

NUCLEO DE THOMSON

ANIMAÇÃO

http://galileoandeinstein.physics.virginia.edu/more_stuff/Applets/rutherford/rutherford2.html

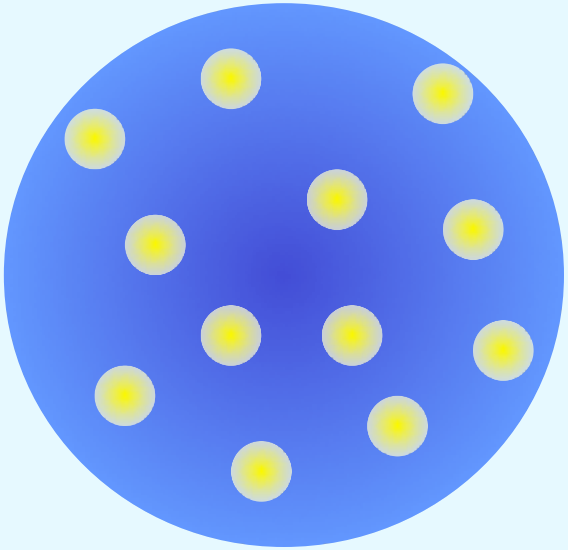

^{24}Mg

NUCLEO DE RUTHERFORD

ANIMAÇÃO

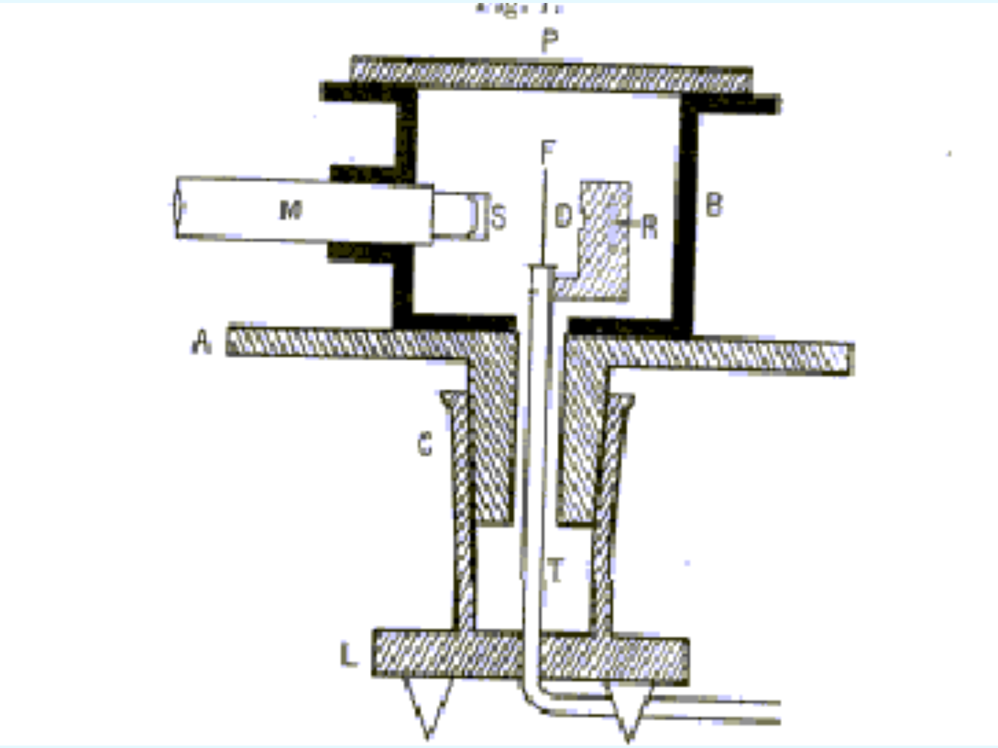

http://galileoandeinstein.physics.virginia.edu/more_stuff/Applets/rutherford/rutherford.html

http://www.nat.vu.nl/~pwgroen/projects/sdm/applets.htm

http://www.nat.vu.nl/~pwgroen/sdm/hyper/anim/anim_DI.html

http://physics.uwstout.edu/physapplets/

http://micro.magnet.fsu.edu/electromag/java/rutherford/

Disproof of the Pudding

The back scattered alpha-particles proved fatal to the plum pudding model. A central assumption of that model was that both the positive charge and the mass of the atom were more or less uniformly distributed over its size, approximately 10-10 meters across or a little more. It is not difficult to calculate the magnitude of electric field from this charge distribution. (Recall that this is the field that must scatter the alphas, the electrons are so light they will jump out of the way with negligible impact on an alpha.)

To be specific, let us consider the gold atom, since the foil used by Rutherford was of gold, beaten into leaf about 400 atoms thick. The gold atom has a positive charge of 79e (balanced of course by that of the 79 electrons in its normal state). Neglecting these electrons -- assume them scattered away -- the maximum electric force the alpha will encounter is that at the surface of the sphere of positive charge,

$$E.2e = \frac{1}{4\pi\varepsilon_0}.\frac{79e.2e}{r_0^2} = 9.10^9.\frac{158.(1.6.10^{-19})^2}{10^{-20}} = 3.64.10^{-6} \text{ newtons}$$

If the alpha particle initially has momentum *p*, for small deflections the angle of deflection (in radians) is given by (*delta_p*)/*p*, where *delta_p* is the sideways momentum resulting from the electrically repulsive force of the positive sphere of charge. Assuming the atomic sphere itself moves negligibly -- it is much heavier than the alpha, so this is reasonable -- the trajectory of the alpha in the inverse square electric field can be found by standard methods. It is the same mathematical problem as finding the elliptic orbits of planets around the sun. Replacing inverse square attraction with inverse square repulsion changes the orbit from an ellipse (or a hyperbola branch swinging around the sun for a comet) to a hyperbola branch lying on one side of the center of repulsion.

Note that since the alpha particle has mass 6.7x10-27 kg, from *F* = *ma*, the electric force at the atomic surface above will give it a sideways acceleration of 5.4x1020 meters per sec per sec (compare *g* = 10!). But the force doesn't have long to act - the alpha is moving at 1.6x107 meters per second. So the time available for the force to act is the time interval a particle needs to cross an atom if the particle gets from New York to Australia in one second.

The time *t*0 = 2*r*0/*v* = 2x10-10/1.6x107 = 1.25x10-17 seconds.

Thus the magnitude of the total sideways velocity picked up is the sideways acceleration multiplied by the time,

1.25x10-17x5.4x1020 = 6750 meters per second.

This is a few ten-thousandths of the alpha's forward speed, so there is only a very tiny deflection. Even if the alpha hit 400 atoms in succession and they all deflected it the same way, an astronomically improbable event, the deflection would only be of order a
In fact, one can get a clear idea of how much deflection comes about without going into the details of the trajectory. Outside the atom, the repulsive electrical force falls away as the inverse square. Inside the atom, the force drops to zero at the center, just as the gravitational force is zero at the center of the earth. The force is maximum right at the surface. Therefore, a good idea of the sideways deflection is given by assuming the alpha experiences that maximal force for a time interval equal to the time it takes the alpha to cross the atom -- say, a distance 2*r*0.
degree. Therefore, the observed deflection through *ninety* degrees and more was completely inexplicable using Thomson's pudding model!

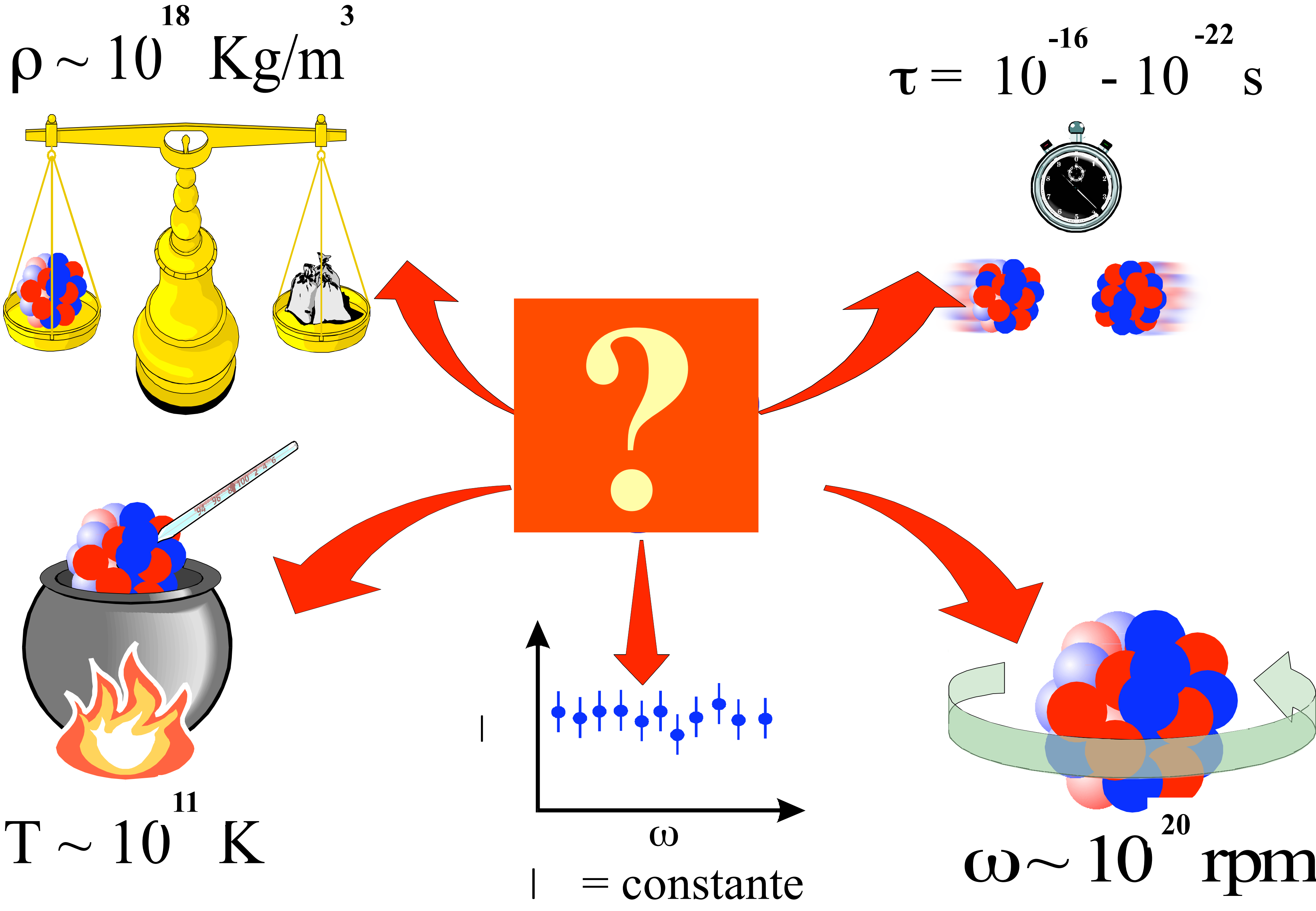

ρ ~ 10^18 Kg/m^3
τ = 10^-16 - 10^-22 s
?
T ~ 10^11 K
ω
= constante
ω ~ 10^20 rpm

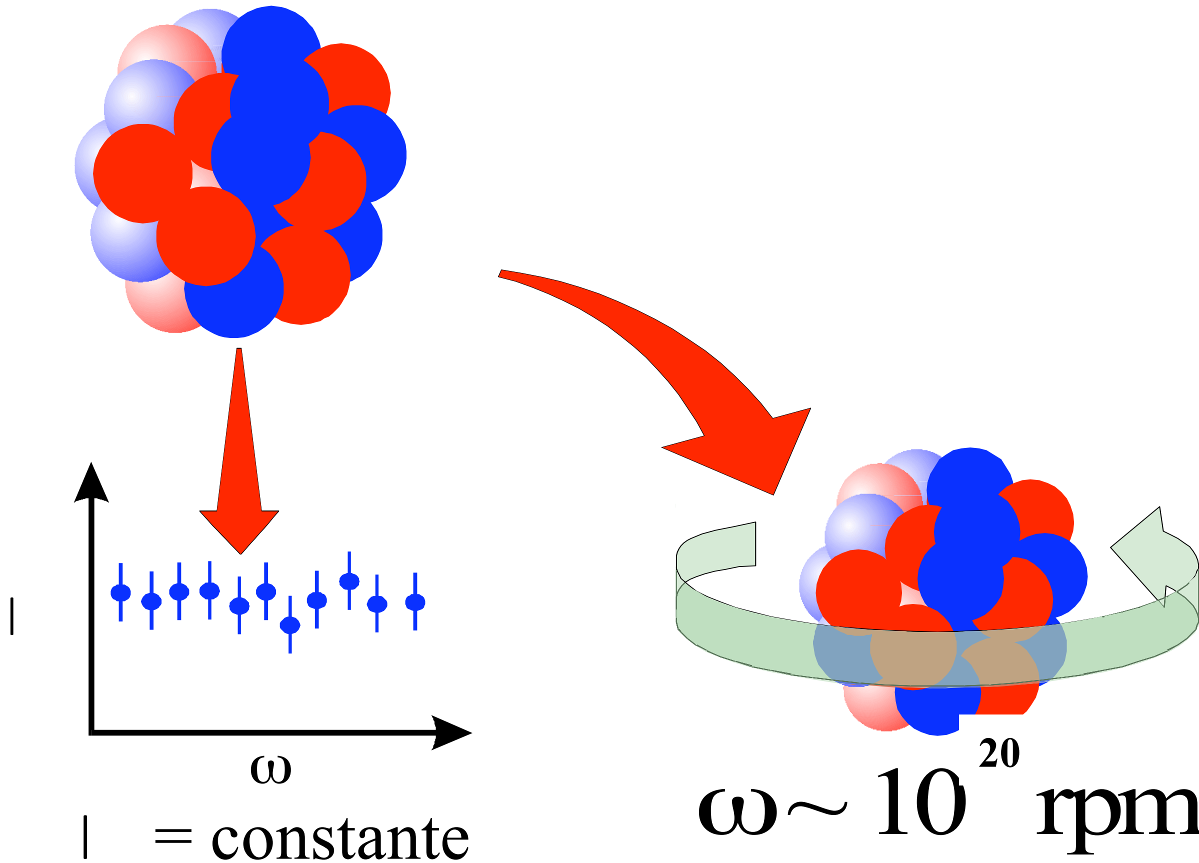
ω
I = constante
ω ~ 10 20 rpm

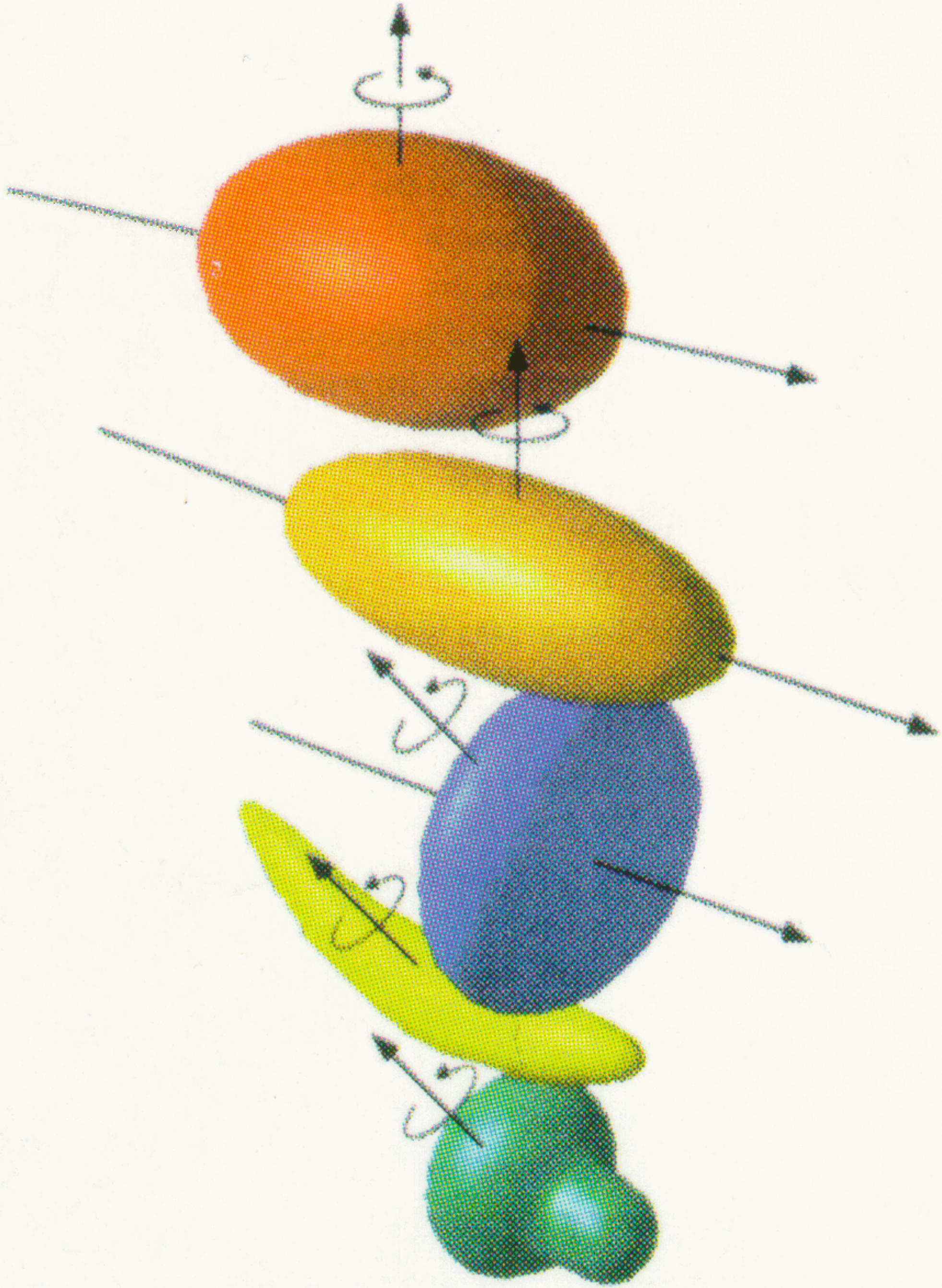

INCLUIR DIAGRAMA DE NIVEIS

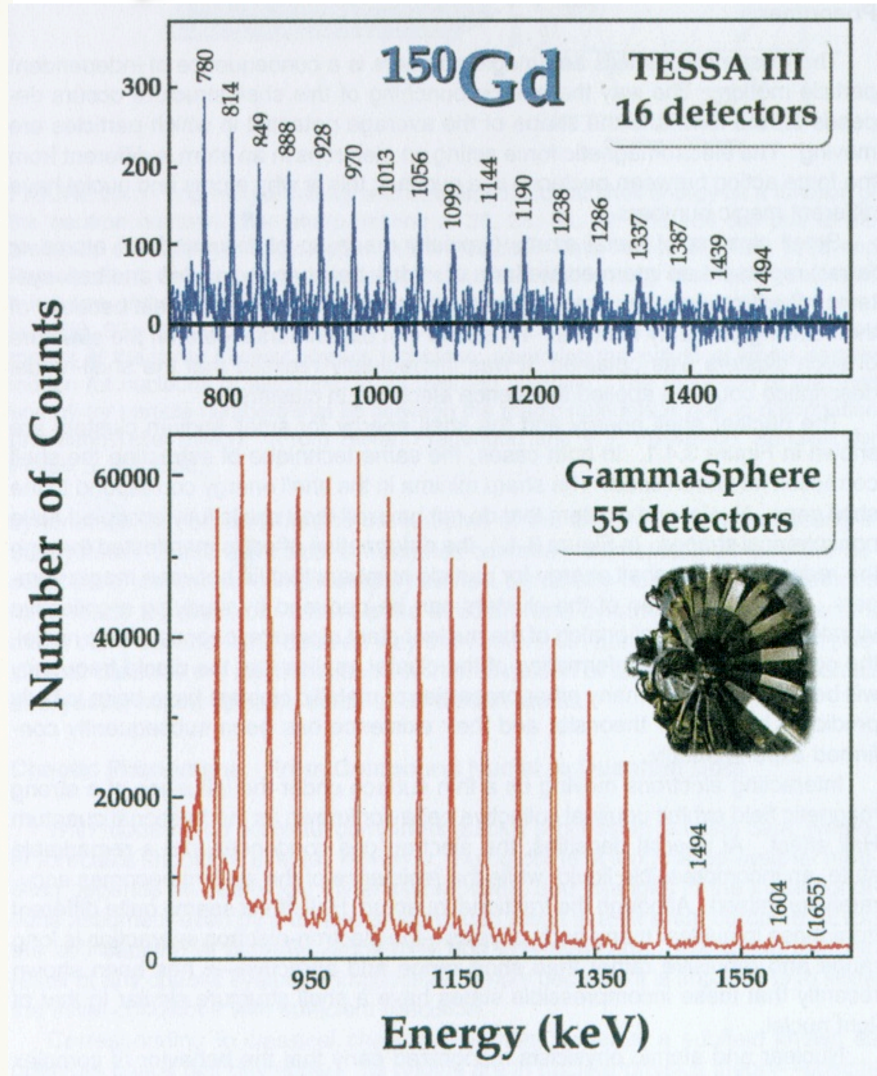

Quark Deconfinement during Pulsar Spin-Down

Deformed Nucleus

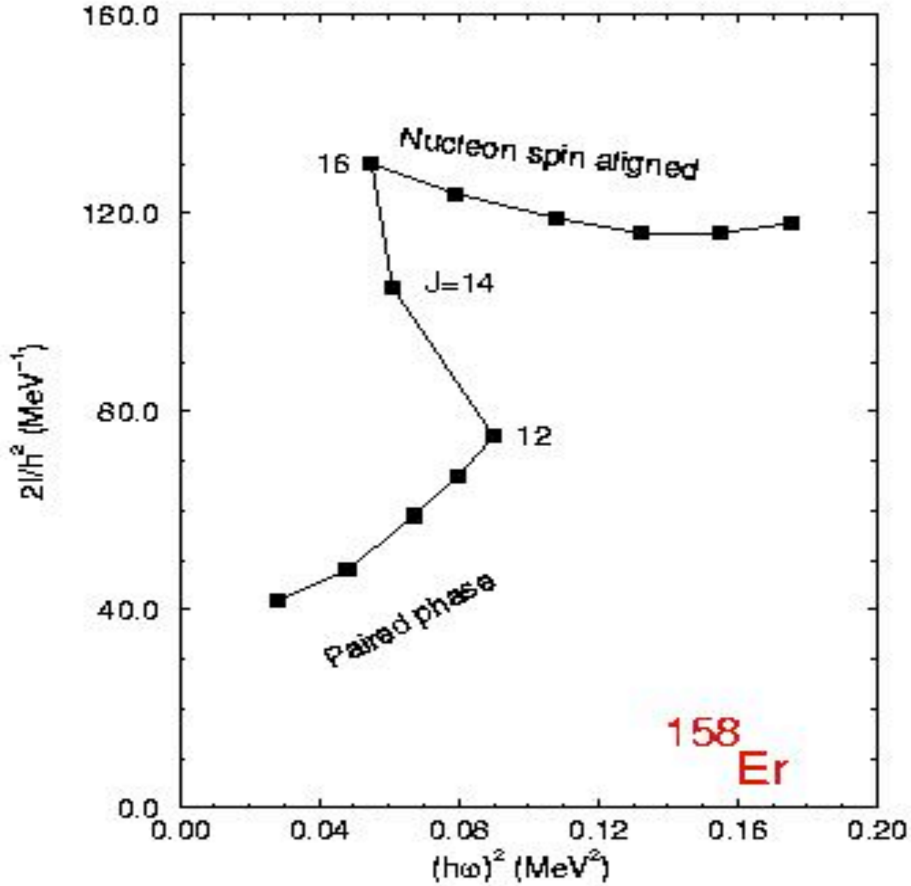

Neutron Star

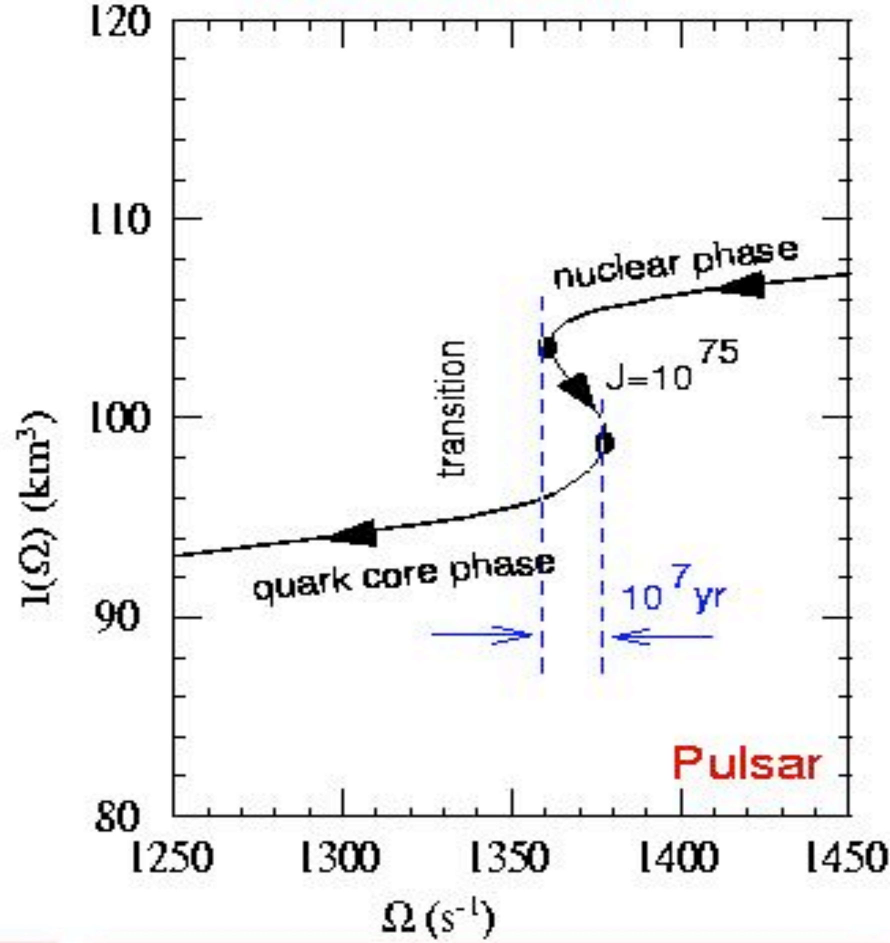

Backbending predicted in 1960 by Mottelson and Valatin (phase transition from spin aligned state at high Ω to pair-correlated super-fluid at low Ω

Backbending in pulsar may result if phase transition occurs.

1)Átomo de Bohr: diagrama de niveis e espectro de raios X
http://www.walter-fendt.de/ph14e/bohrh.htm

2) Espectro nuclear de raios Gamma

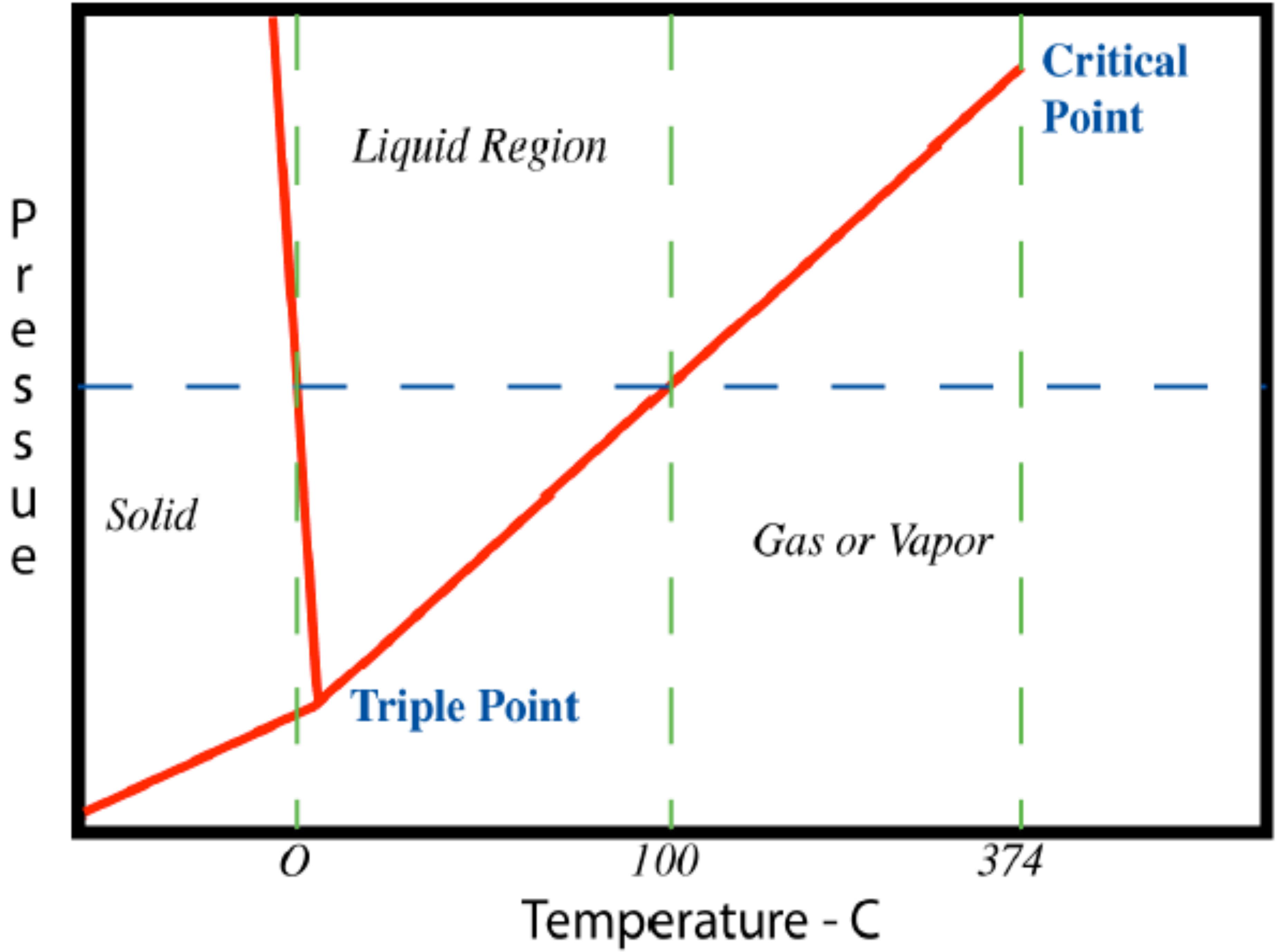
Critical Point
Liquid Region
P r e s s u e
Solid
Gas or Vapor
Triple Point
O
100
374
Temperature - C

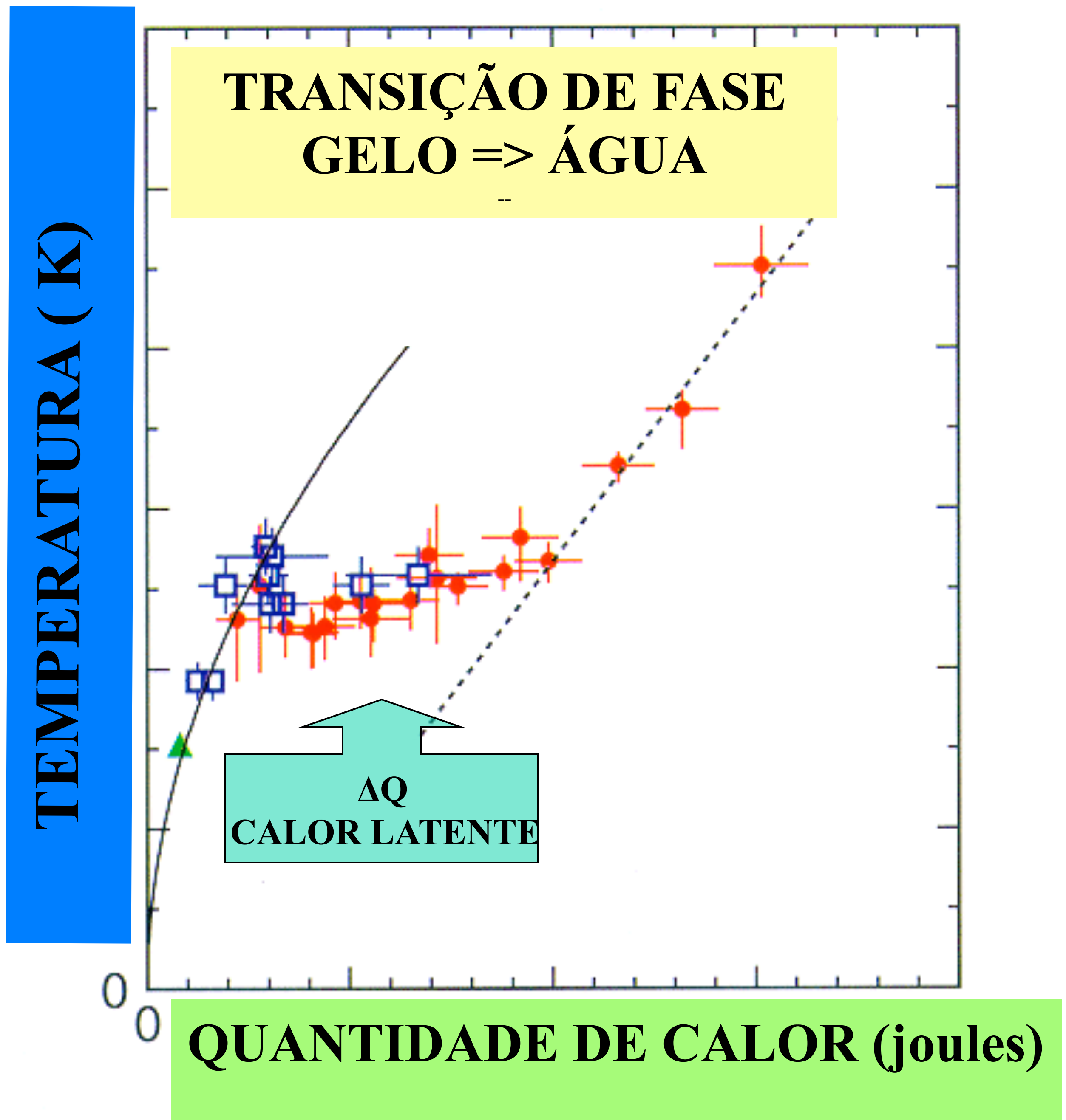

TRANSIÇÃO DE FASE
GELO => ÁGUA
TEMPERATURA (K)
ΔQ
CALOR LATENTE
0
0
QUANTIDADE DE CALOR (joules)

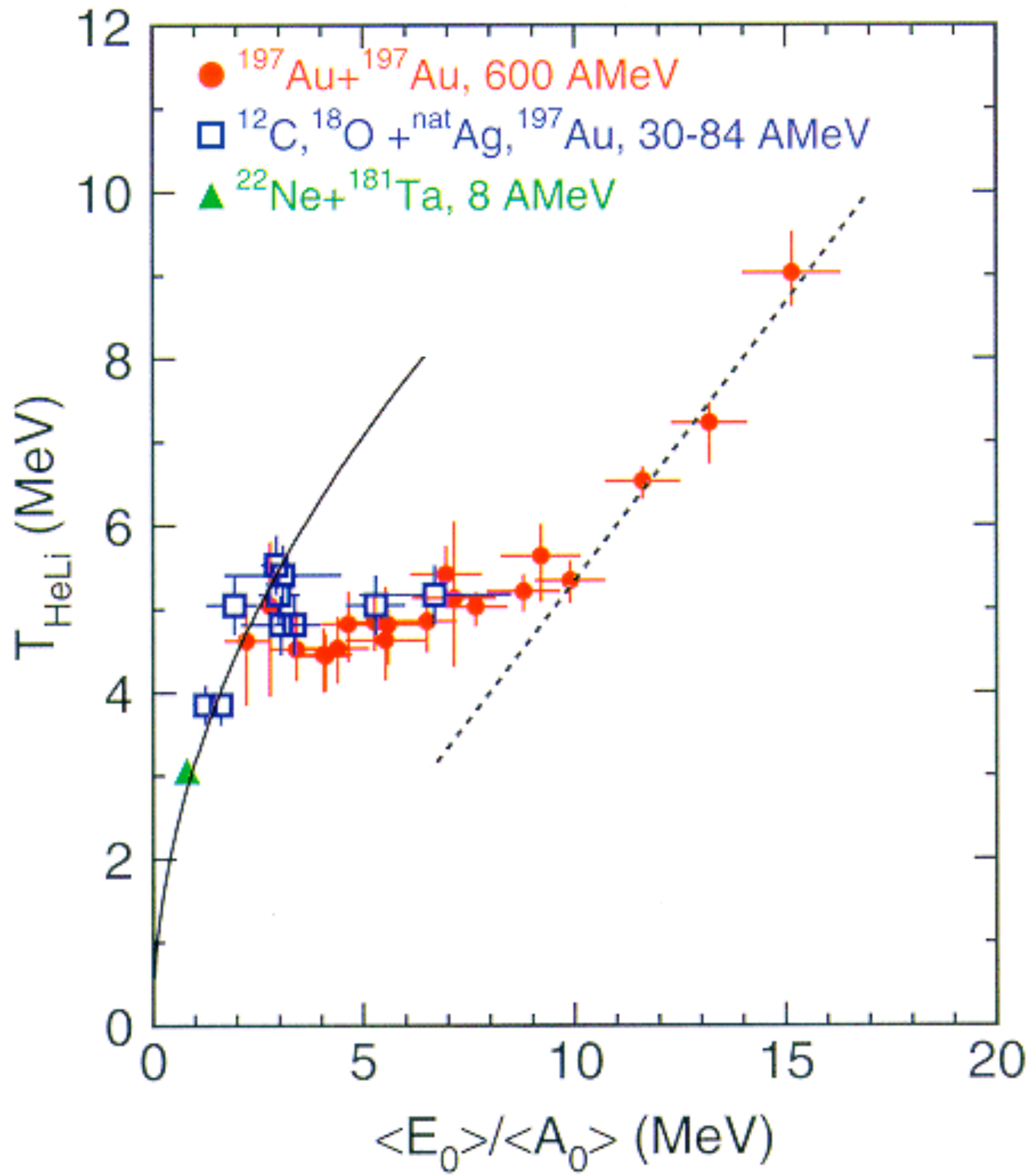

^{197}Au+^{197}Au, 600 AMeV
^{12}C,^{18}O +^{nat}Ag,^{197}Au, 30-84 AMeV
^{22}Ne+^{181}Ta, 8 AMeV
T_{HeLi} (MeV)
$\langle E_0\rangle/\langle A_0\rangle$ (MeV)
0
2
4
6
8
10
12
0
5
10
15
20

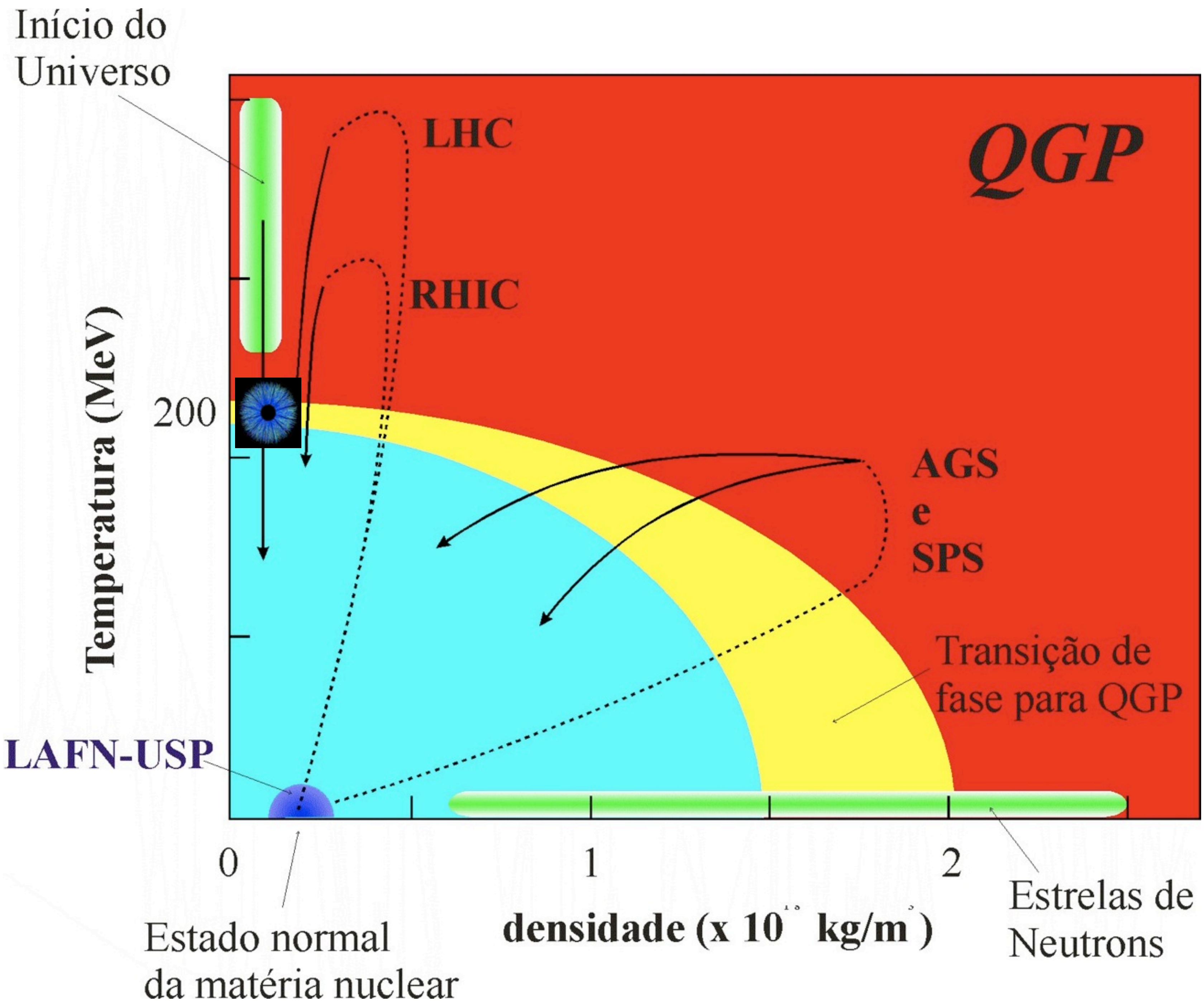
Início do
Universo
LHC
QGP
RHIC
Temperatura (MeV)
200
AGS
e
SPS
Transição de
fase para QGP
LAFN-USP
0
1
2
Estrelas de
Neutrons
densidade (x 10 kg/m)
Estado normal
da matéria nuclear

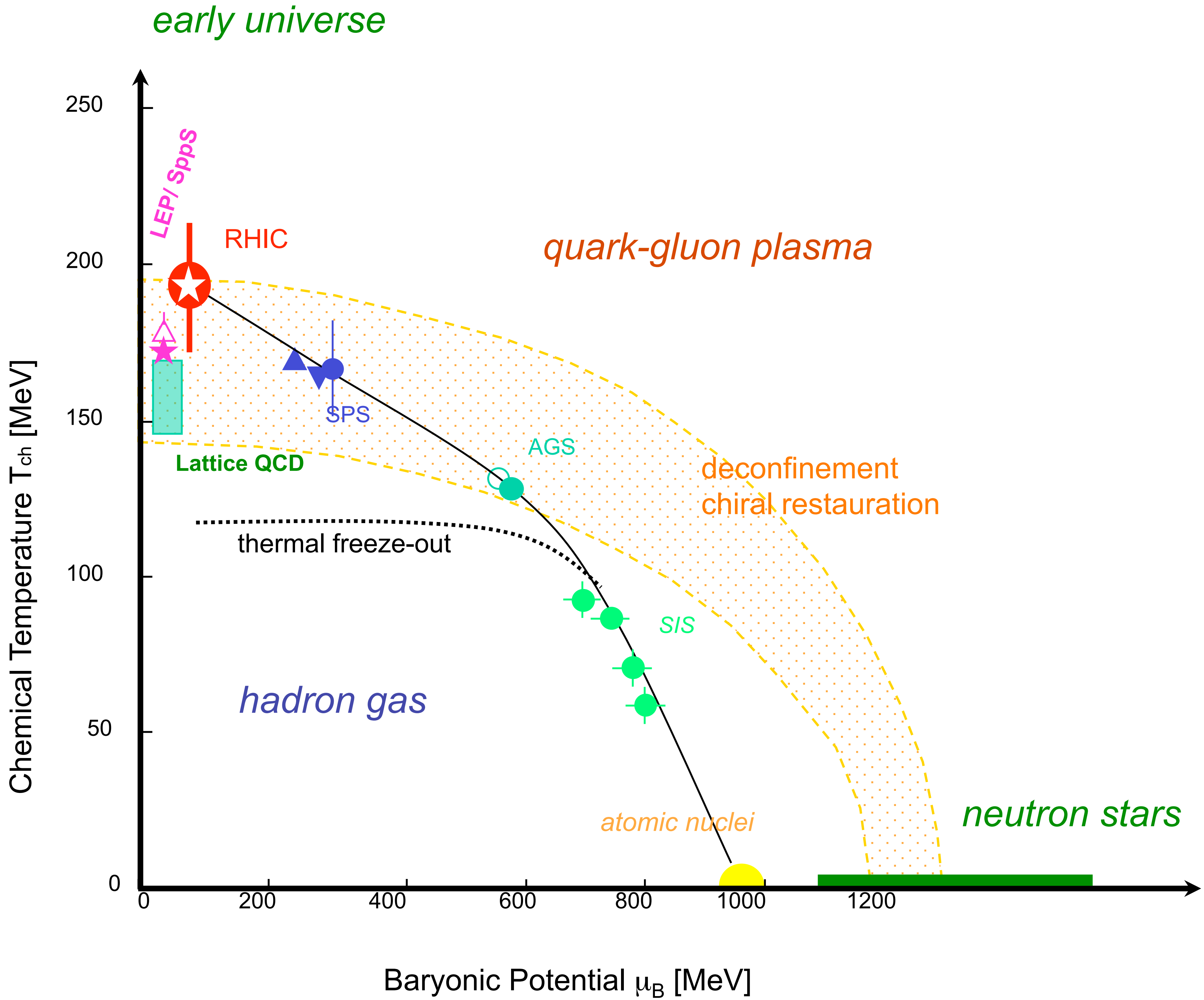

early universe
LEP/ SppS
RHIC
quark-gluon plasma
SPS
AGS
Lattice QCD
deconfinement
chiral restauration
thermal freeze-out
SIS
hadron gas
atomic nuclei
neutron stars
Chemical Temperature T_{ch} [MeV]
Baryonic Potential μ_B [MeV]
0
50
100
150
200
250
0
200
400
600
800
1000
1200

$\rho \sim 10^{18}\ Kg/m^{3}$

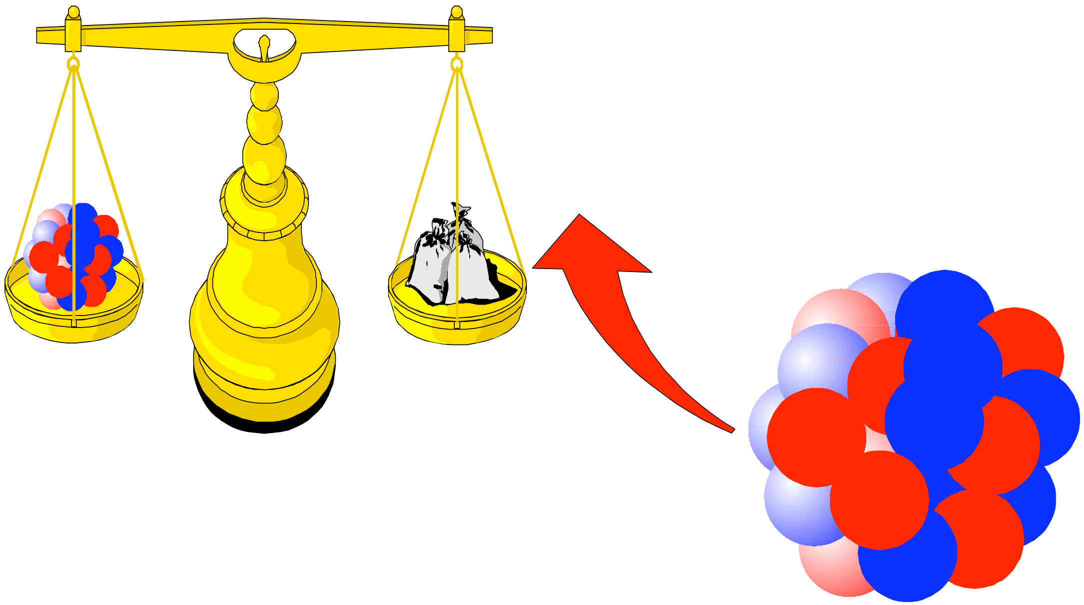

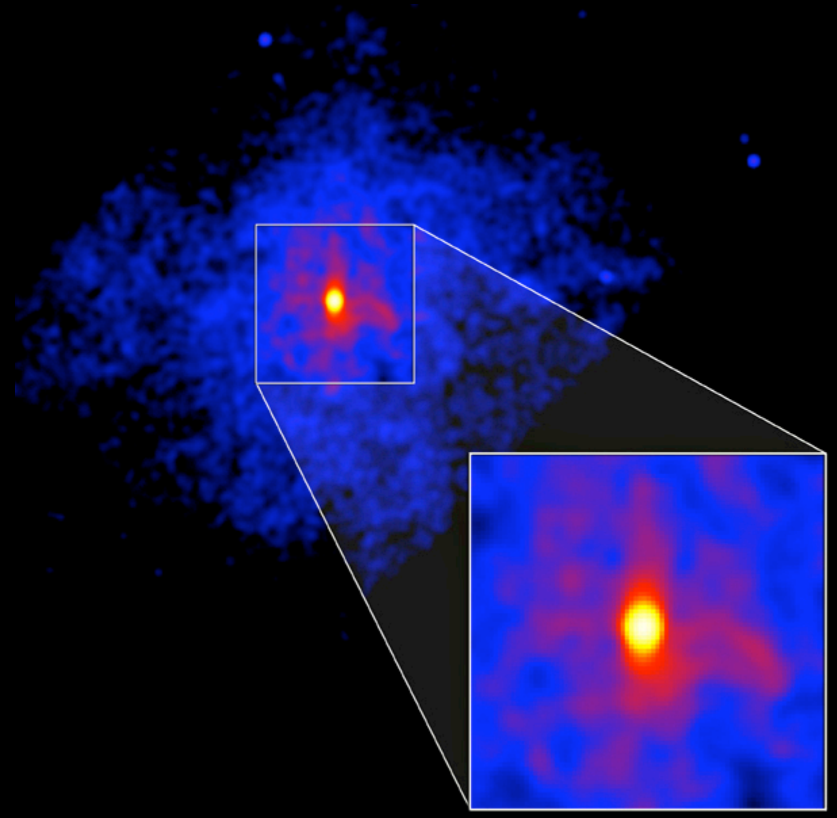

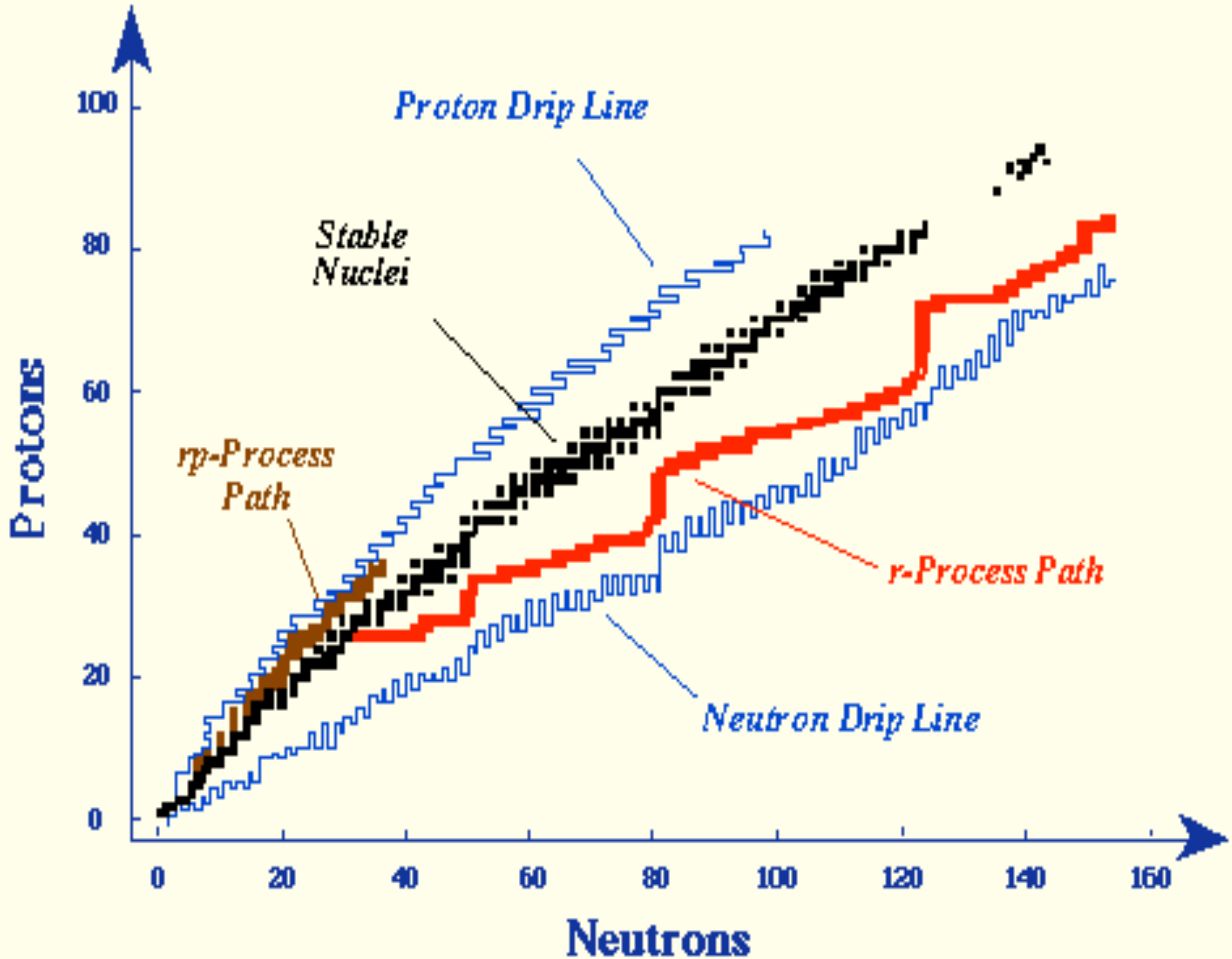
Proton Drip Line
Stable Nuclei
rp-Process Path
r-Process Path
Neutron Drip Line
Protons
Neutrons
0
20
40
60
80
100
0
20
40
60
80
100
120
140
160

COLISÃO DISTANTE

COLISÃO RASANTE

COLISÃO FRONTAL

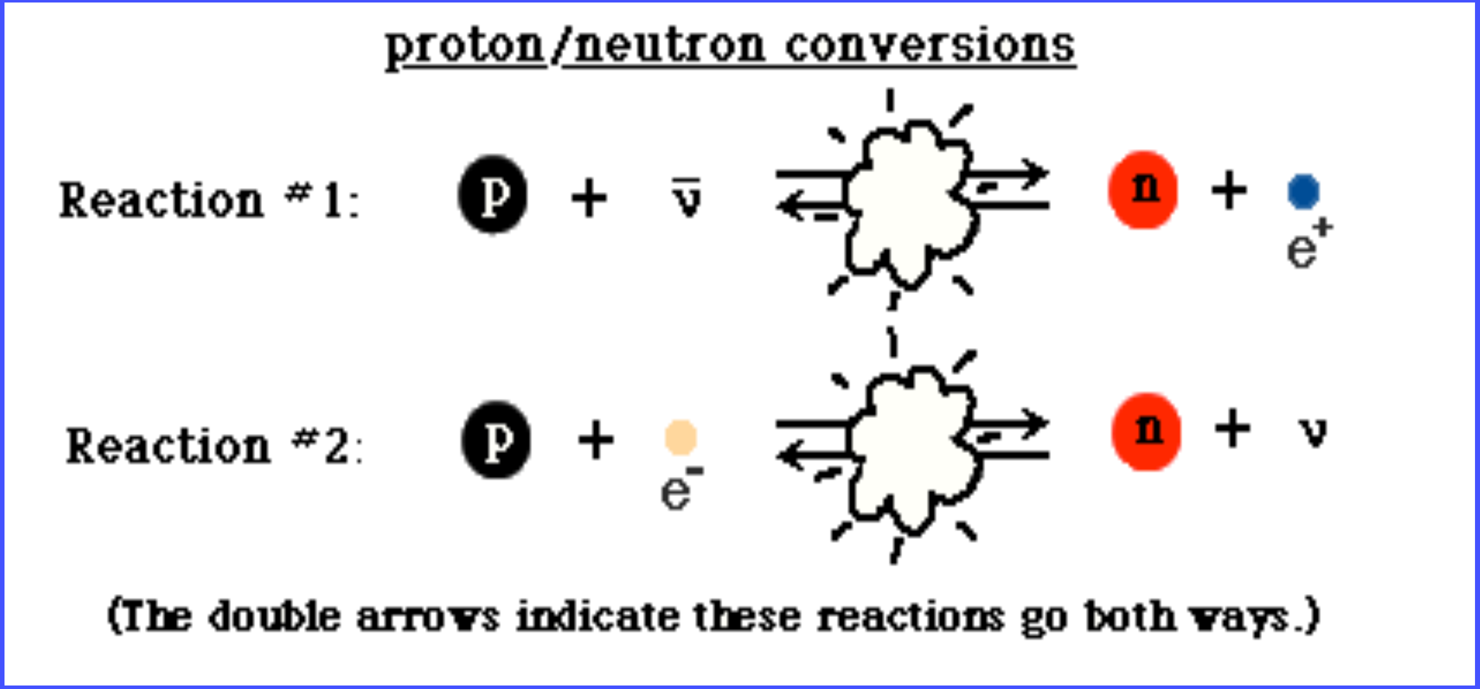
proton/neutron conversions
Reaction #1:
p + ν̄
n + e+
Reaction #2:
p + e-
n + ν
(The double arrows indicate these reactions go both ways.)

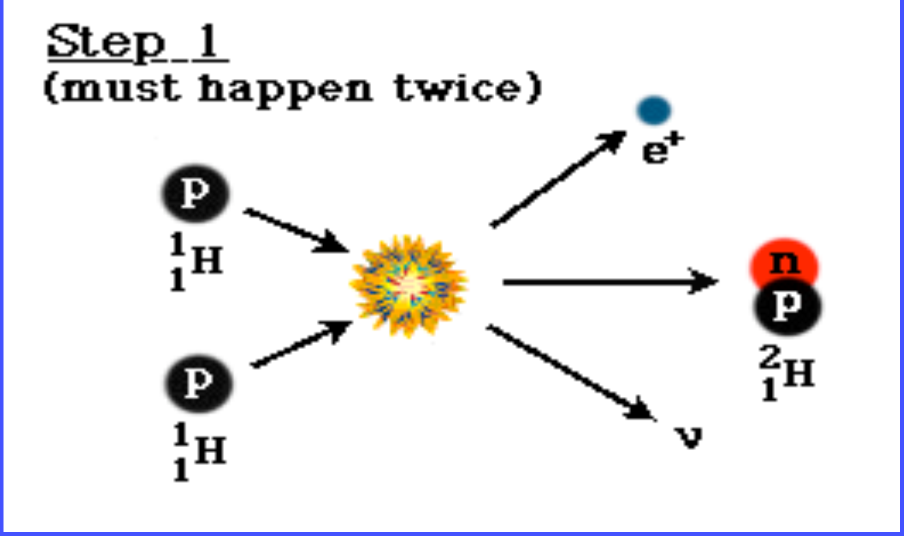
Step 1
(must happen twice)
p
1 1 H
p
1 1 H
e+
n p
2 1 H
ν

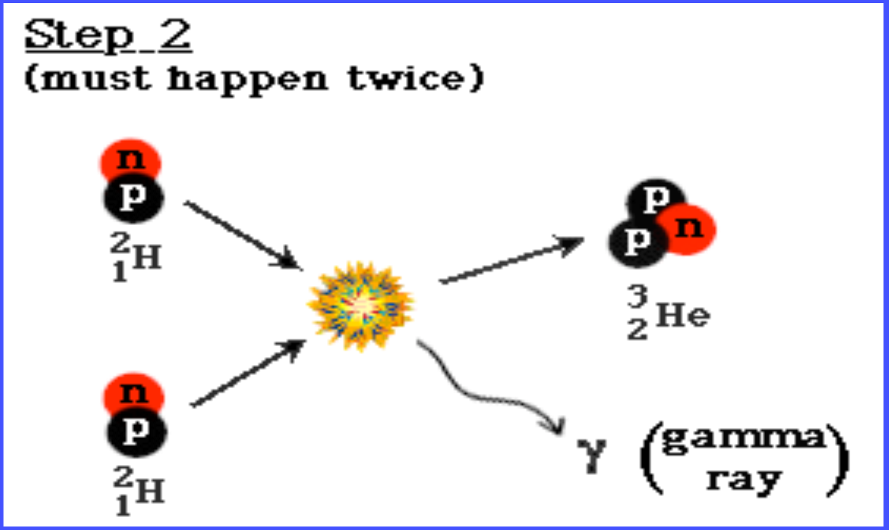
Step 2
(must happen twice)
n p
2 1 H
n p
2 1 H
p p n
3 2 He
γ (gamma ray)

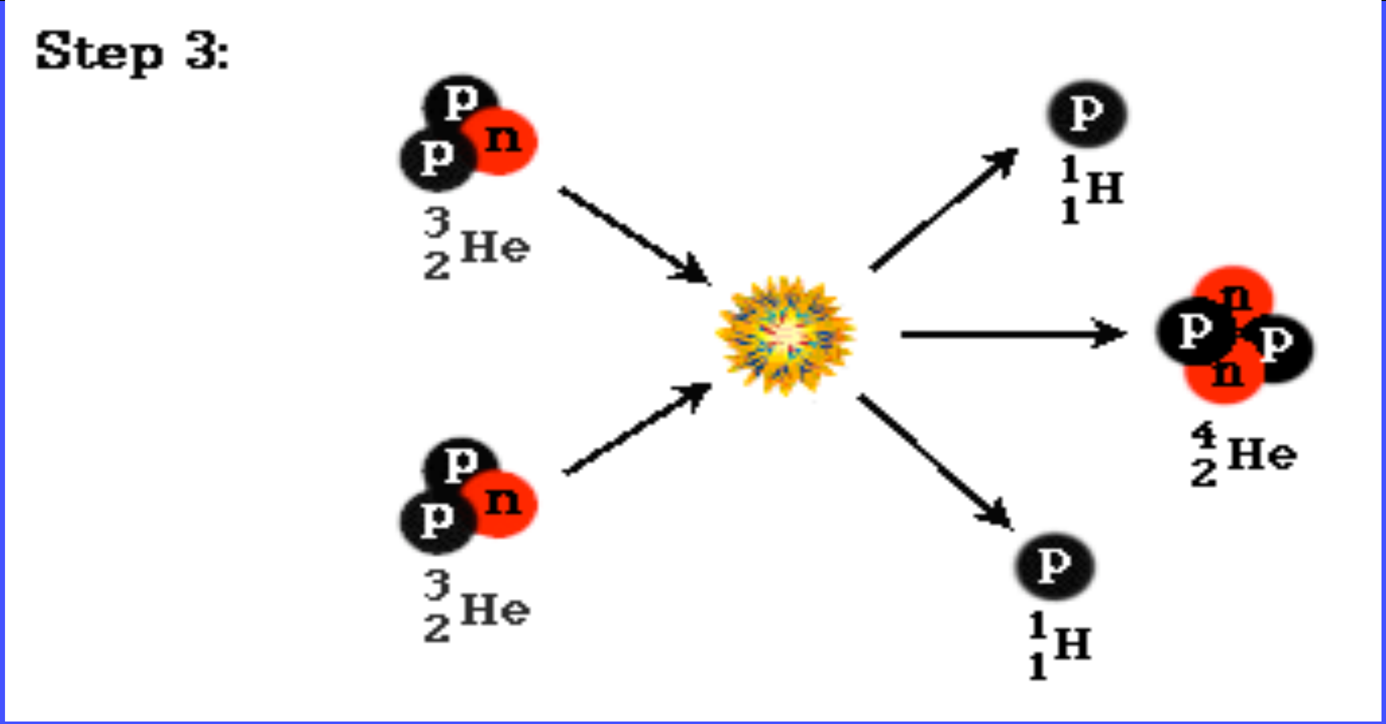
Step 3:
p
n
p
3
2 He
p
n
p
3
2 He
p
1
1 H
n
p
p
n
4
2 He
p
1
1 H

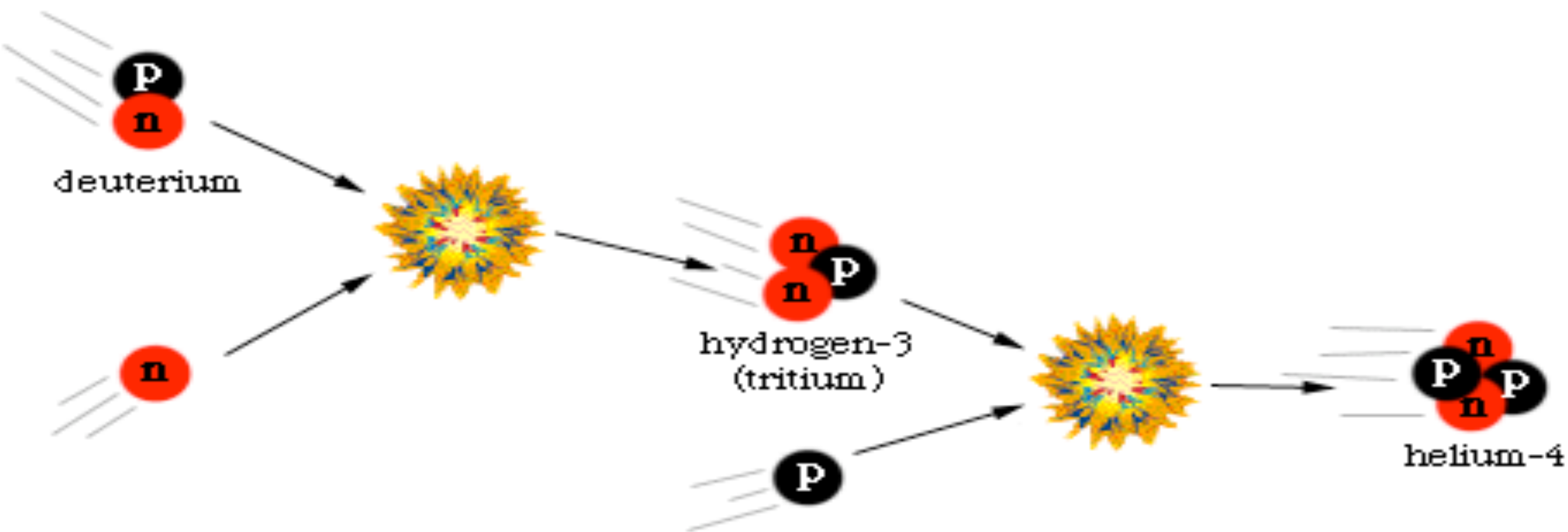
p
n
deuterium
n
n
p
n
hydrogen-3
(tritium)
p
n
p
p
n
helium-4

n =1.00866 u.m.a.
p = 1.0079 u.m.a.
d = 2.01410 u.m.a.
t = 3.01860 u.m.a.
^{4}He = 4. 00260 u.m.a.
^{6}Li = 6. 01512 u.m.a.
^{12}C = 0.00000 u.m.a.

p+p+n+n=ALPHA
d+t=n+ALPHA

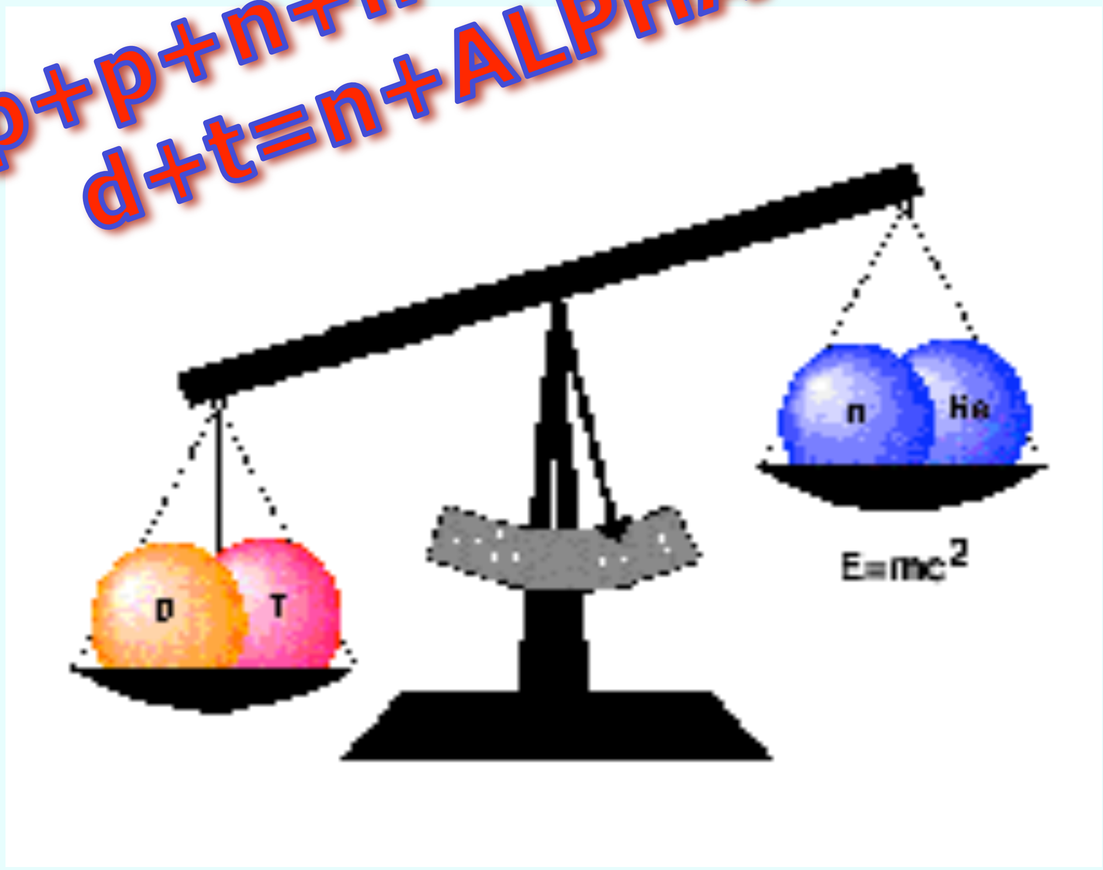

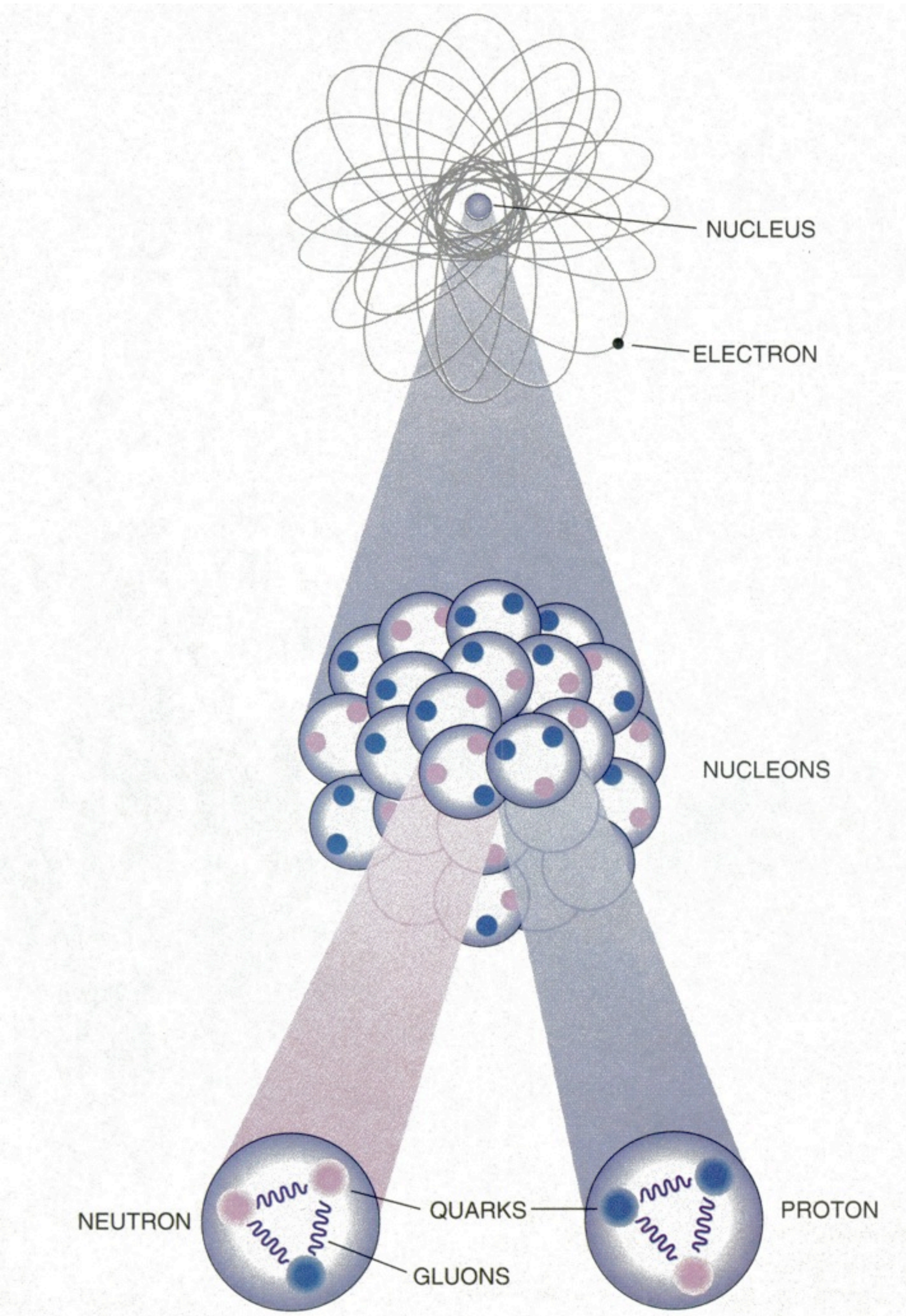

$M_{(proton)} = M_p = 938.27$ MeV

$M_{(neutron)} = M_n = 939.56$ MeV

$M_{(eletron)} = M_e = 0.511$ MeV

$M_{(\text{átomo de Hidrogênio})} = M_H = 938.58$ MeV

$M_p + M_e = 938.27 + 0.511 = 938.78$MeV

$M_H = 938.58$ MeV

$M_{(16O)} = 14\,899.17$ MeV

$8M_p + 8M_n = 15\,022.64$ MeV

$\Delta M = 123.47$ MeV

p = (u + u + d)

$M_{(u)} \approx 3$ MeV

$M_{(d)} \approx 6$ MeV

$2\,M(u) + M(d) \approx 12$MeV

$Mp = 938.27$ MeV

$\Delta M \approx 926$ MeV

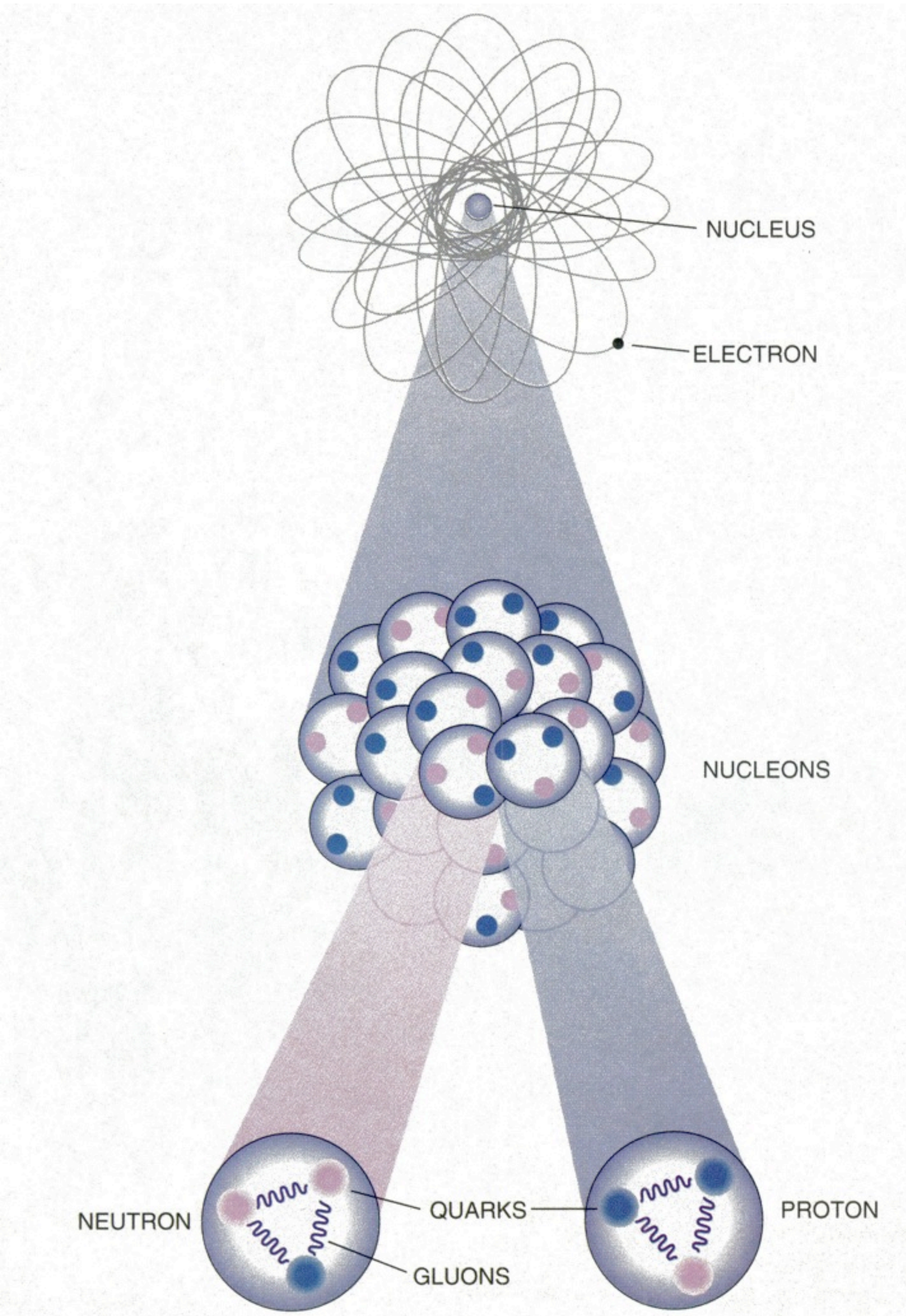

$M_{(neutron)} = M_n = 1.008664904$ u

$M_{(proton)} = M_p = 1.007276470$ u

$M_{(eletron)} = M_e = 0.000548580$ u

$M_{(\text{átomo de Hidrogênio})} = M_H = 1.007825032$ u

$M_p + M_e = 1.007815050$ u

$M_{(16O)} = 14\,899.17$ MeV

$8M_p + 8M_n = 15\,022.64$ MeV

$\Delta M = 123.47$ MeV

$p = (u + u + d)$

$M_{(u)} \approx 3$ MeV

$M_{(d)} \approx 6$ MeV

$2\,M(u) + M(d) \approx 12$MeV

$Mp = 938.27$ MeV

$\Delta M \approx 926$ MeV

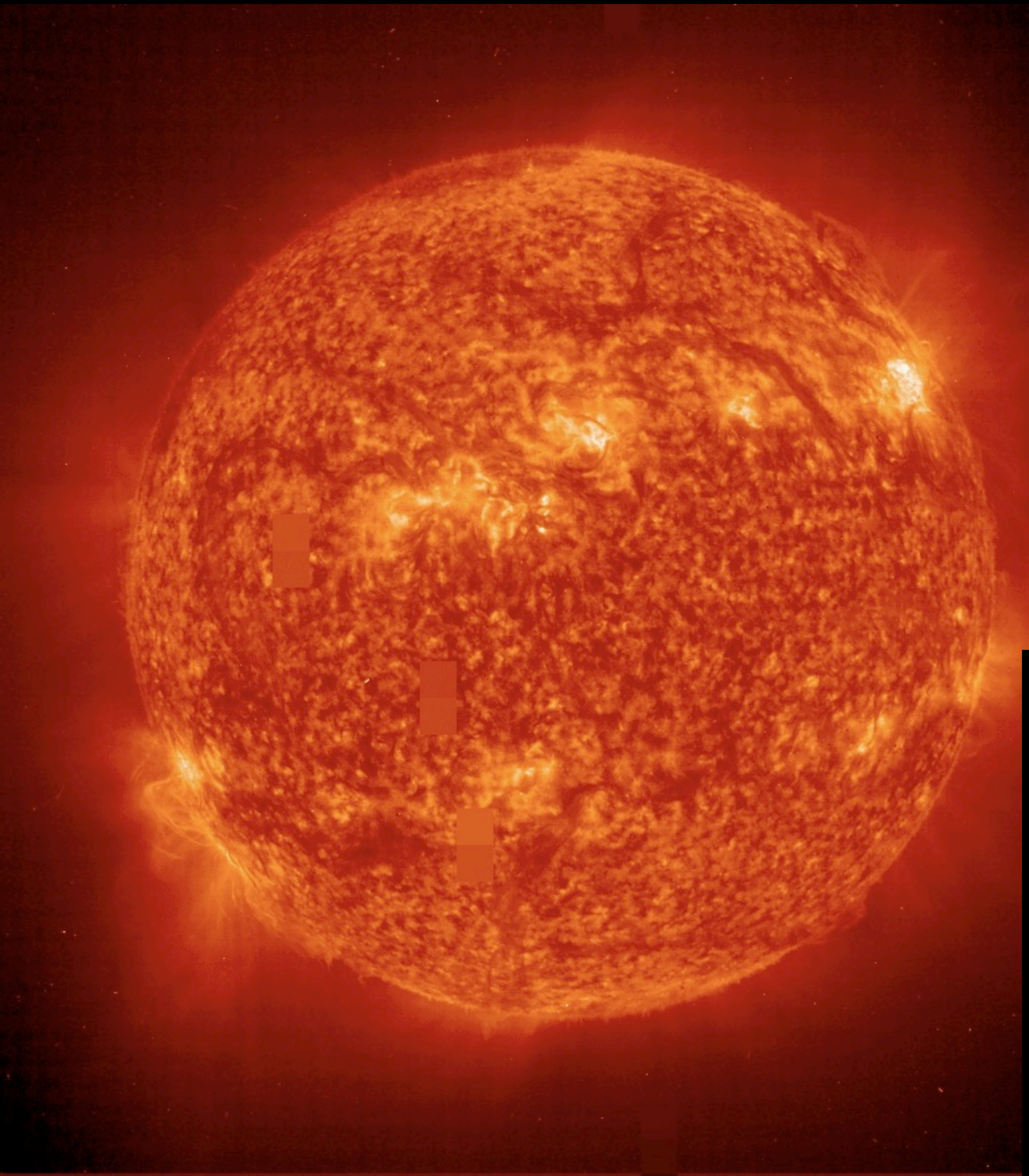

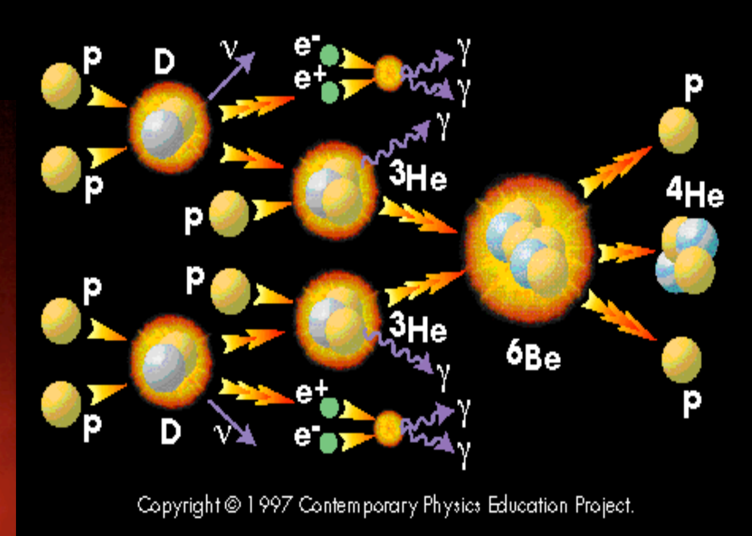
p
p
D
ν
e^-
e^+
γ
γ
γ
p
^3He
^6Be
p
^4He
p
p
p
p
^3He
γ
D
ν
e^+
e^-
γ
γ
p
Copyright © 1997 Contemporary Physics Education Project.

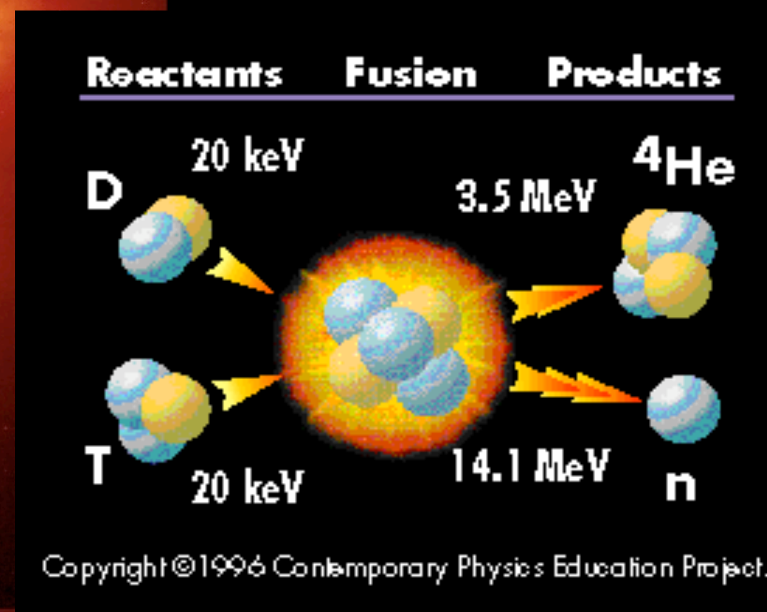
Reactants
Fusion
Products
D
20 keV
3.5 MeV
^4He
T
20 keV
14.1 MeV
n
Copyright ©1996 Contemporary Physics Education Project.

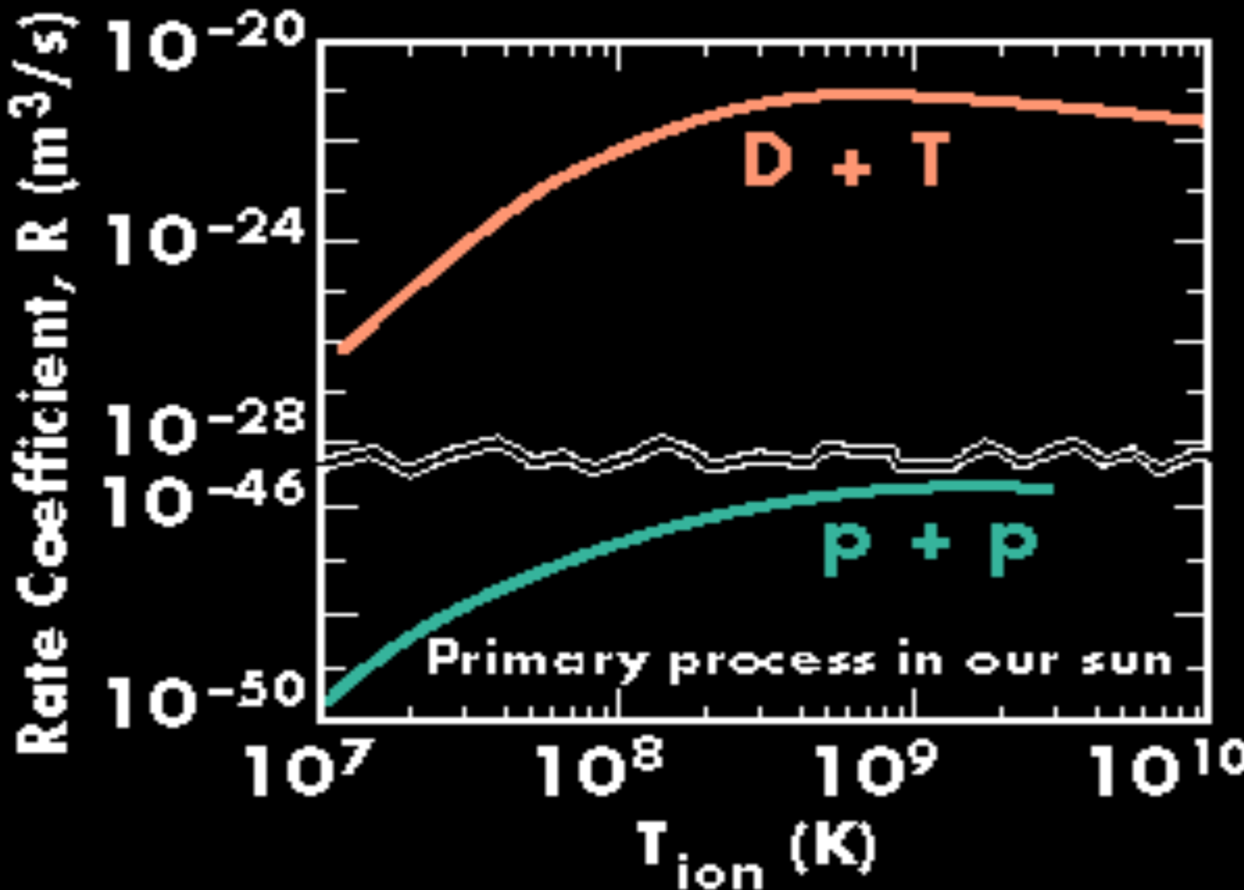

Rate Coefficient, R (m3/s)
10-20
10-24
10-28
10-46
10-50
D + T
p + p
Primary process in our sun
107
108
109
1010
Tion (K)

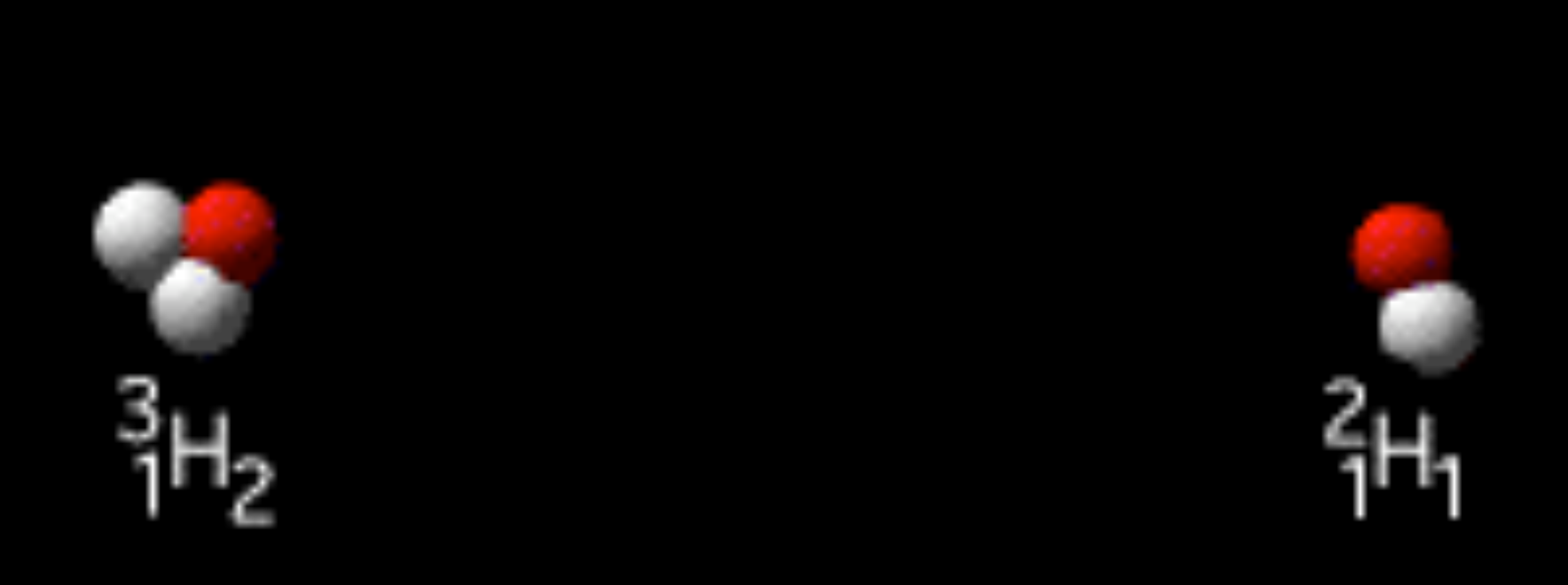
$^{3}_{1}H_{2}$
$^{2}_{1}H_{1}$

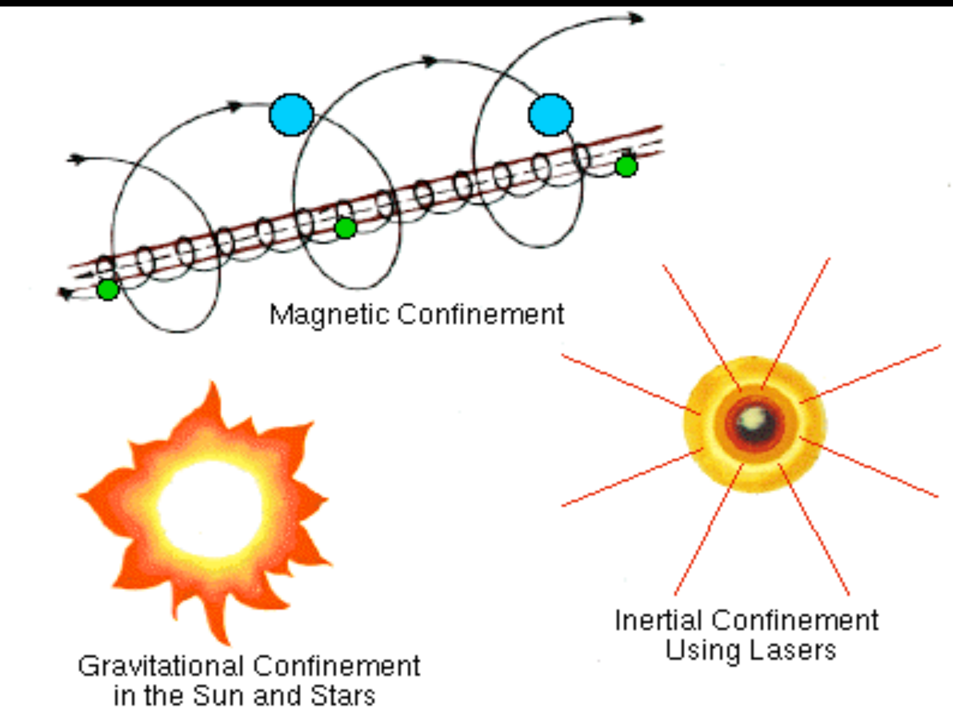
Magnetic Confinement
Inertial Confinement
Using Lasers
Gravitational Confinement
in the Sun and Stars

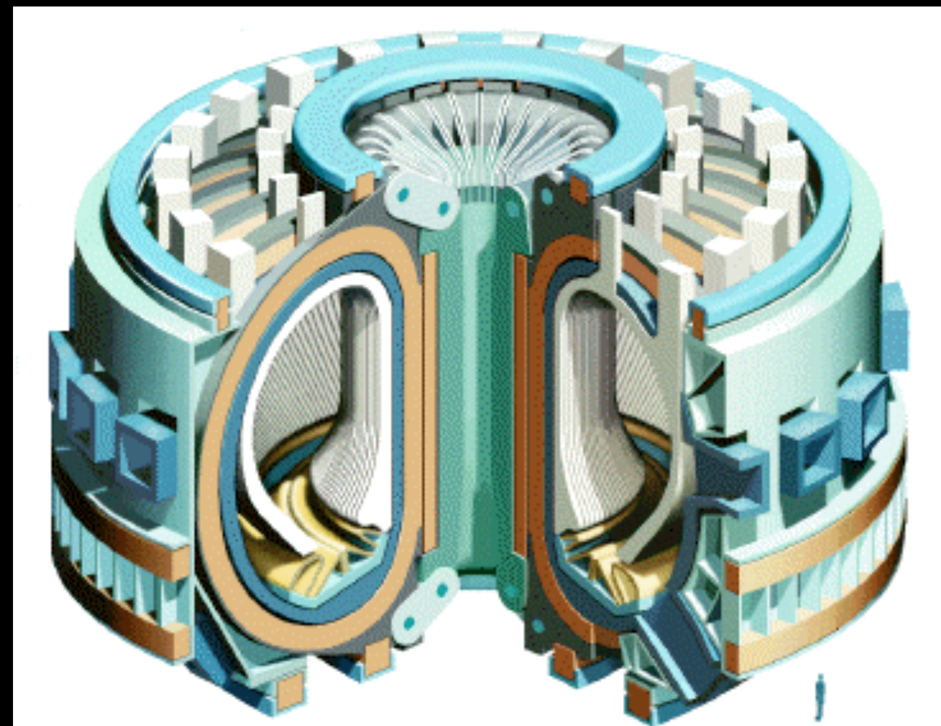

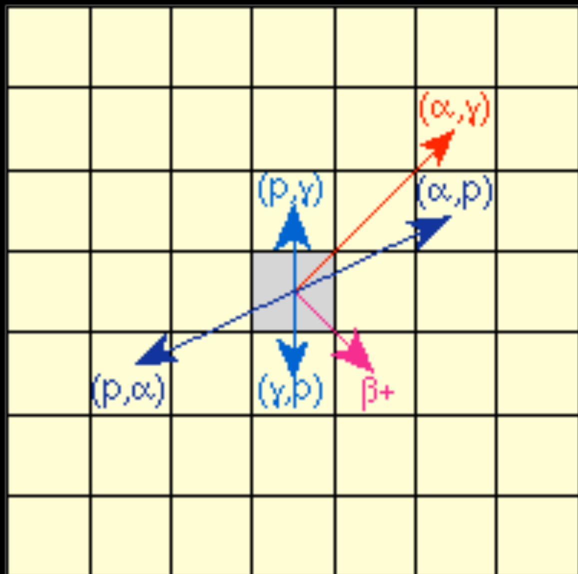

Carbon- Nitrogen- Oxygen Cycle

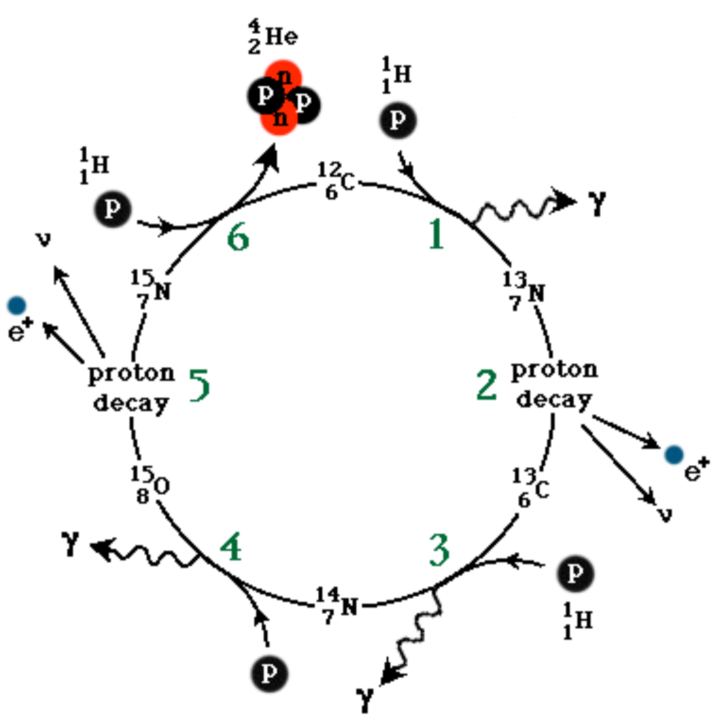

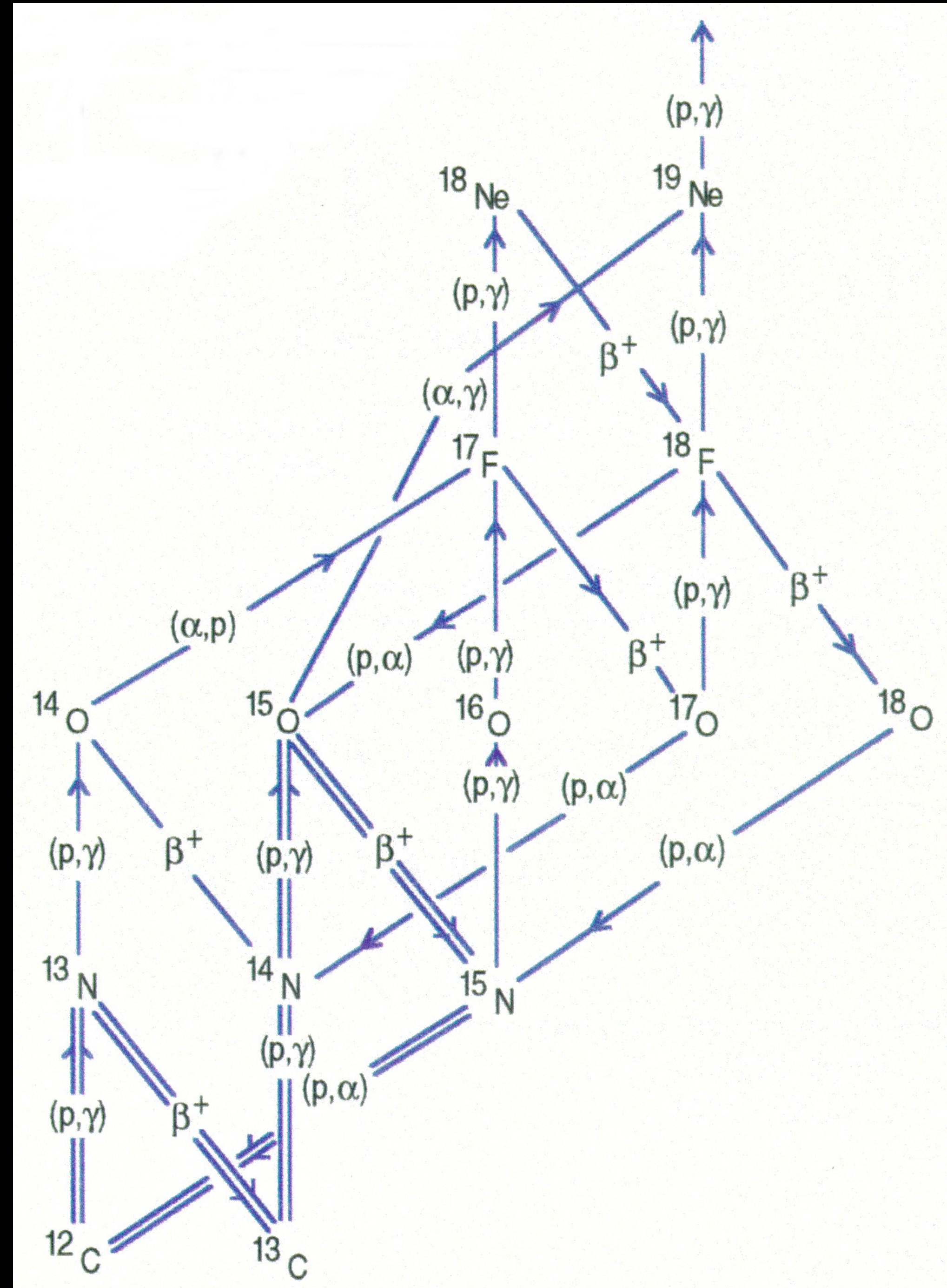

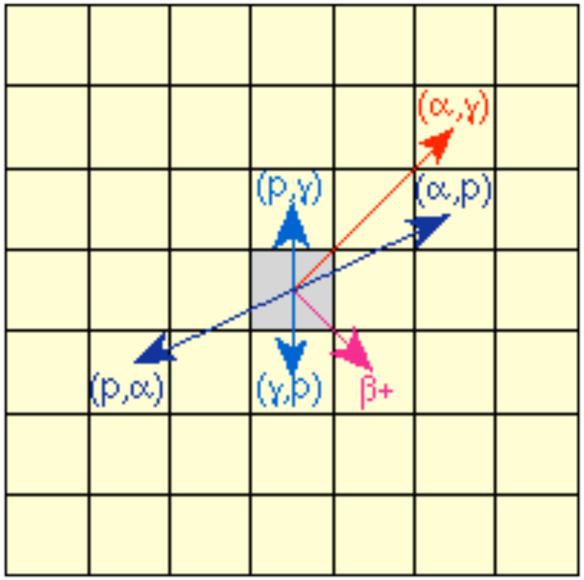

Reaction Vectors

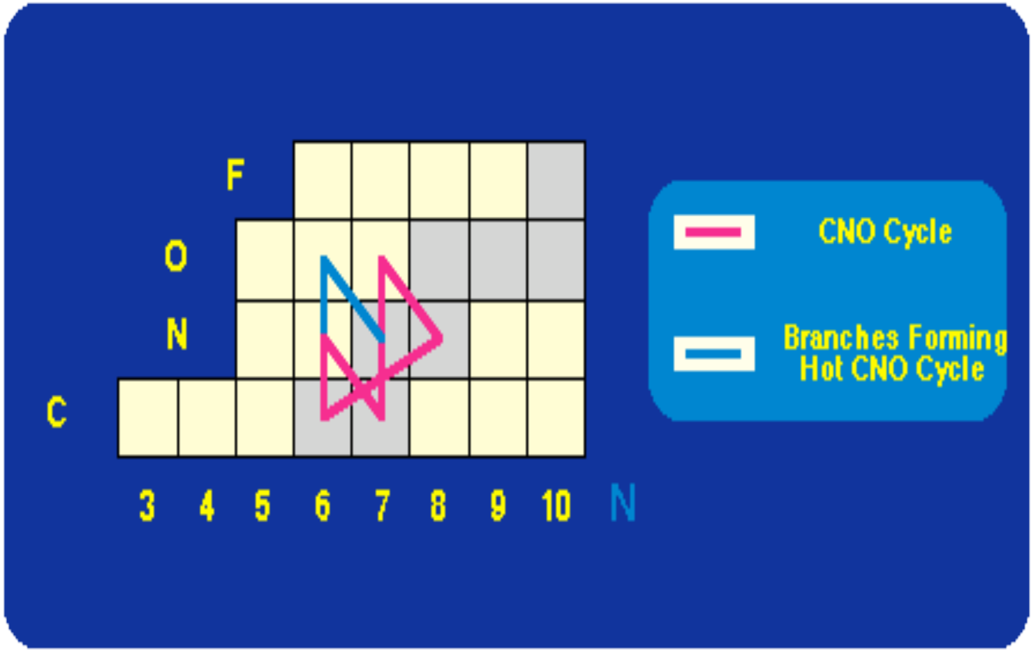

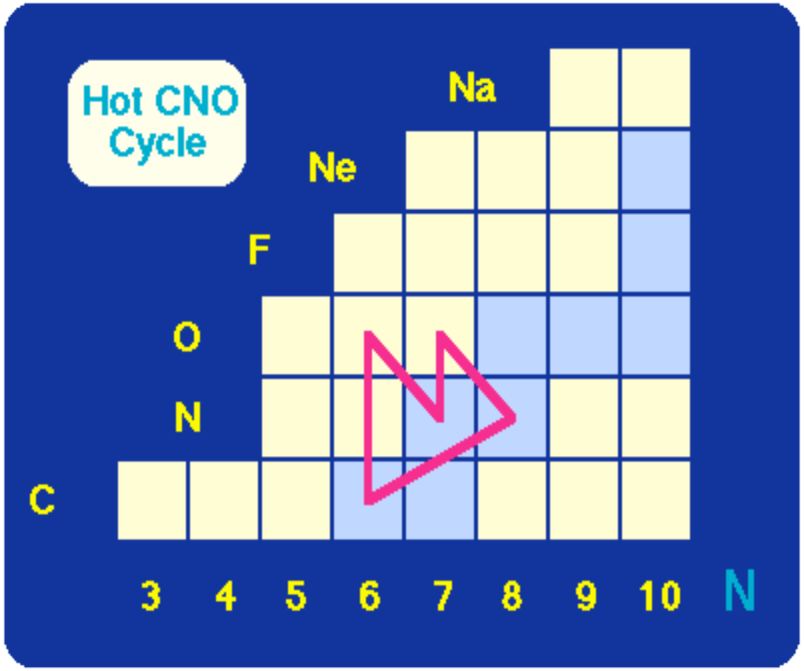

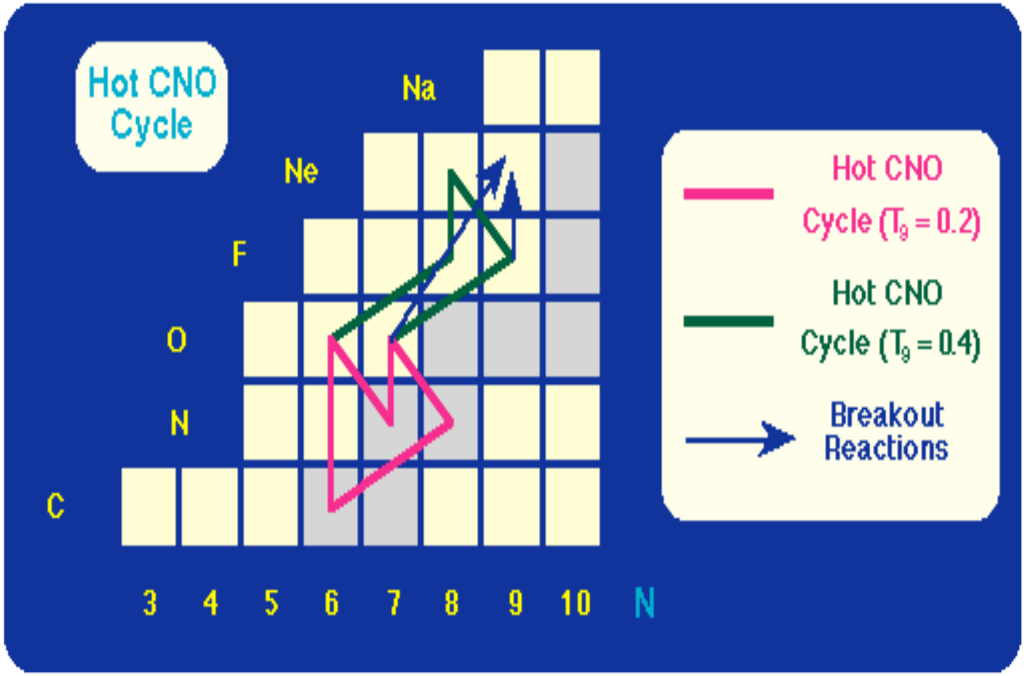

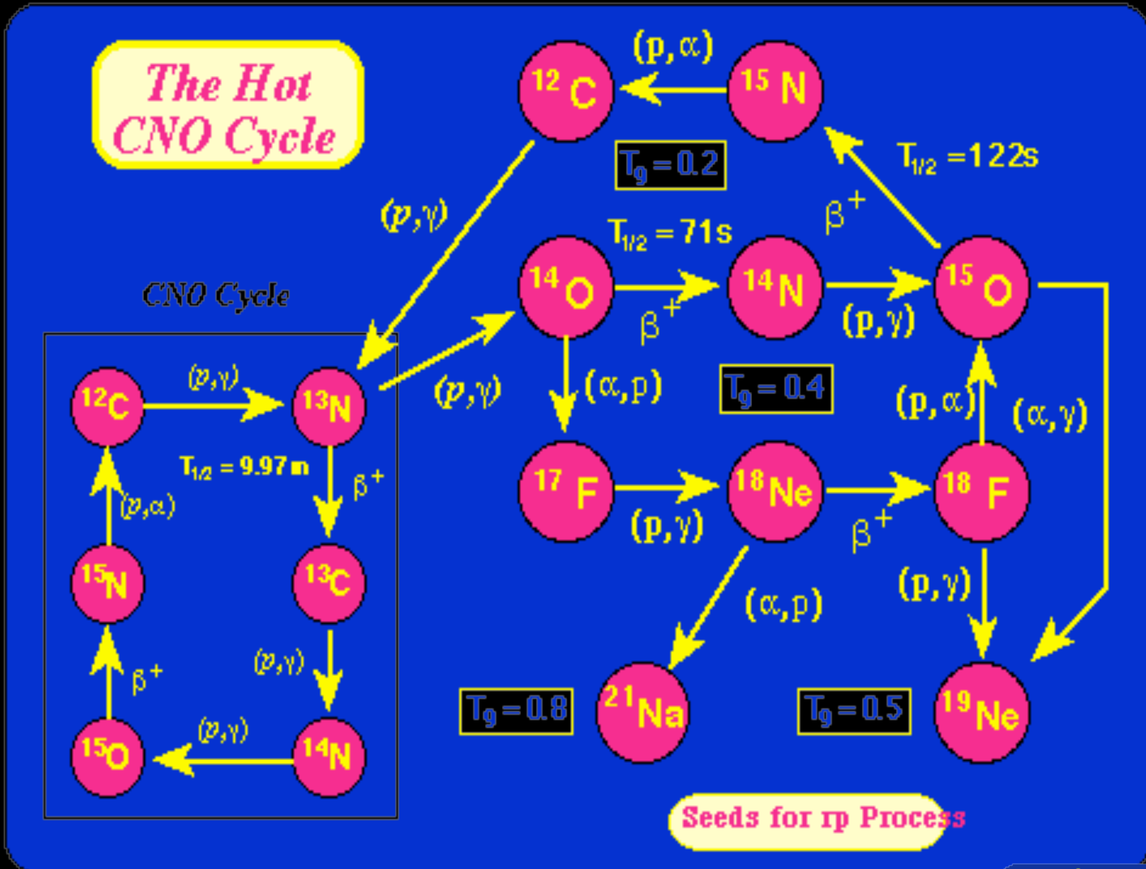

The Hot CNO Cycle
CNO Cycle
12C
13N
13C
14N
15O
15N
(p,γ)
β+
(p,α)
T1/2 = 9.97 m
12 C
15 N
(p,α)
Tg = 0.2
T1/2 = 122s
(p,γ)
14 O
14 N
15 O
T1/2 = 71s
β+
(p,γ)
(α,p)
Tg = 0.4
(p,α)
(α,γ)
17 F
18 Ne
18 F
(p,γ)
β+
(α,p)
(p,γ)
Tg = 0.8
21 Na
Tg = 0.5
19 Ne
Seeds for rp Process

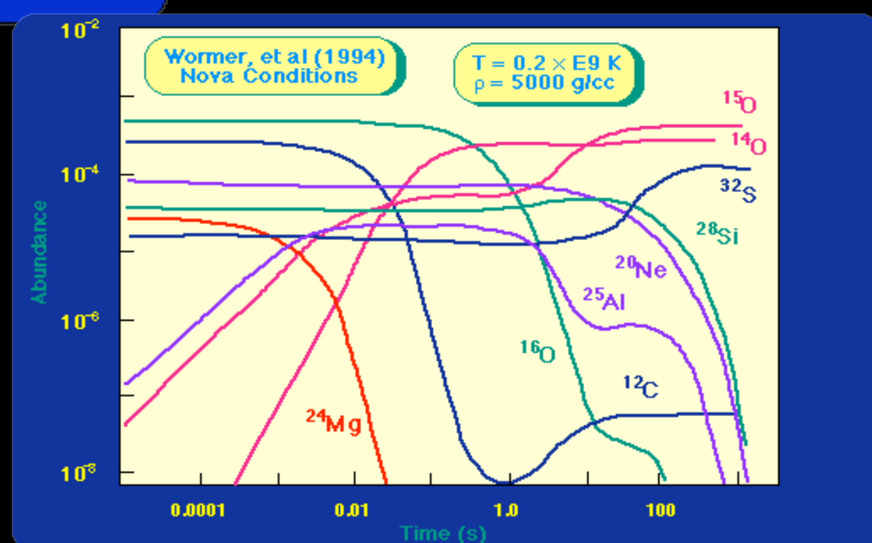

Wormer, et al (1994)
Nova Conditions
T = 0.2 × E9 K
ρ = 5000 g/cc
15O
14O
32S
28Si
20Ne
25Al
16O
12C
24Mg
Abundance
10-2
10-4
10-6
10-8
0.0001
0.01
1.0
100
Time (s)

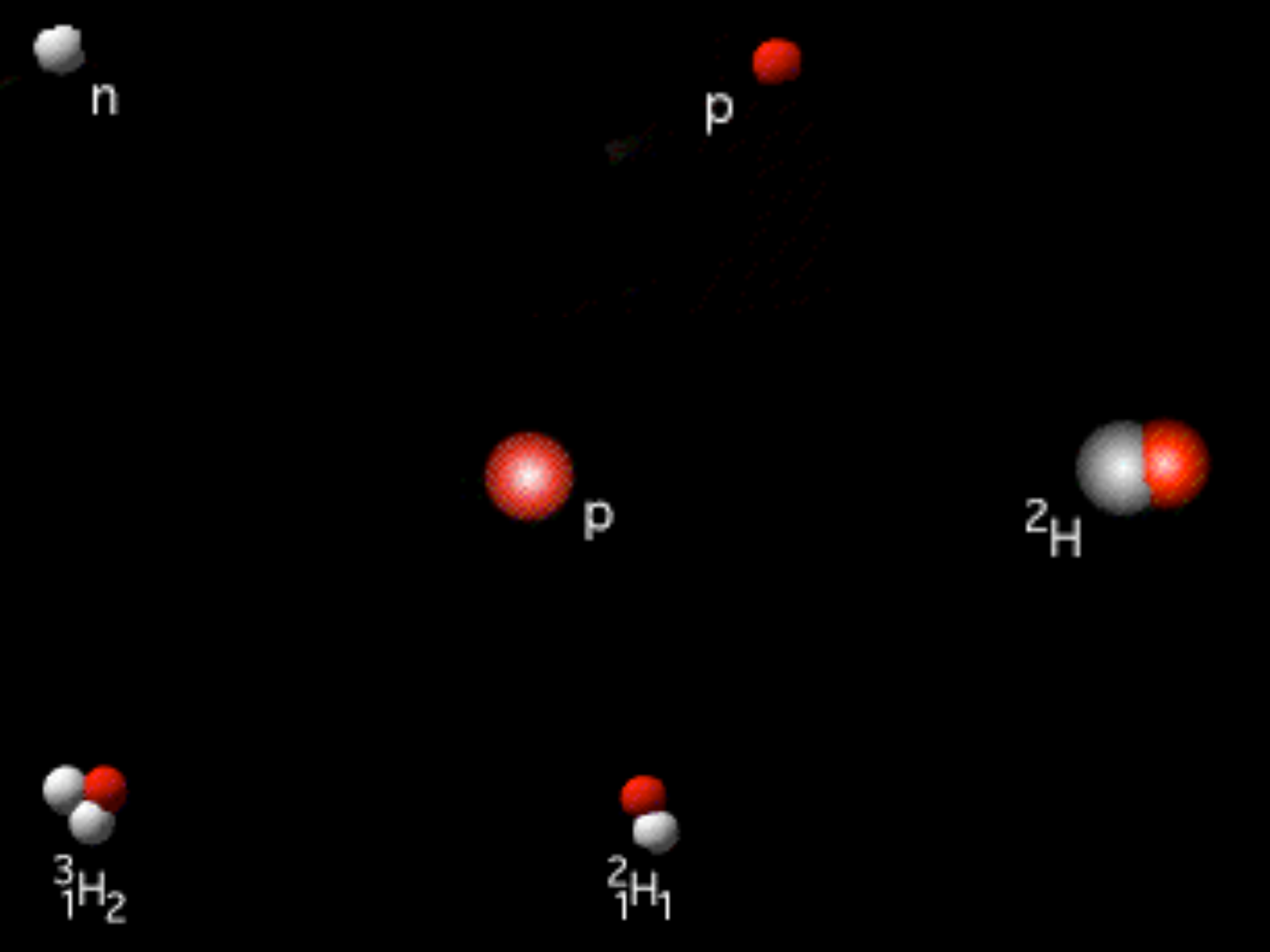
n
p
p
^{2}H
$^{3}_{1}H_{2}$
$^{2}_{1}H_{1}$

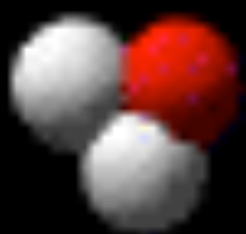

${}^{3}_{1}H_{2}$

${}^{2}_{1}H_{1}$

ESPALHAMENTO

TUNELAMENTO

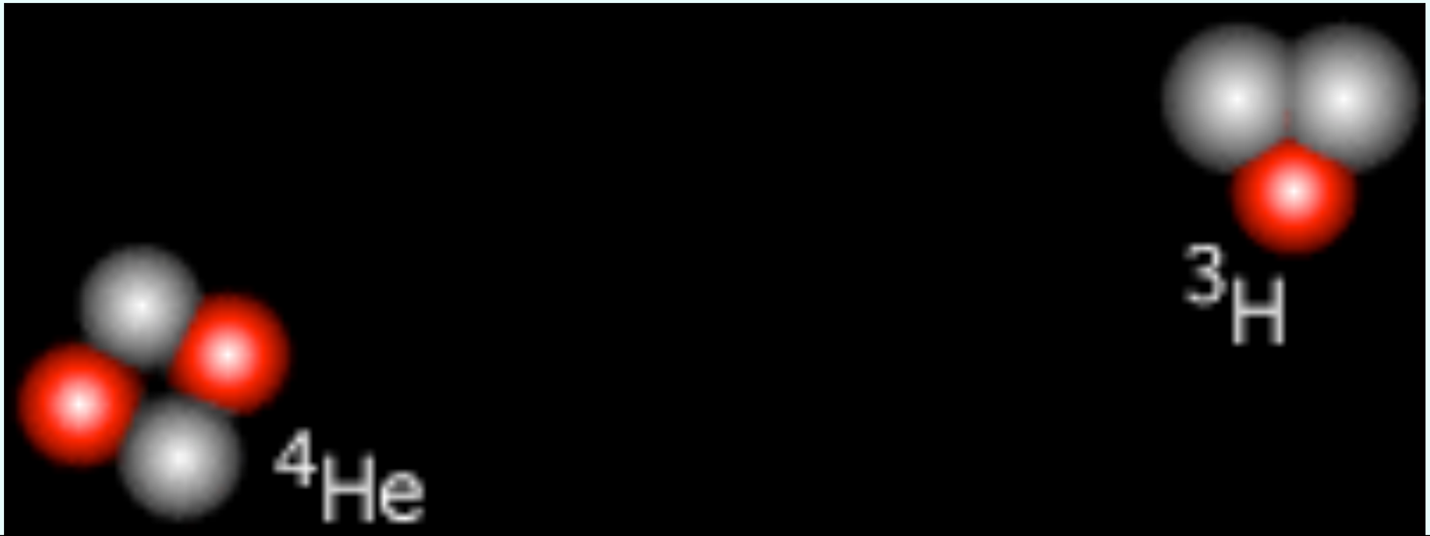

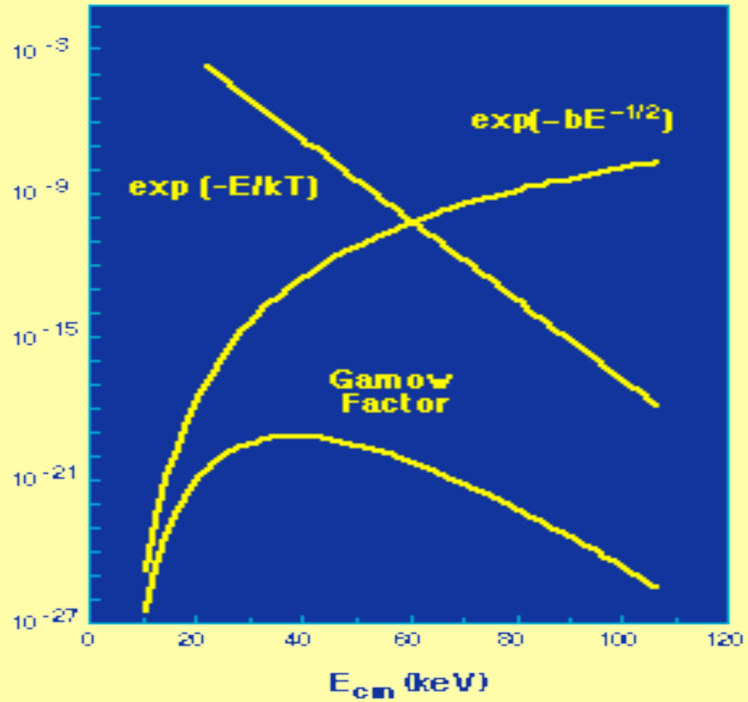

Gamow Factor

For charged-particle reactions there is an optimum energy for reactions that represents a tradeoff between a Coulomb barrier penetration factor that increases exponentially with the square root of energy, and the Boltzmann factor that decreases exponentially with energy. The maximum of the product of these two functions is termed the *Gamow Peak*.

Element Production Networks

Cross Sections:

$$\sigma = \frac{\text{Number of Reactions/Target/Second}}{\text{Incoming Flux}} = \frac{r/n_j}{n_k \upsilon}$$

Reaction Rates:

$$\langle j,k \rangle \equiv \langle \sigma \upsilon \rangle_{j,k} = \left(\frac{8}{\mu \pi} \right)^{1/2} (kT)^{-3/2} \int_0^\infty E \sigma(E) e^{(-E/kT)} dE$$

Differential Equations for Nuclear Abundances Y:

$$\dot{Y} = \sum_j c_j^i Y_j + \sum_{j,k} c_{jk}^i Y_j Y_k + \sum_{j,k,l} c_{jkl}^i Y_j Y_k Y_l$$

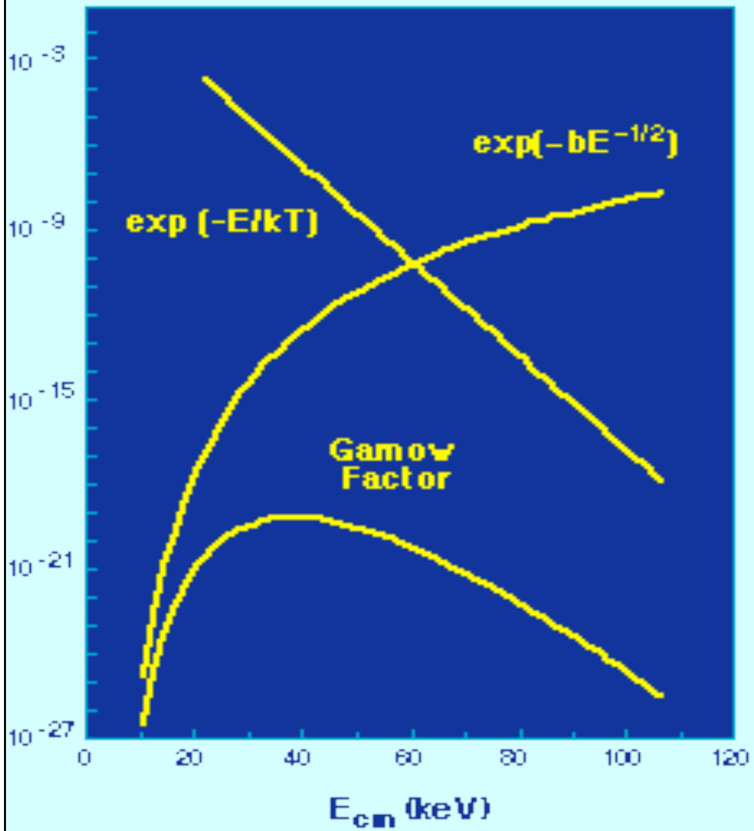
10^{-3}
10^{-9}
10^{-15}
10^{-21}
10^{-27}
exp(-bE^-1/2)
exp (-E/kT)
Gamow Factor
0 20 40 60 80 100 120
E_{cm} (keV)

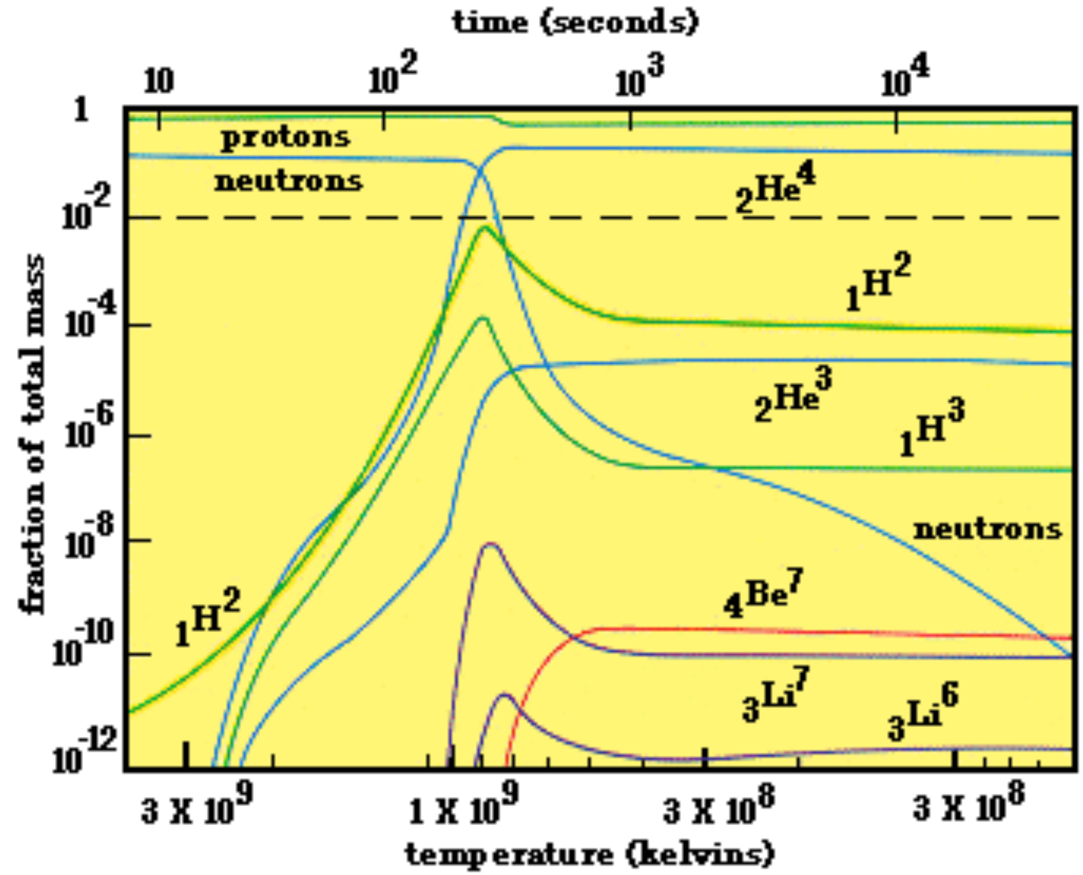
time (seconds)
10 10^2 10^3 10^4
1
10^{-2}
10^{-4}
10^{-6}
10^{-8}
10^{-10}
10^{-12}
protons
neutrons
$_2He^4$
$_1H^2$
$_2He^3$
$_1H^3$
neutrons
$_4Be^7$
$_1H^2$
$_3Li^7$
$_3Li^6$
fraction of total mass
3 X 10^9
1 X 10^9
3 X 10^8
3 X 10^8
temperature (kelvins)

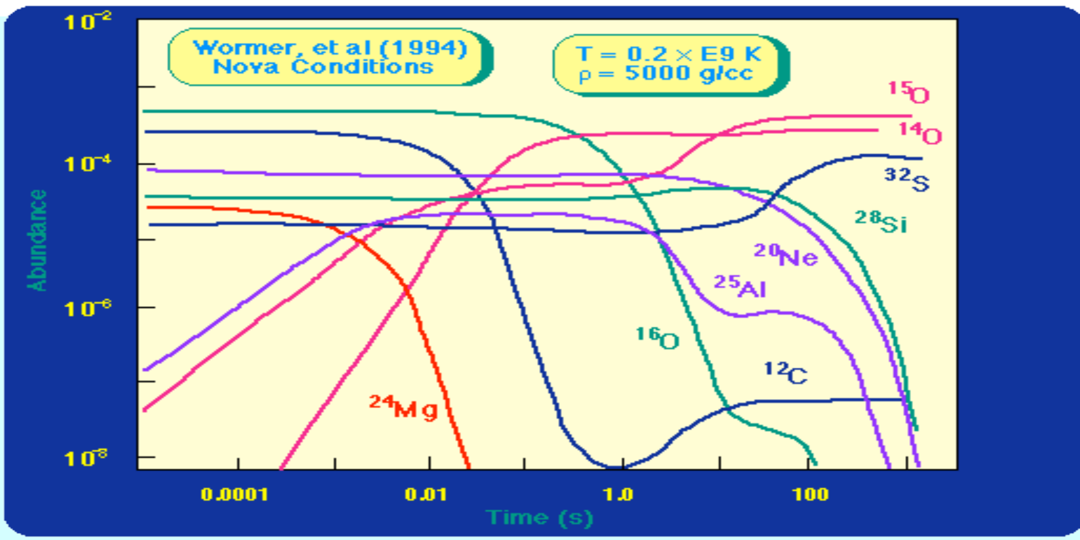
Wormer, et al (1994)
Nova Conditions
T = 0.2 × E9 K
ρ = 5000 g/cc
10^{-2}
10^{-4}
10^{-6}
10^{-8}
Abundance
^{15}O
^{14}O
^{32}S
^{28}Si
^{20}Ne
^{25}Al
^{16}O
^{12}C
^{24}Mg
0.0001
0.01
1.0
100
Time (s)

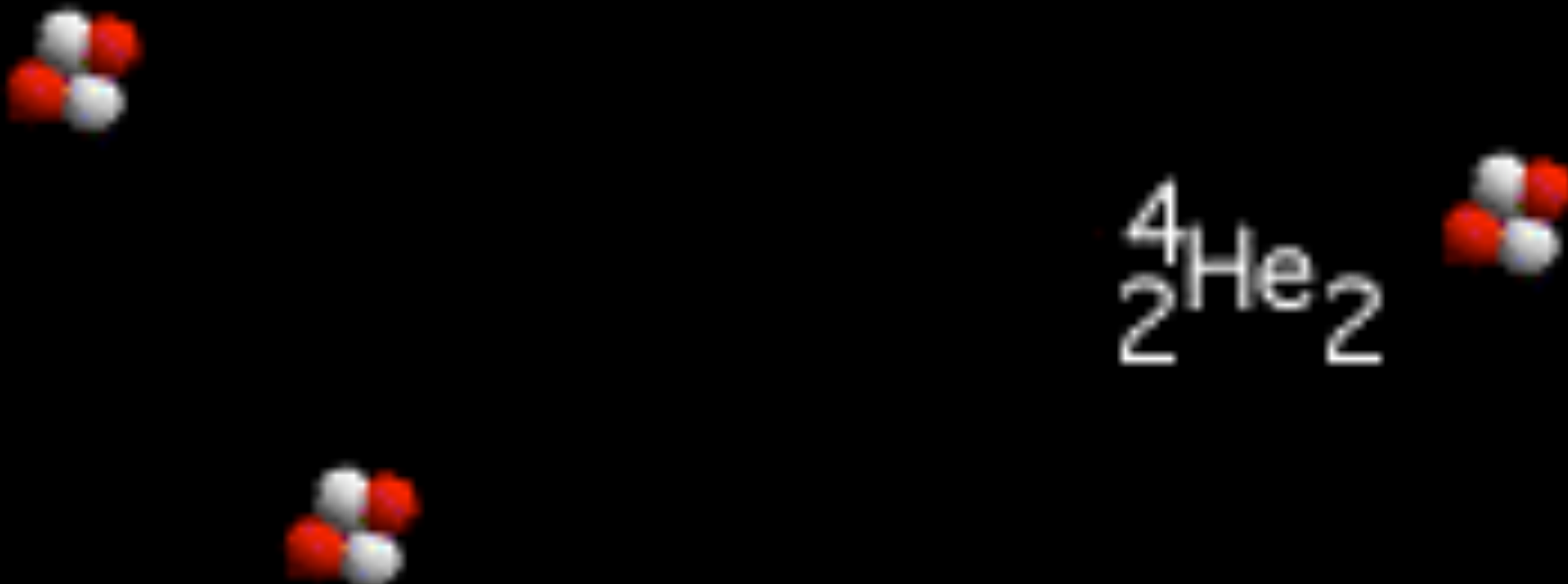
${}^{4}_{2}He_{2}$

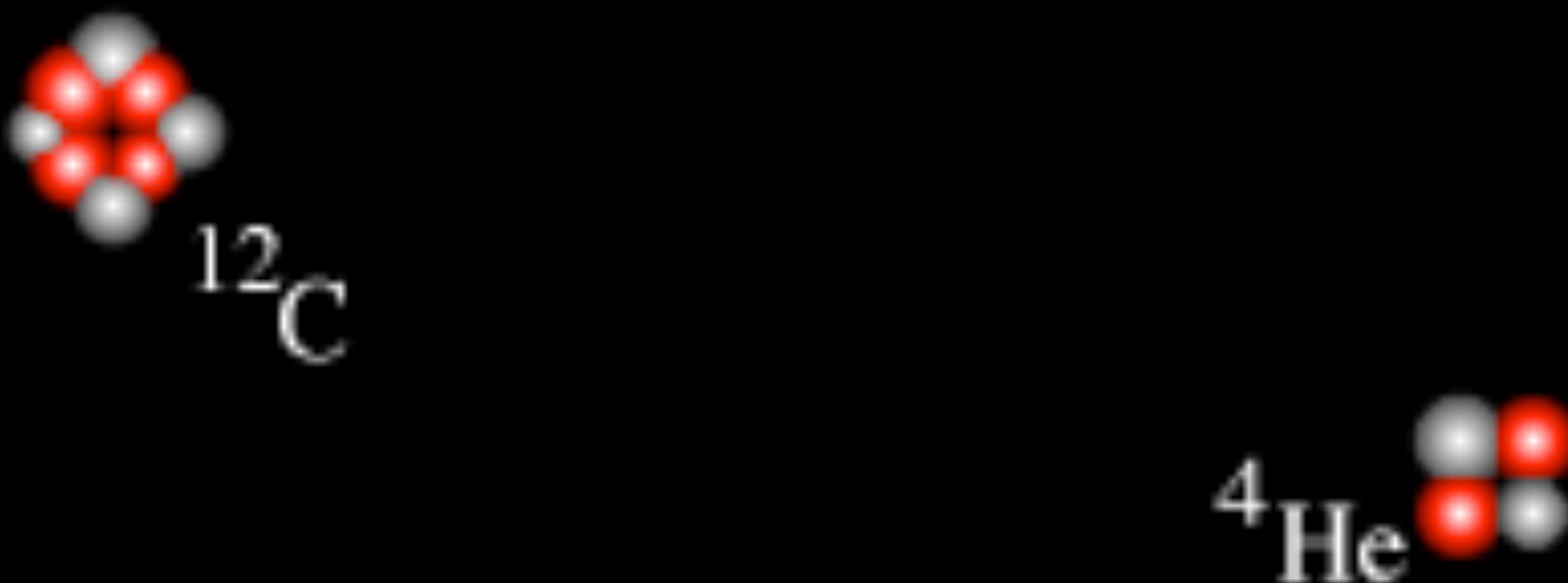

^{12}C
^{4}He

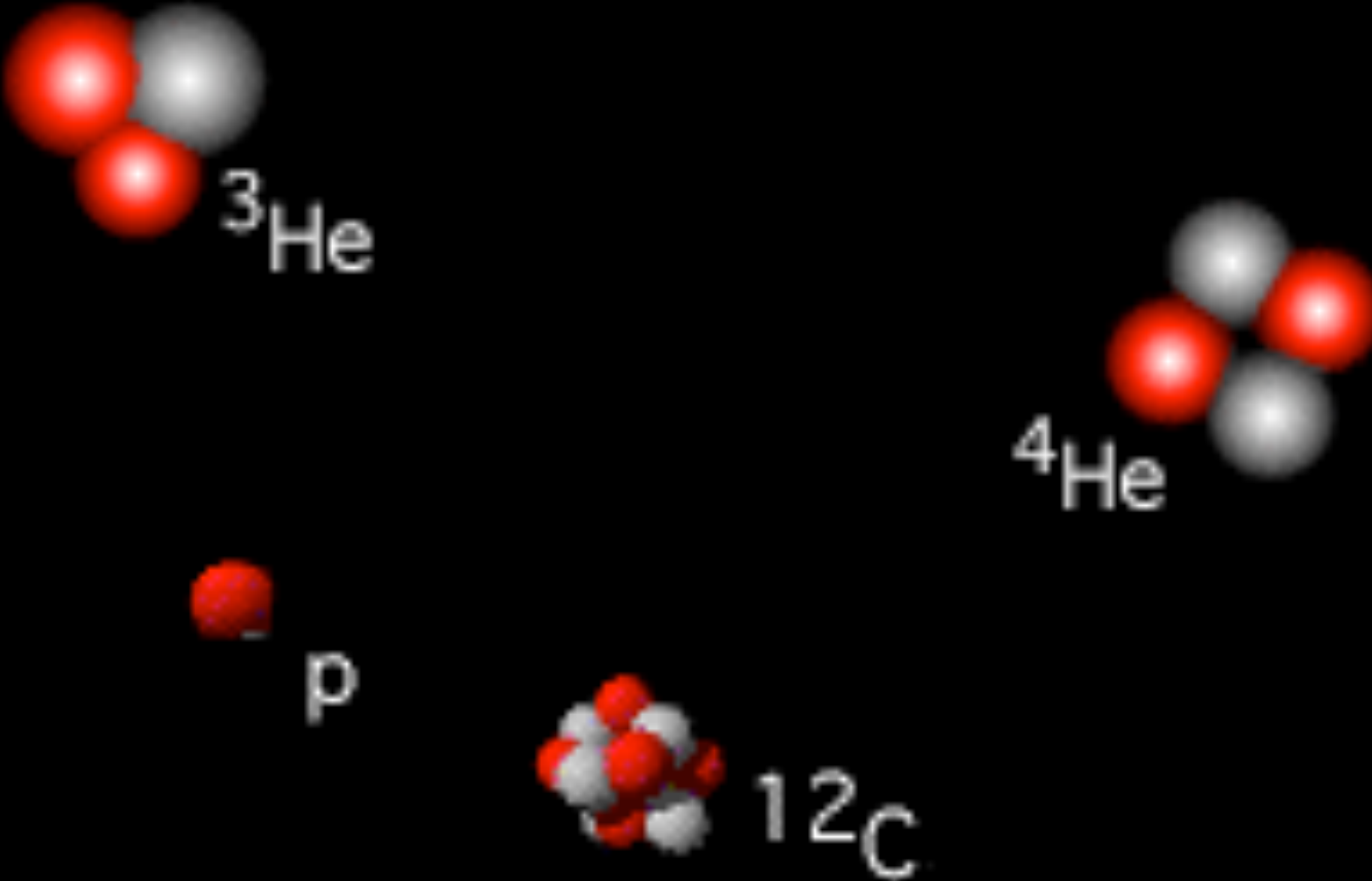

³He
⁴He
p
¹²C


n
235U
92
143

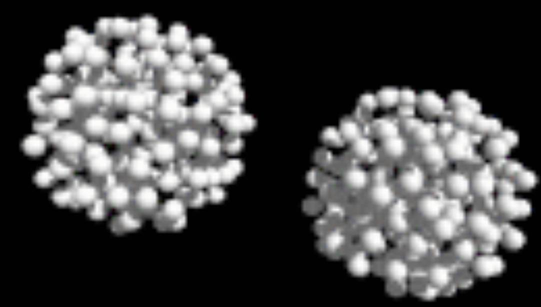

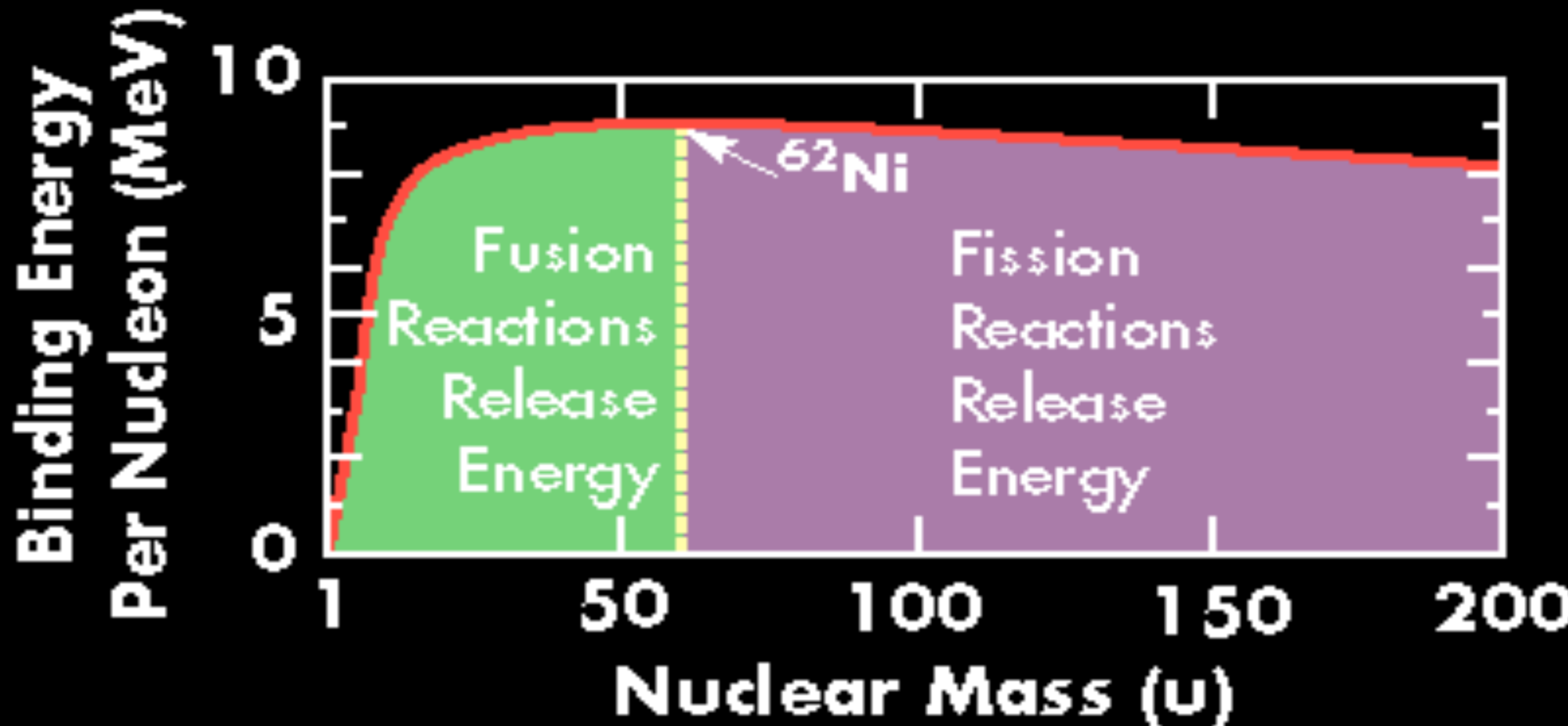
Binding Energy
Per Nucleon (MeV)
10
5
0
^{62}Ni
Fusion
Reactions
Release
Energy
Fission
Reactions
Release
Energy
1
50
100
150
200
Nuclear Mass (u)

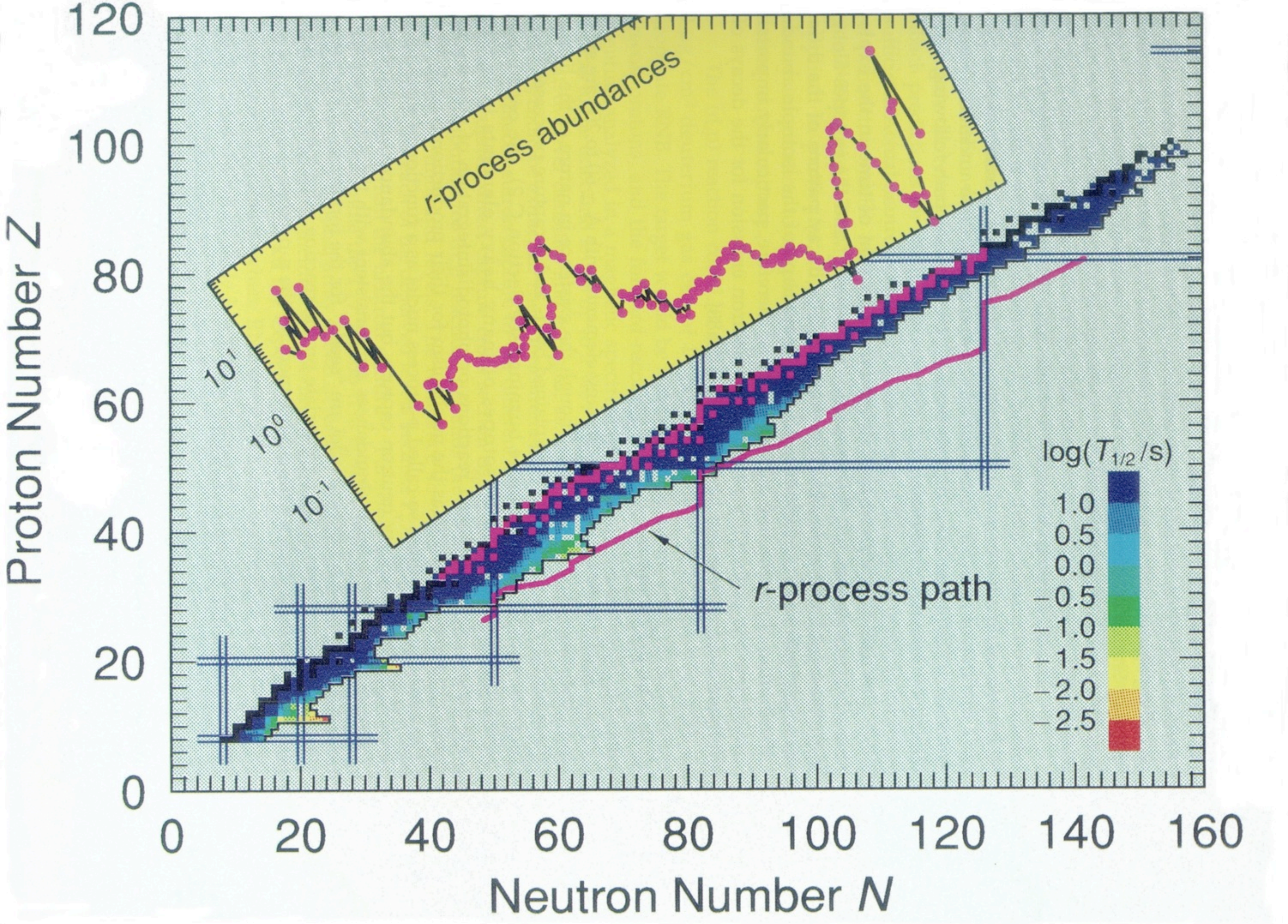

r-process abundances
r-process path
log($T_{1/2}$/s)
1.0
0.5
0.0
−0.5
−1.0
−1.5
−2.0
−2.5
10^1
10^0
10^{-1}
Proton Number Z
Neutron Number N
0
20
40
60
80
100
120
140
160

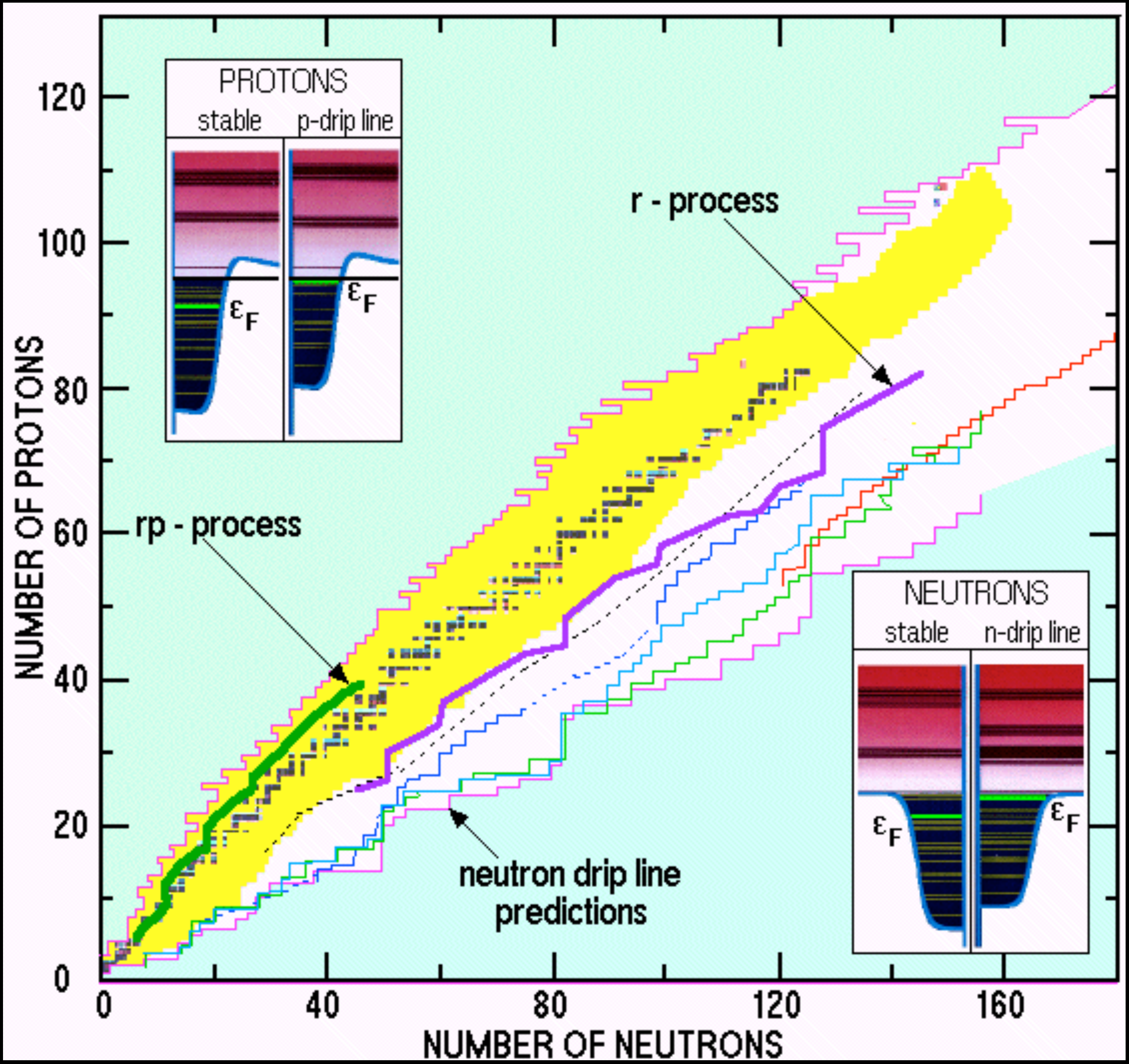

PROTONS
stable
p-drip line
ε_F
ε_F
r - process
rp - process
neutron drip line predictions
NEUTRONS
stable
n-drip line
ε_F
ε_F
NUMBER OF PROTONS
NUMBER OF NEUTRONS
0
20
40
60
80
100
120
0
40
80
120
160

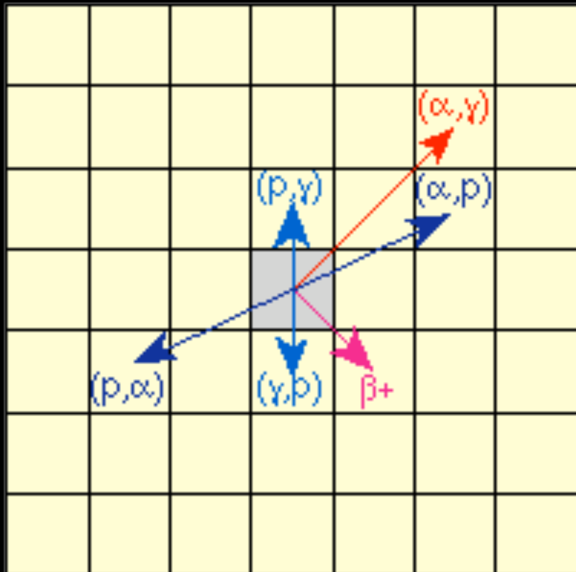

Carbon-Nitrogen-Oxygen Cycle

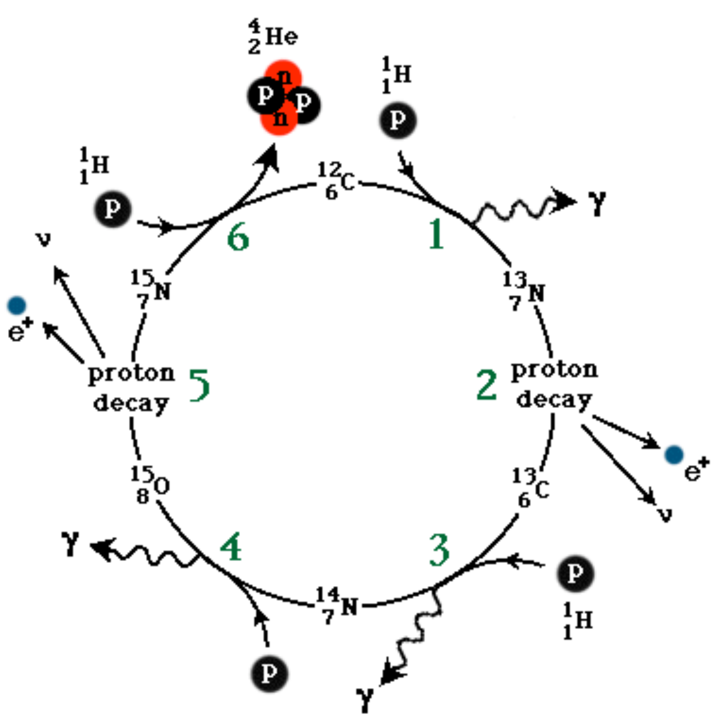

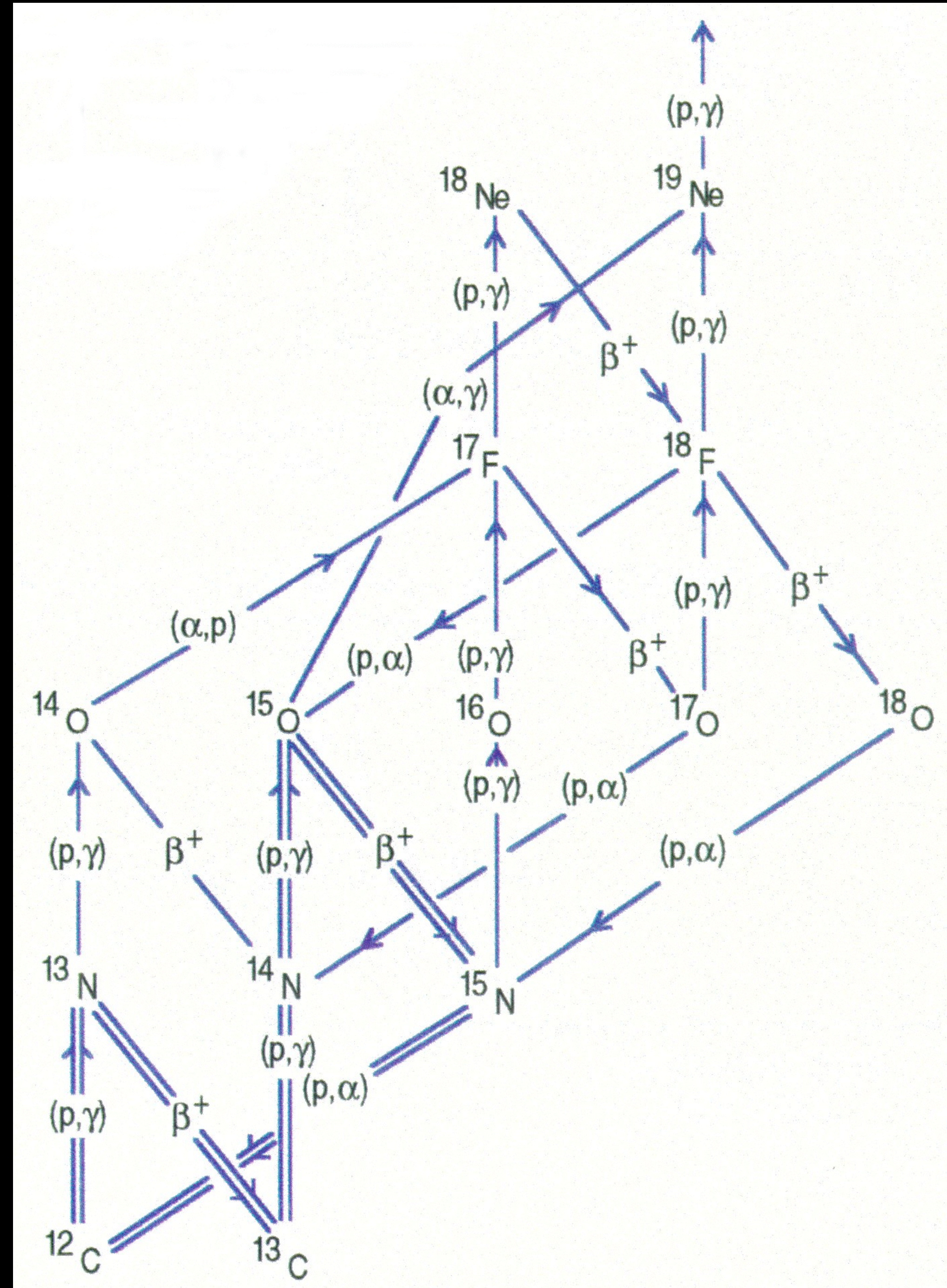

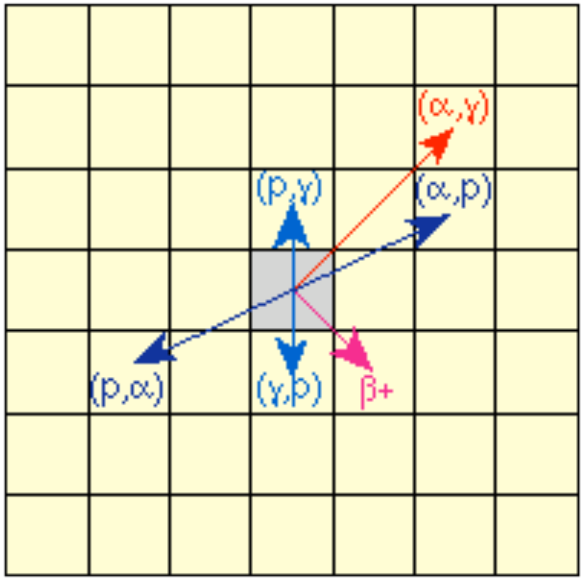

Reaction Vectors

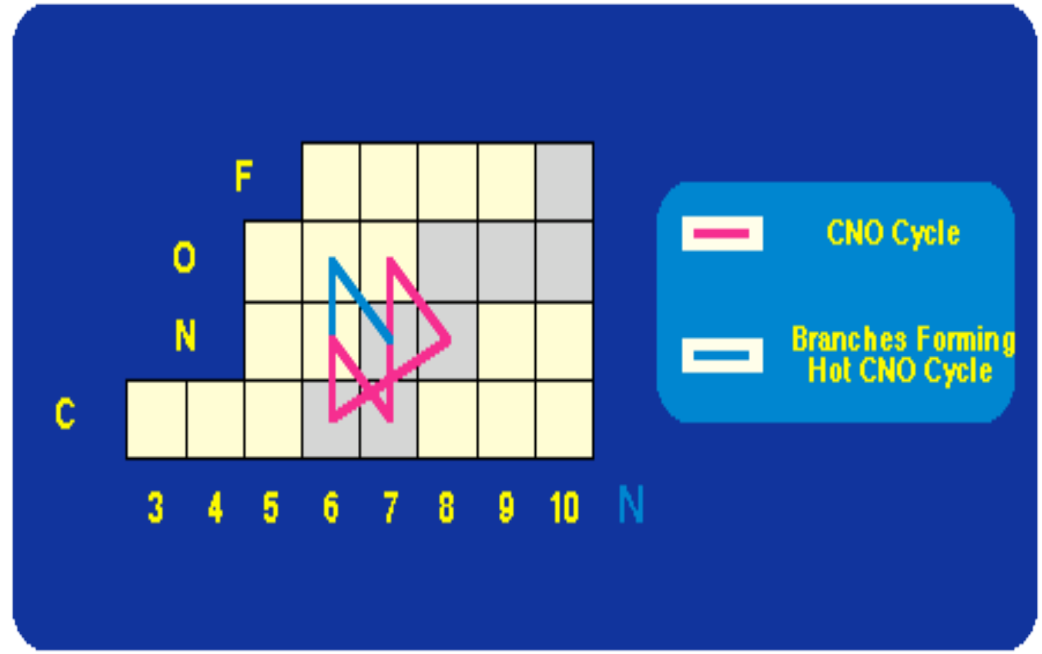

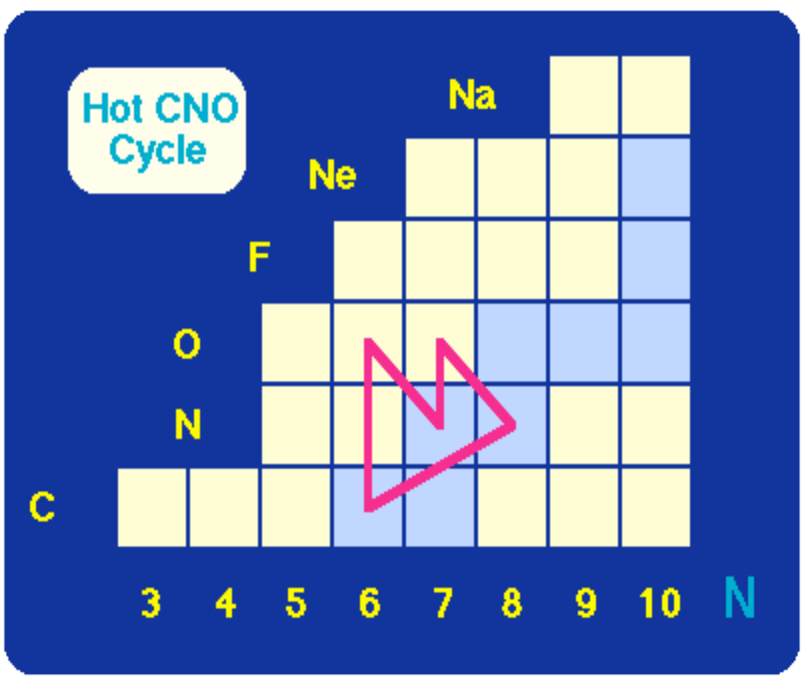

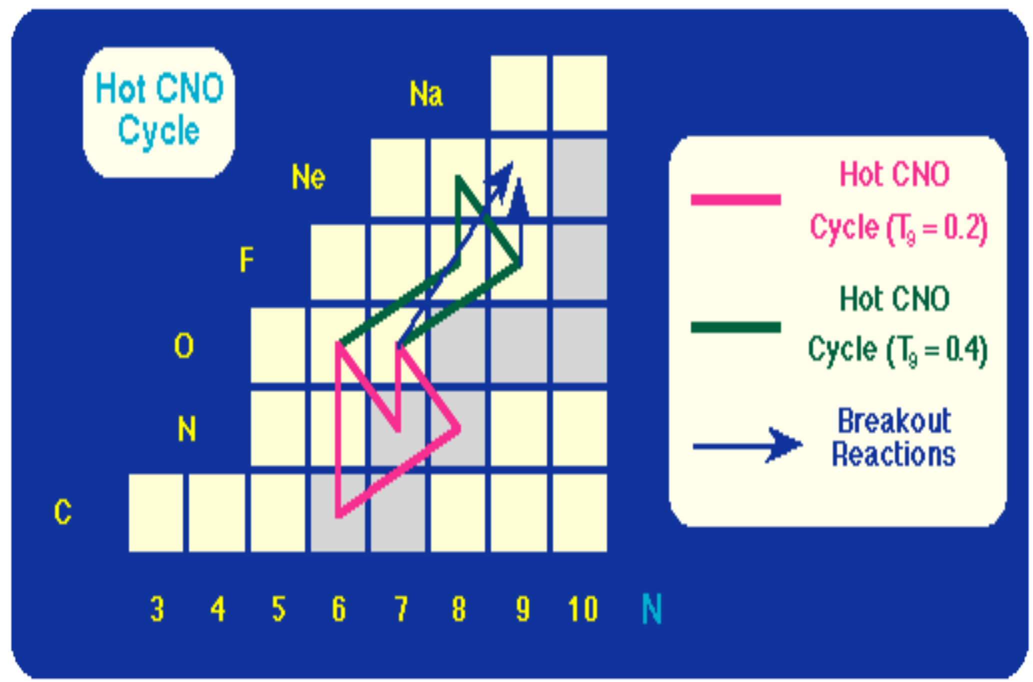

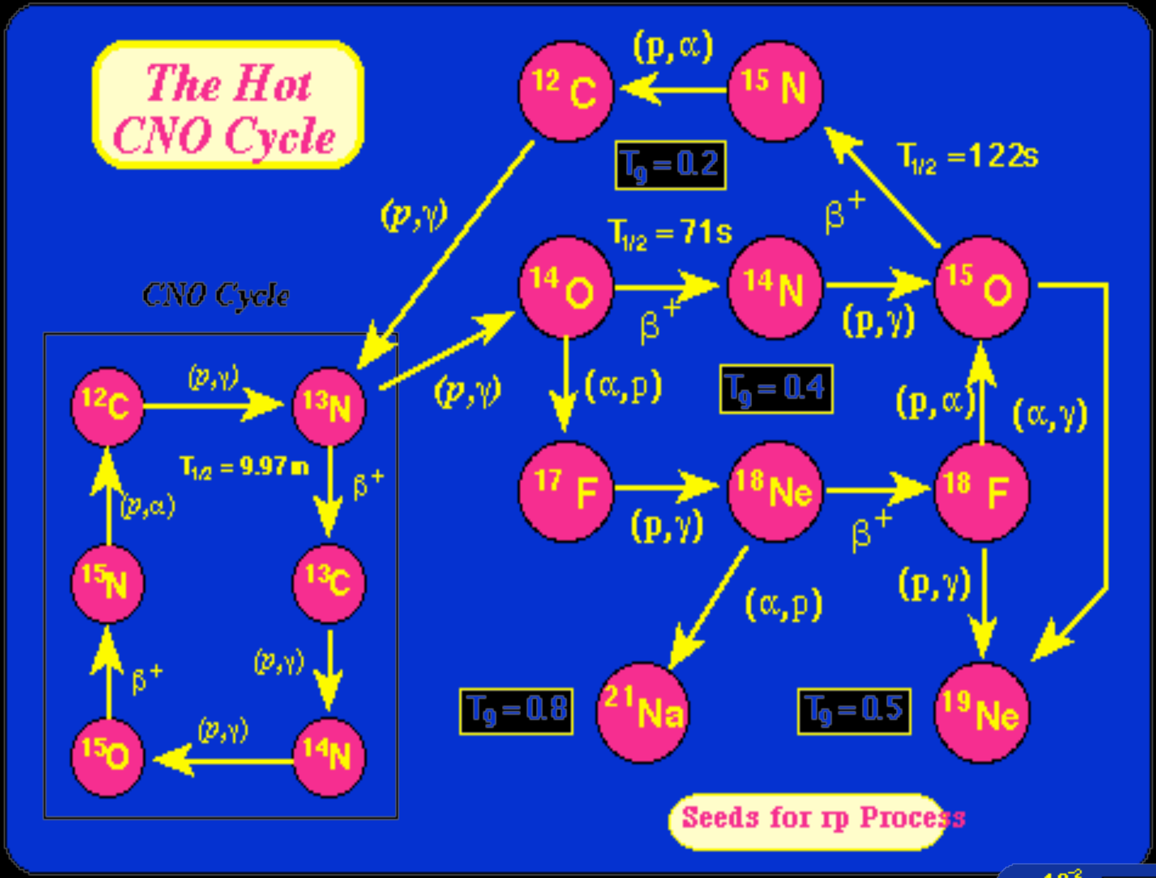
The Hot CNO Cycle
CNO Cycle
12C
13N
13C
14N
15O
15N
(p,γ)
β+
(p,α)
T1/2 = 9.97 m
12 C
15 N
(p,α)
T9 = 0.2
T1/2 = 122s
14 O
14 N
15 O
T1/2 = 71s
T9 = 0.4
(α,p)
(α,γ)
17 F
18 Ne
18 F
T9 = 0.8
21 Na
T9 = 0.5
19 Ne
Seeds for rp Process

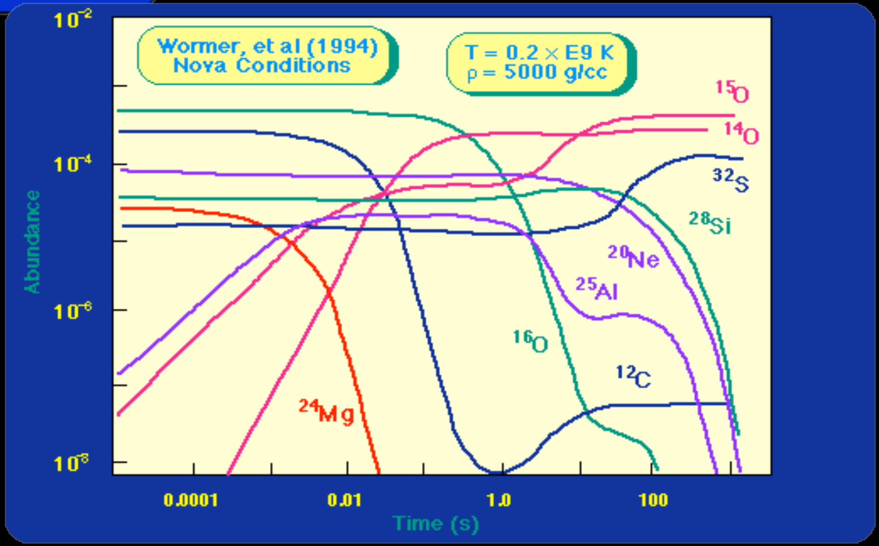
Wormer, et al (1994)
Nova Conditions
T = 0.2 × E9 K
ρ = 5000 g/cc
Abundance
Time (s)
15O
14O
32S
28Si
20Ne
25Al
16O
12C
24Mg

ESTRUTURA NUCLEAR

MECANISMO DE REAÇÕES

DINÂMICA DE REAÇÕES

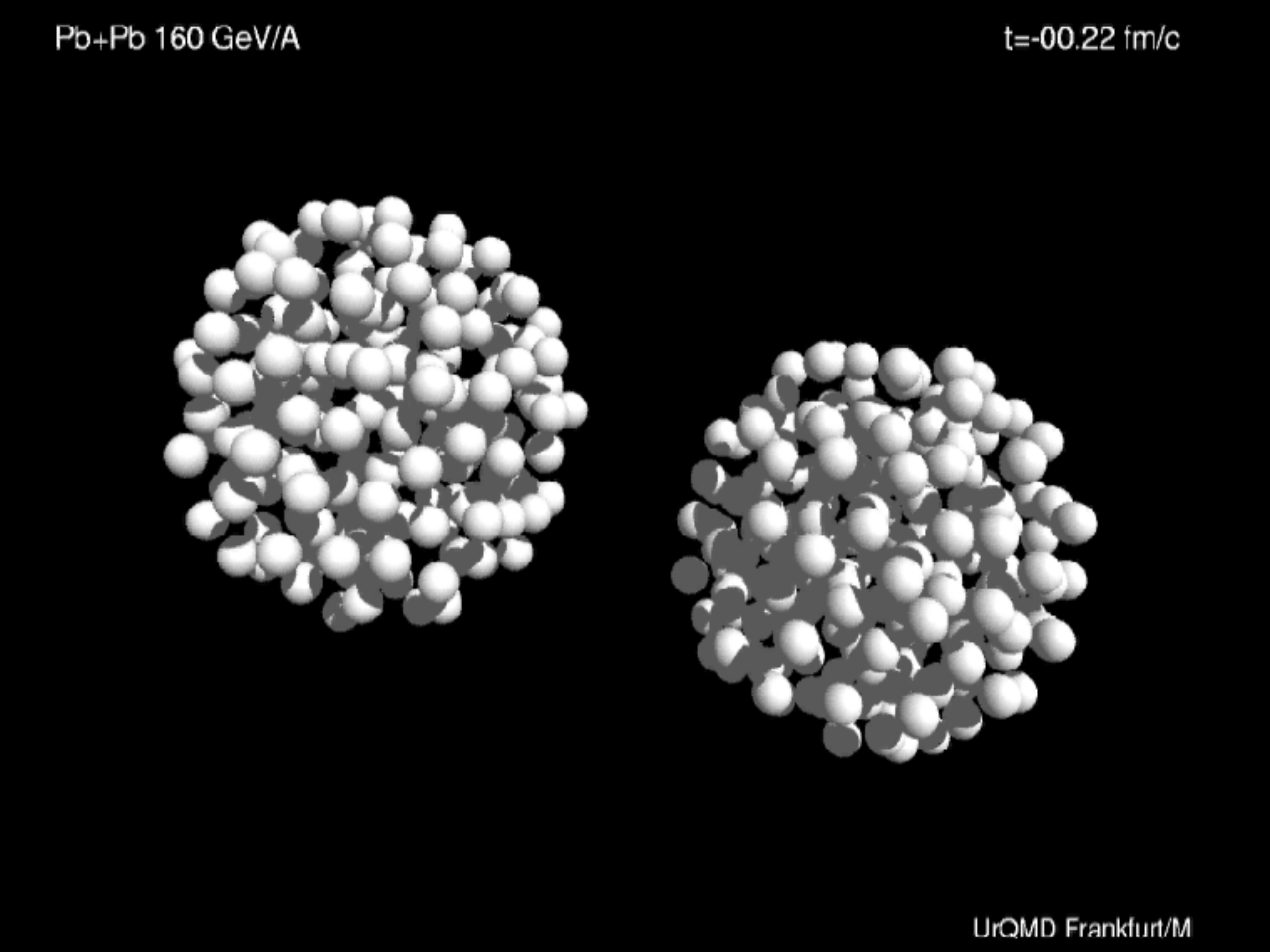
Pb+Pb 160 GeV/A
t=-00.22 fm/c
UrQMD Frankfurt/M

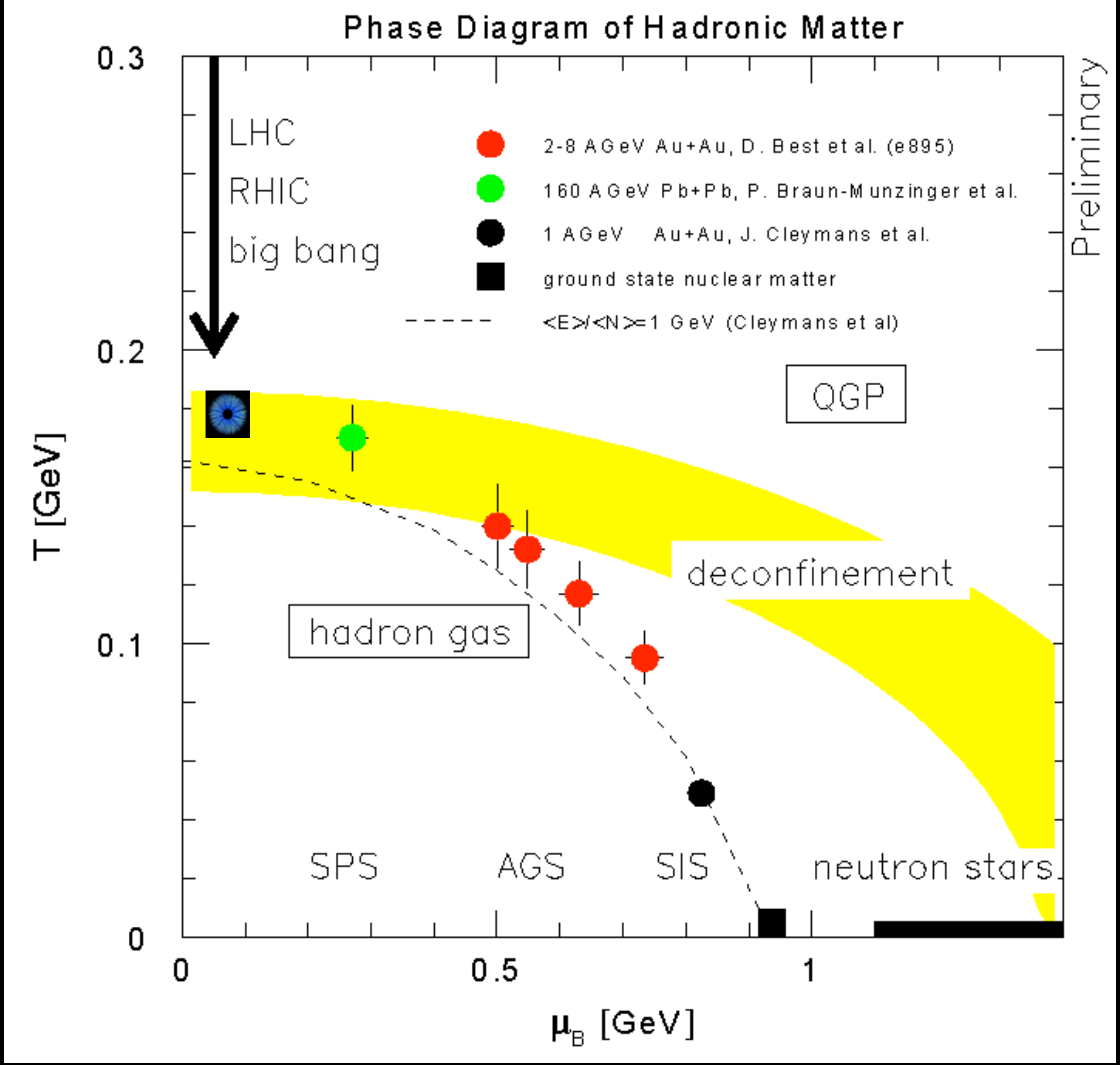
Phase Diagram of Hadronic Matter
0.3
0.2
0.1
0
T [GeV]
0
0.5
1
μ_B [GeV]
LHC
RHIC
big bang
2-8 AGeV Au+Au, D. Best et al. (e895)
160 AGeV Pb+Pb, P. Braun-Munzinger et al.
1 AGeV Au+Au, J. Cleymans et al.
ground state nuclear matter
<E>/<N>=1 GeV (Cleymans et al)
Preliminary
QGP
deconfinement
hadron gas
SPS
AGS
SIS
neutron stars

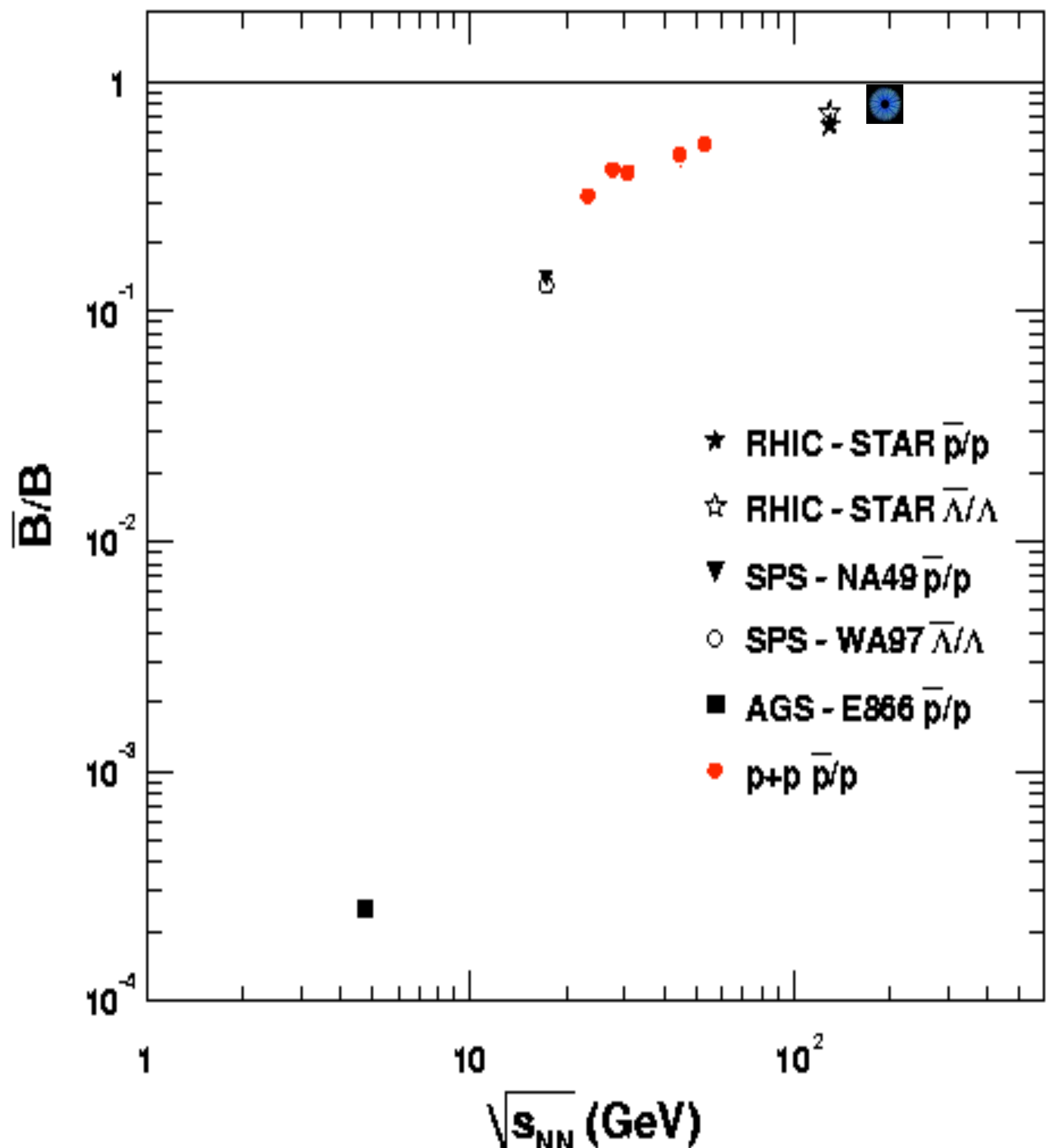

$\overline{B}/B$
1
10^{-1}
10^{-2}
10^{-3}
10^{-4}
1
10
10^{2}
$\sqrt{s_{NN}}$ (GeV)
RHIC - STAR $\overline{p}/p$
RHIC - STAR $\overline{\Lambda}/\Lambda$
SPS - NA49 $\overline{p}/p$
SPS - WA97 $\overline{\Lambda}/\Lambda$
AGS - E866 $\overline{p}/p$
p+p $\overline{p}/p$

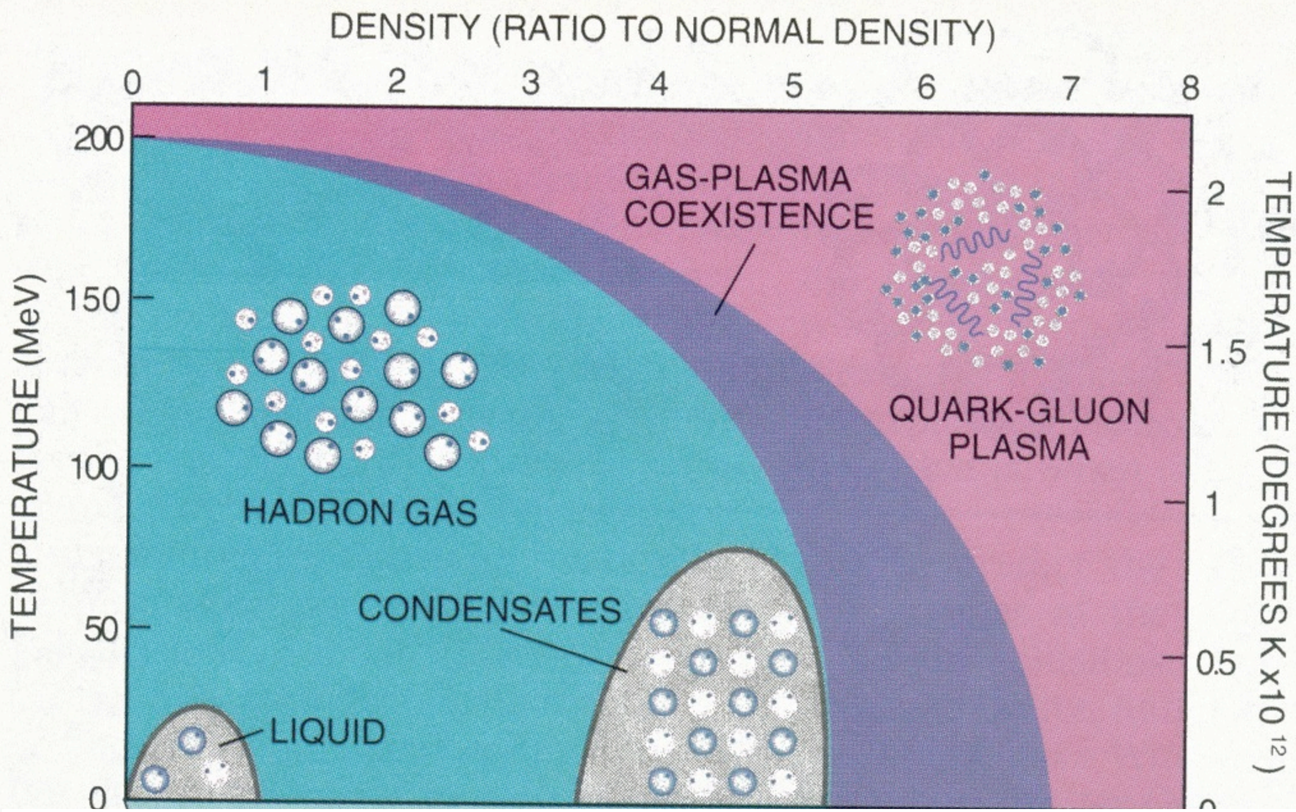

DENSITY (RATIO TO NORMAL DENSITY)
0
1
2
3
4
5
6
7
8
200
150
100
50
0
TEMPERATURE (MeV)
2
1.5
1
0.5
0
TEMPERATURE (DEGREES K x10 12)
GAS-PLASMA
COEXISTENCE
QUARK-GLUON
PLASMA
HADRON GAS
CONDENSATES
LIQUID

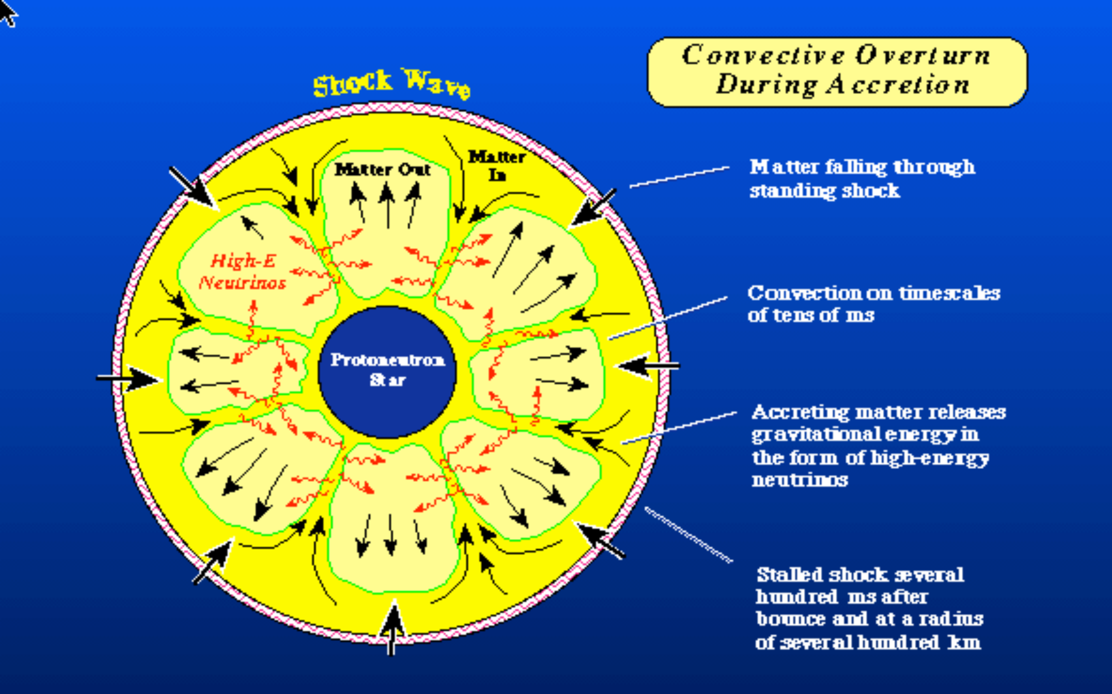
Convective Overturn
During Accretion
Shock Wave
Matter Out
Matter In
High-E Neutrinos
Protoneutron Star
Matter falling through standing shock
Convection on timescales of tens of ms
Accreting matter releases gravitational energy in the form of high-energy neutrinos
Stalled shock several hundred ms after bounce and at a radius of several hundred km

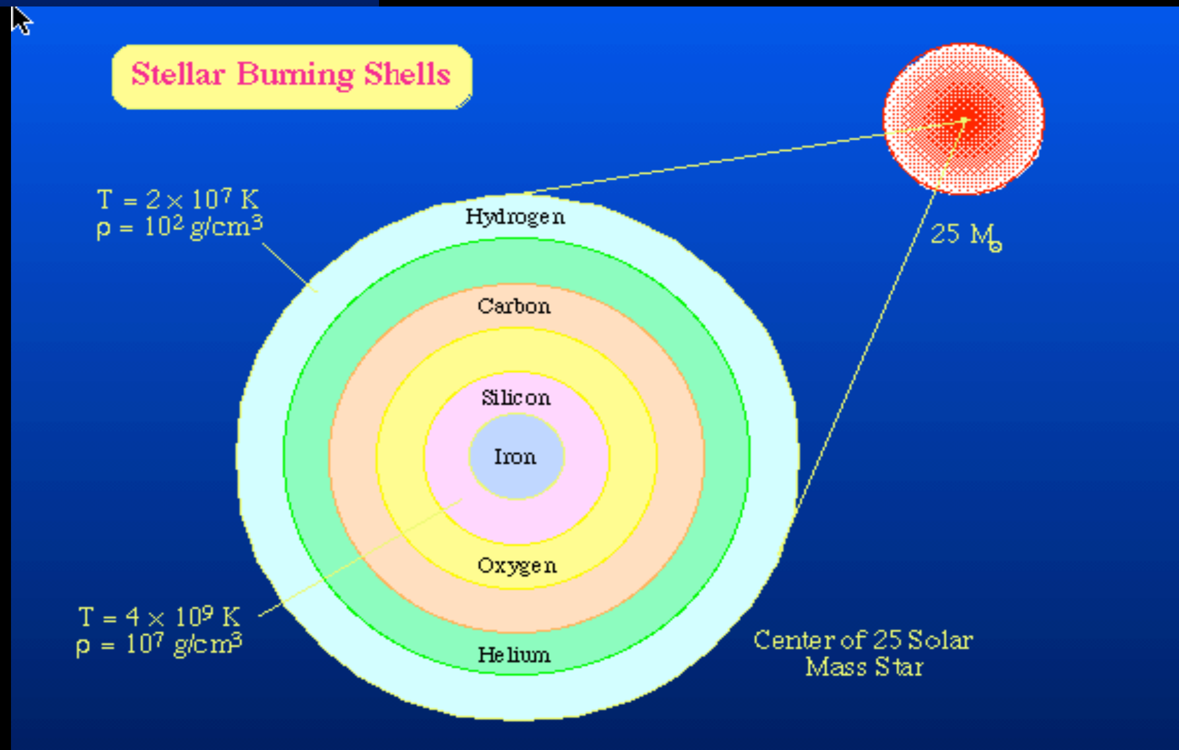
Stellar Burning Shells
T = 2 × 10^7 K
ρ = 10^2 g/cm^3
Hydrogen
Carbon
Silicon
Iron
Oxygen
Helium
T = 4 × 10^9 K
ρ = 10^7 g/cm^3
25 M☉
Center of 25 Solar Mass Star

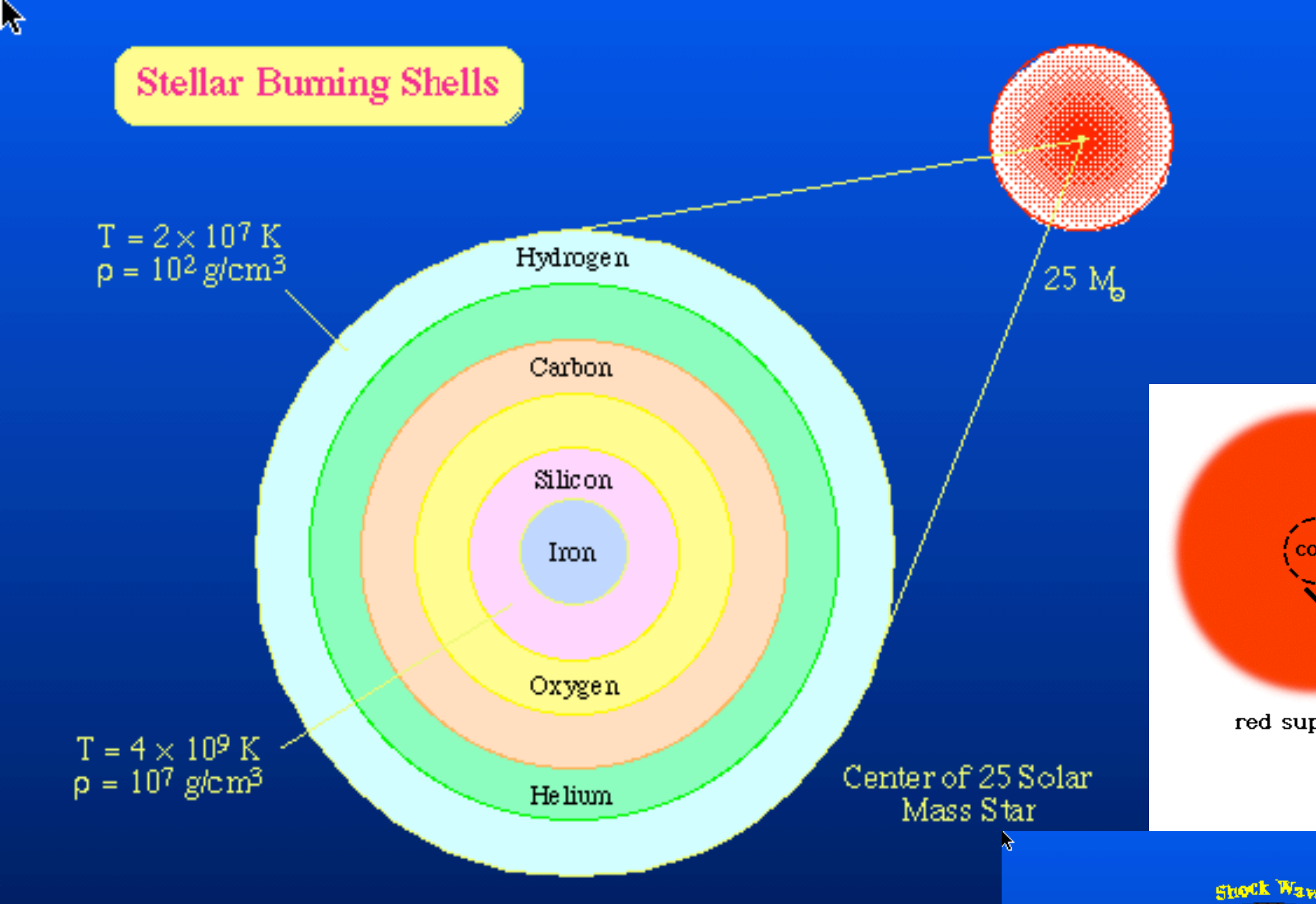

Stellar Burning Shells
T = 2 × 10^7 K
ρ = 10^2 g/cm^3
Hydrogen
Carbon
Silicon
Iron
Oxygen
Helium
T = 4 × 10^9 K
ρ = 10^7 g/cm^3
25 M☉
Center of 25 Solar Mass Star

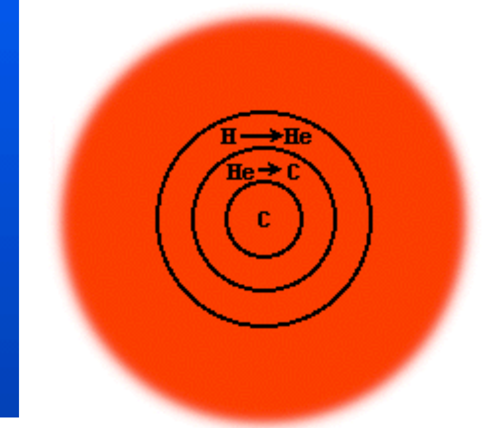

H → He
He → C
C

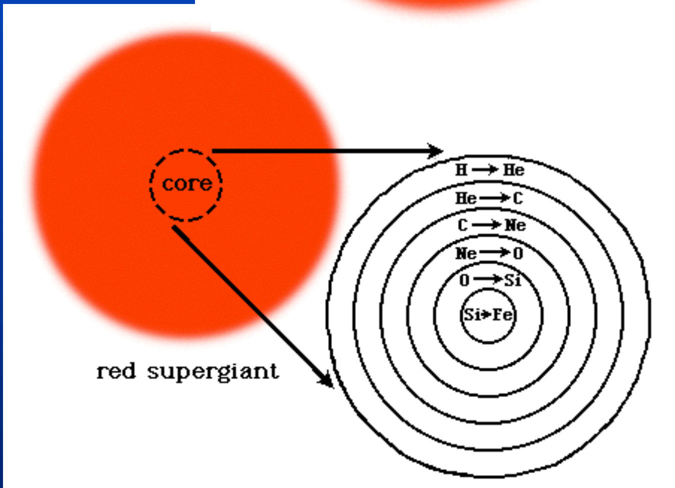

core
red supergiant
H → He
He → C
C → Ne
Ne → O
O → Si
Si → Fe

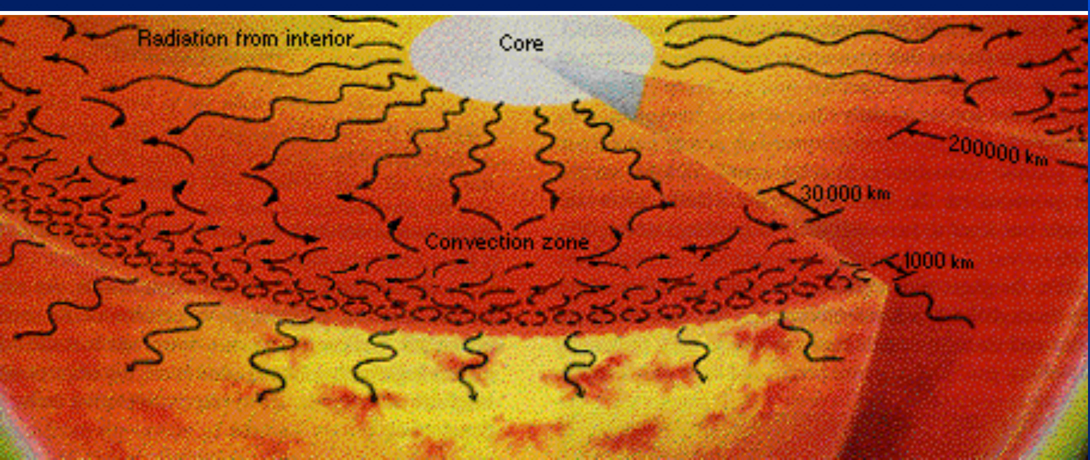

Radiation from interior
Core
200000 km
30,000 km
Convection zone
1000 km

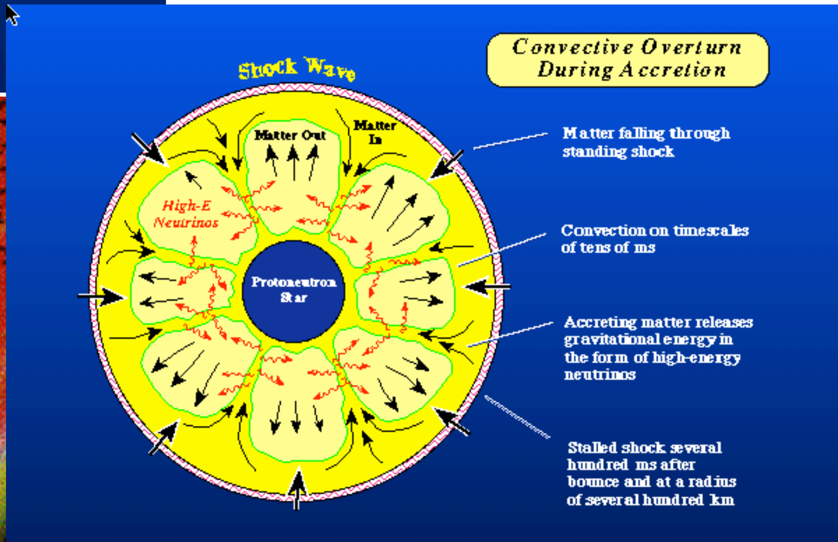

Shock Wave
Convective Overturn During Accretion
Matter Out
Matter In
High-E Neutrinos
Protoneutron Star
Matter falling through standing shock
Convection on timescales of tens of ms
Accreting matter releases gravitational energy in the form of high-energy neutrinos
Stalled shock several hundred ms after bounce and at a radius of several hundred km

RX J1856.5-3754 and 3C58: Cosmic X-rays May Reveal New Form of Matter

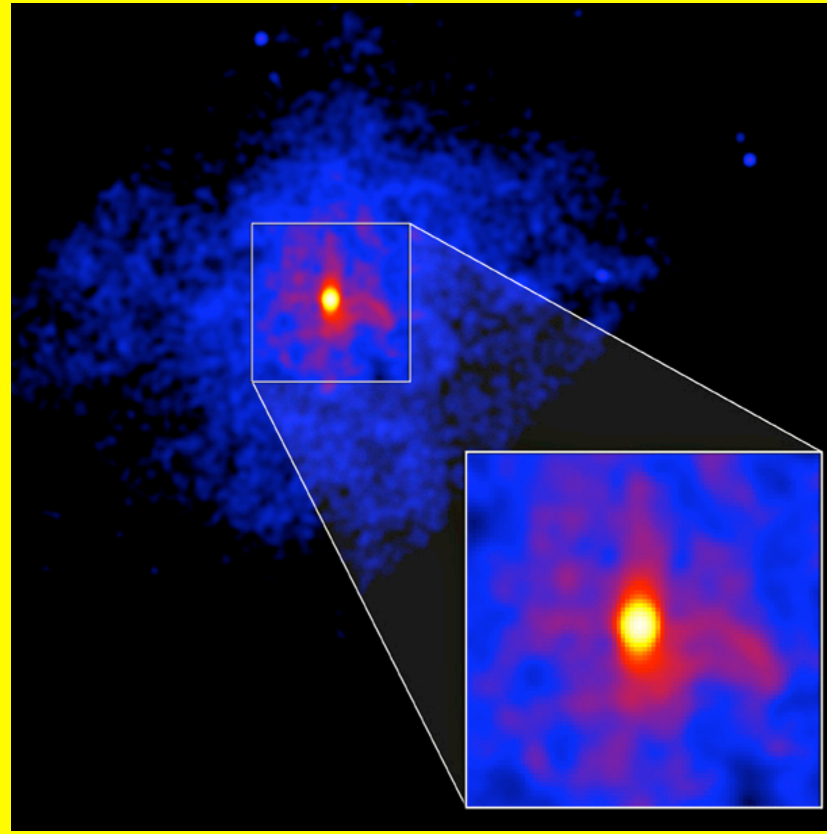

Chandra observations of RX J1856.5-3754 and the pulsar in 3C58 suggest that the matter in these collapsed stars is even denser than nuclear matter, the most dense matter found on Earth. This raises the possibility that these stars are composed of free quarks or crystals of sub-nuclear particles, rather than neutrons. .... One exciting possibility, predicted by some theories, is that the neutrons in the star have dissolved at very high density into a soup of "up," "down" and "strange"quarks to form a "strange quark star" which would explain the smaller radius.

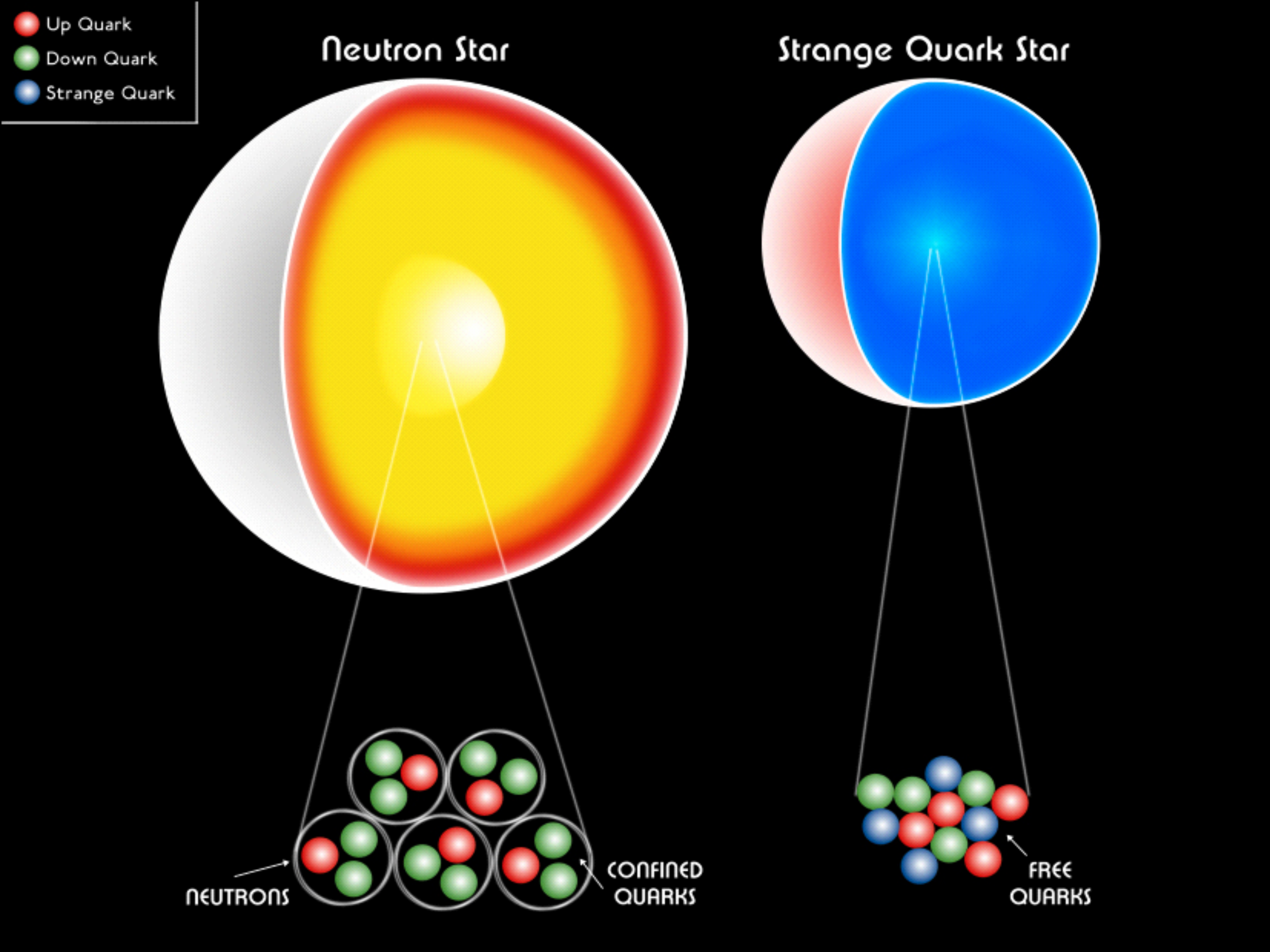
Up Quark
Down Quark
Strange Quark
Neutron Star
Strange Quark Star
NEUTRONS
CONFINED QUARKS
FREE QUARKS

Unlocking the Mysteries of the Universe with state–of–the–art Telescopes

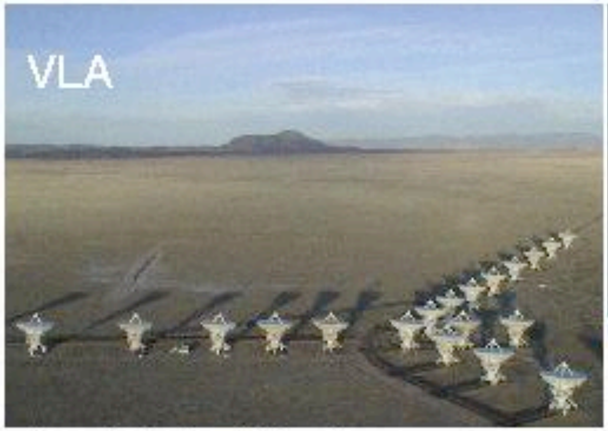

Search for 'exotic' pulsars

First lone NS,
RXJ 185635–3754

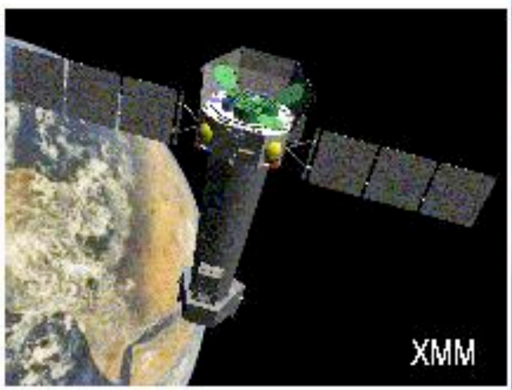

First accreting ms pulsar, J1808–369

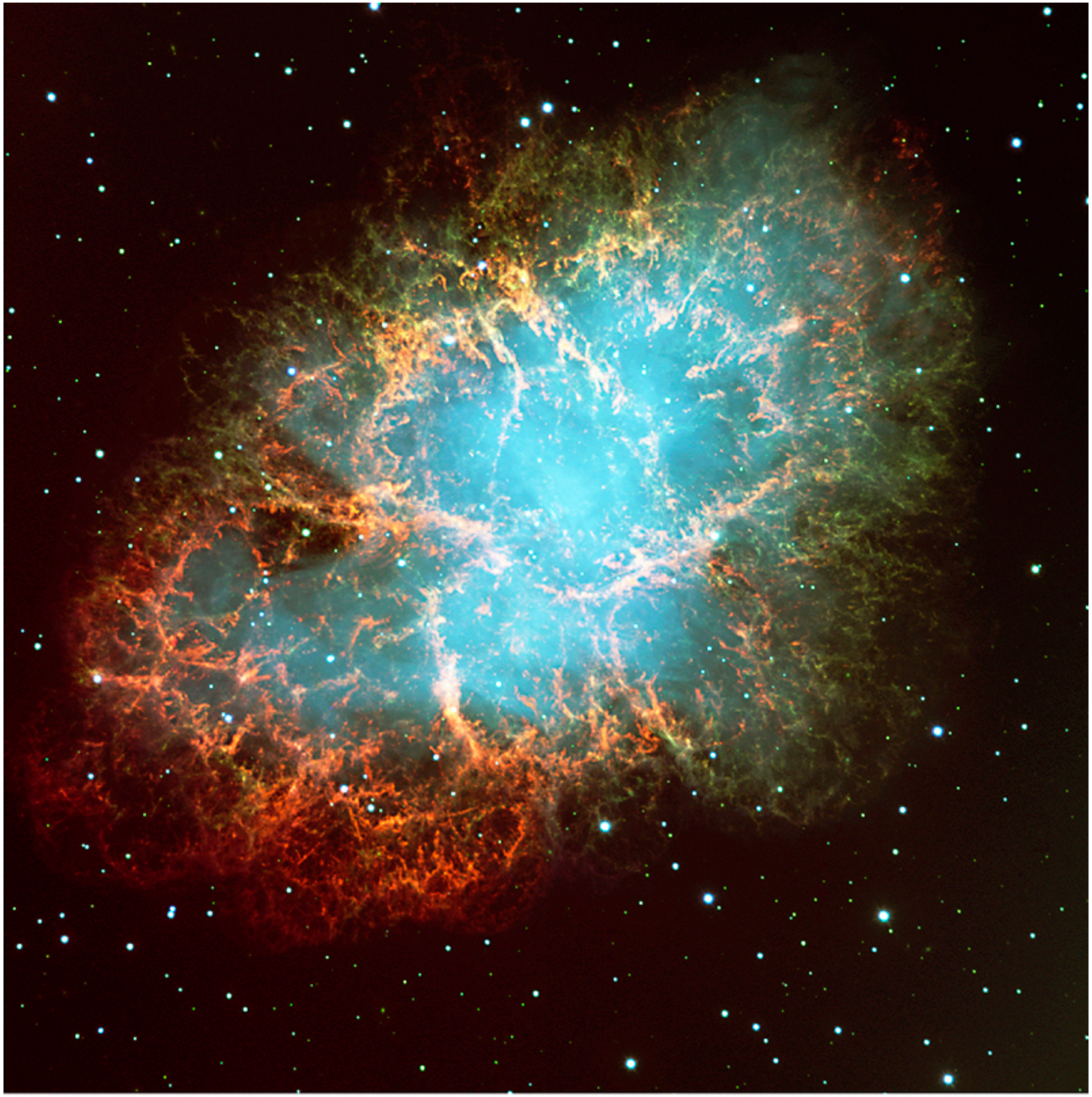

The Crab Nebula in Taurus (VLT KUEYEN + FORS2)

ESO PR Photo 40f/99 (17 November 1999)

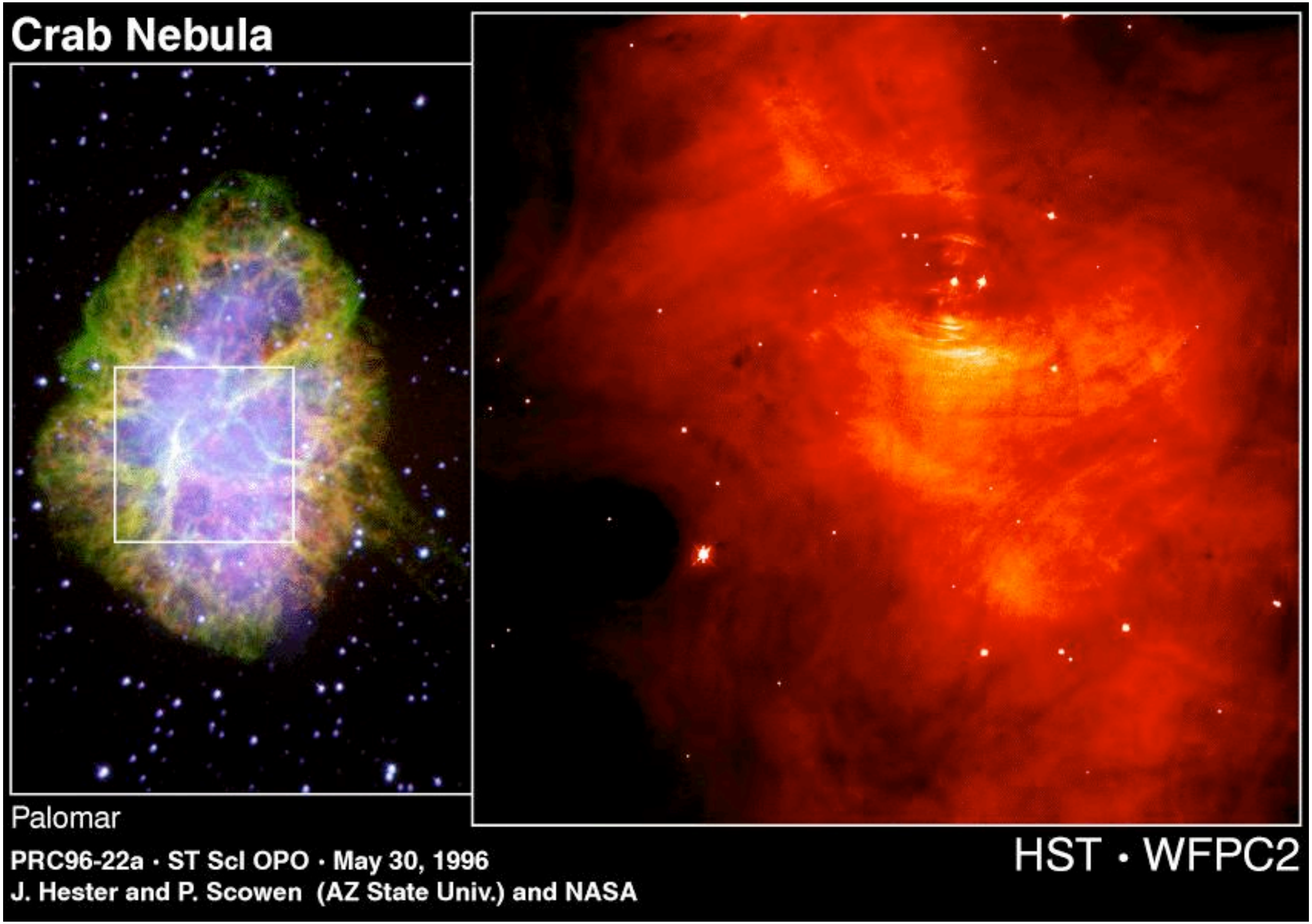
Crab Nebula
Palomar
HST • WFPC2
PRC96-22a • ST ScI OPO • May 30, 1996
J. Hester and P. Scowen (AZ State Univ.) and NASA

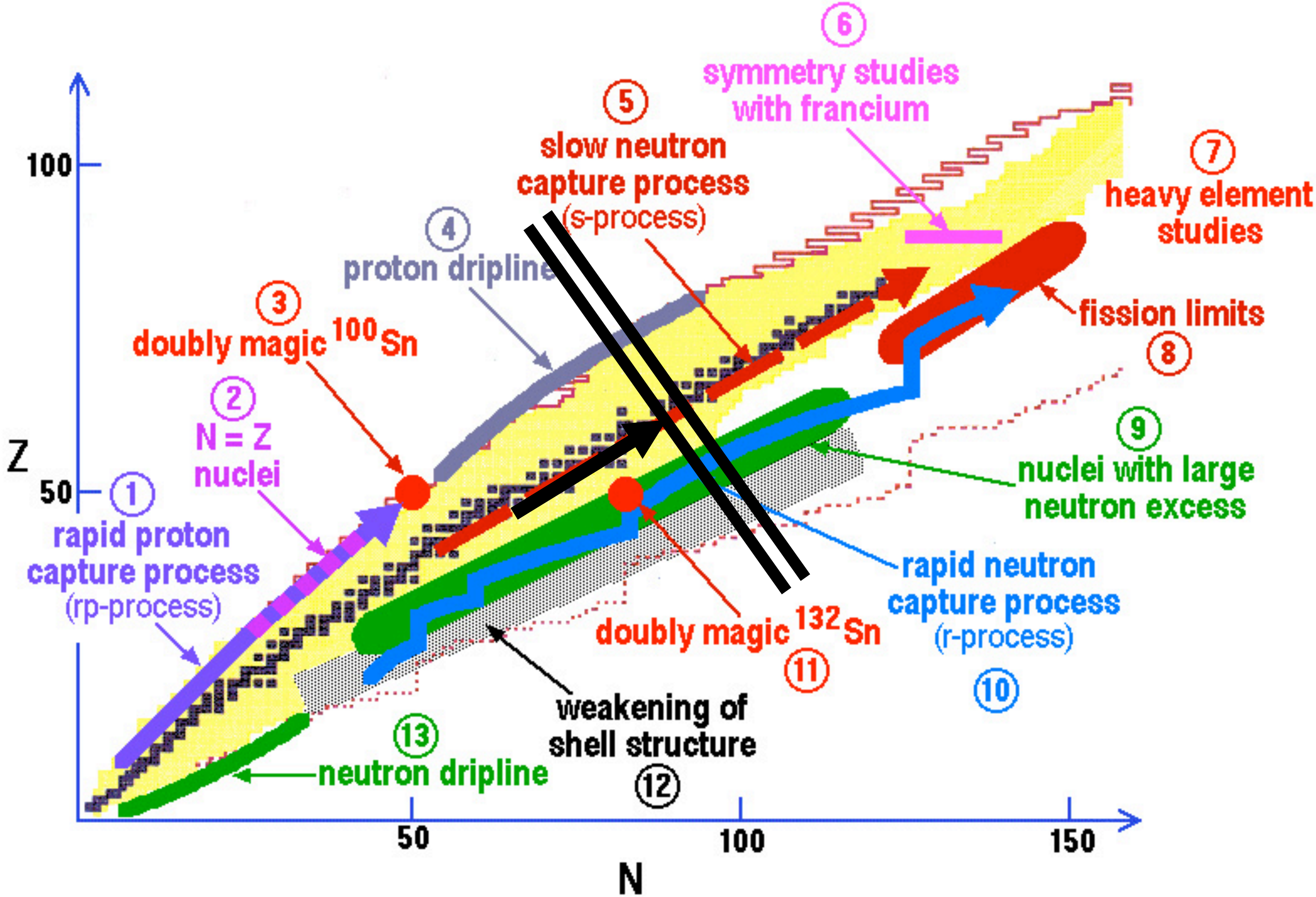

100
50
Z
N
50
100
150
1
rapid proton
capture process
(rp-process)
2
N = Z
nuclei
3
doubly magic 100Sn
4
proton dripline
5
slow neutron
capture process
(s-process)
6
symmetry studies
with francium
7
heavy element
studies
fission limits
8
9
nuclei with large
neutron excess
rapid neutron
capture process
(r-process)
10
doubly magic 132Sn
11
weakening of
shell structure
12
13
neutron dripline

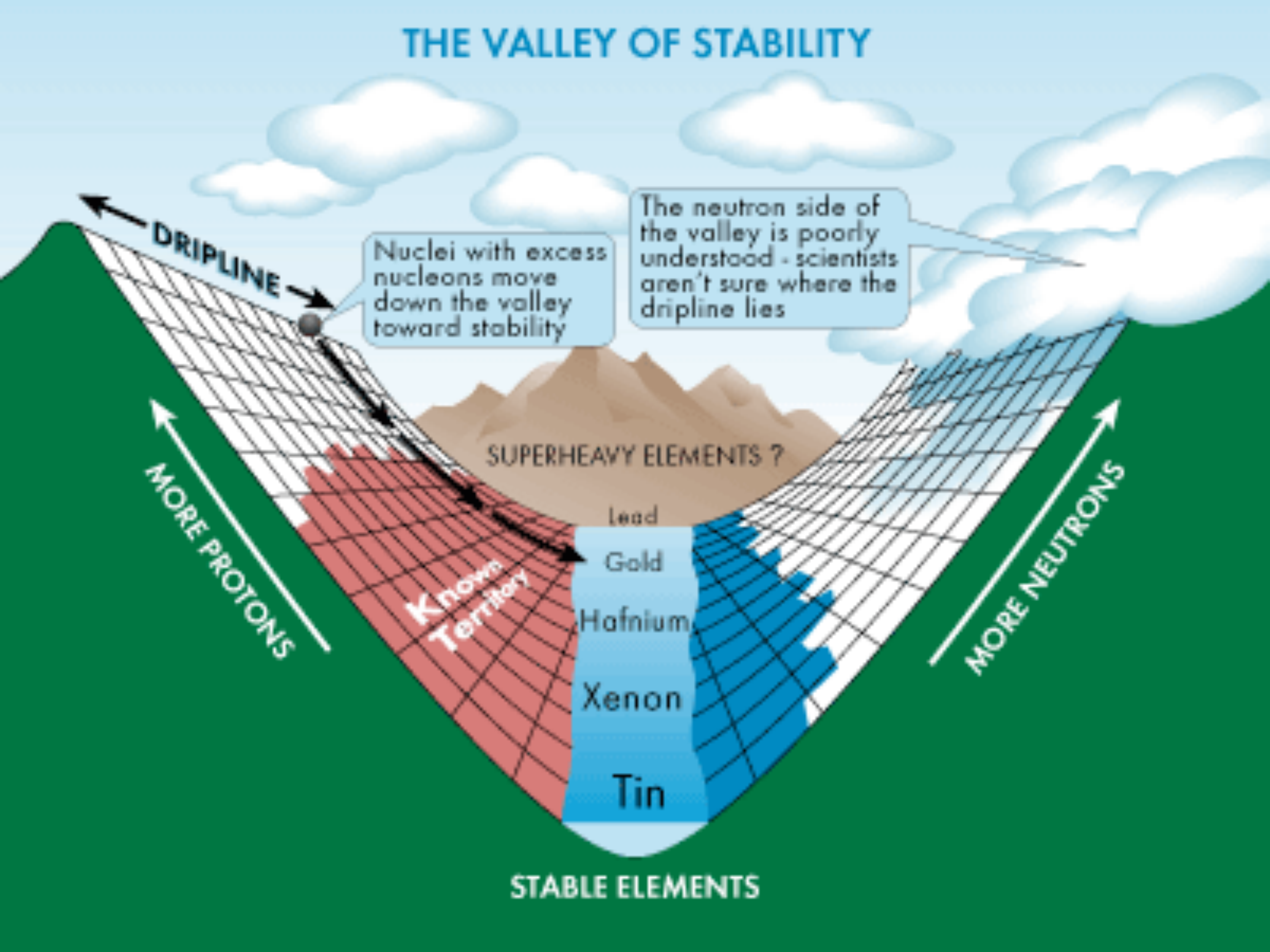
THE VALLEY OF STABILITY
DRIPLINE
Nuclei with excess nucleons move down the valley toward stability
The neutron side of the valley is poorly understood - scientists aren't sure where the dripline lies
SUPERHEAVY ELEMENTS ?
Lead
Gold
Hafnium
Xenon
Tin
Known Territory
MORE PROTONS
MORE NEUTRONS
STABLE ELEMENTS

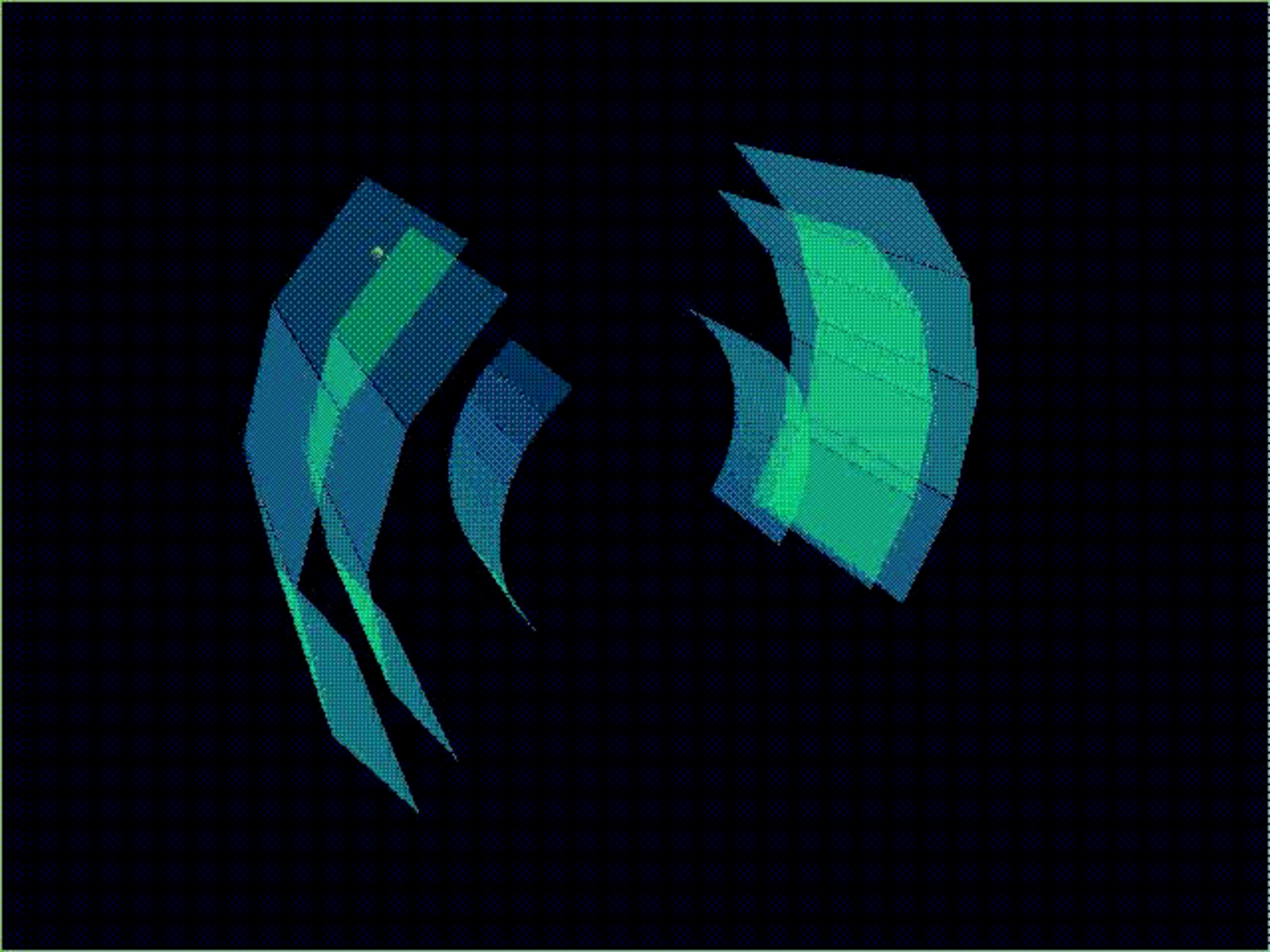

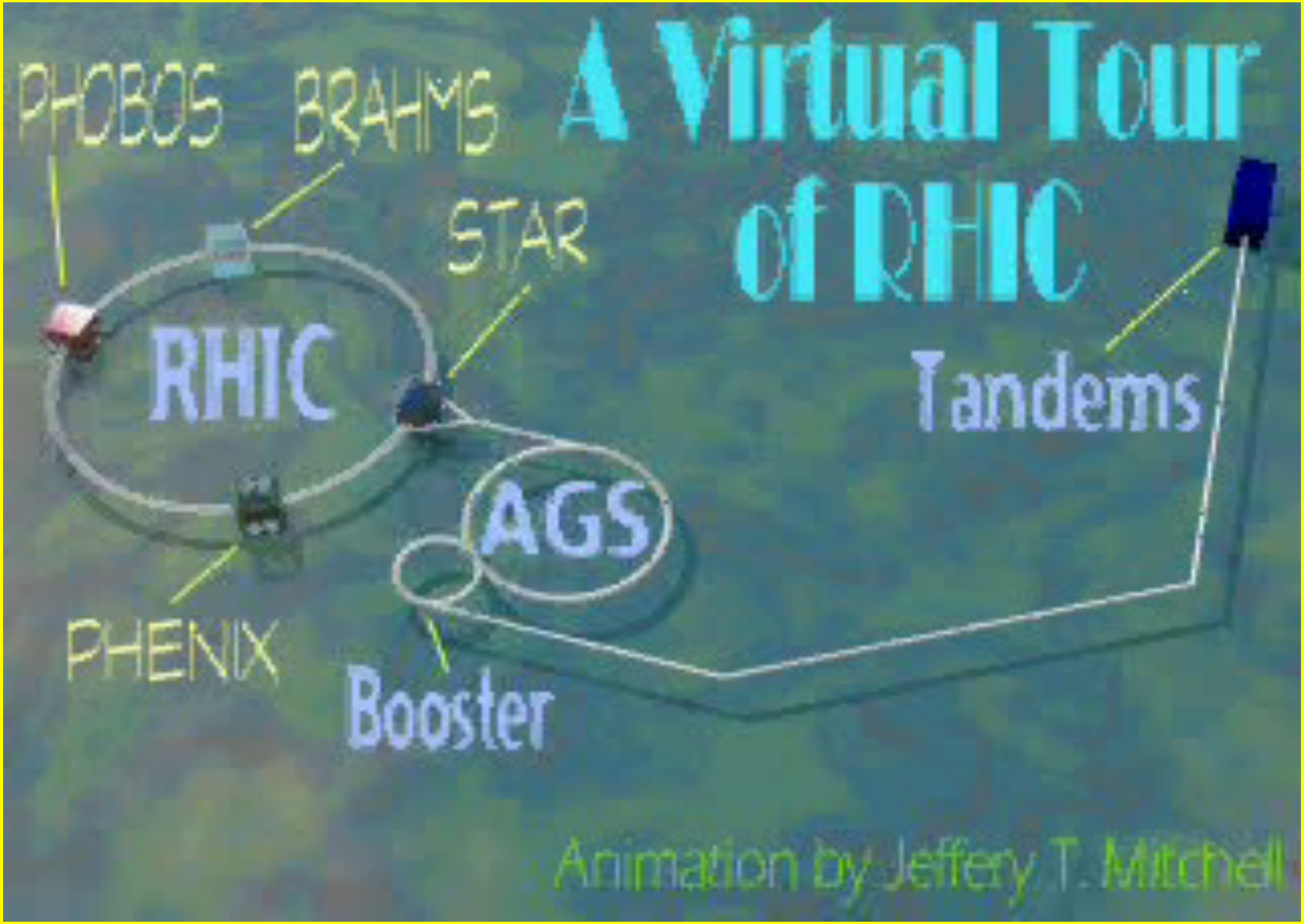
A Virtual Tour of RHIC
PHOBOS
BRAHMS
STAR
RHIC
Tandems
AGS
PHENIX
Booster
Animation by Jeffery T. Mitchell

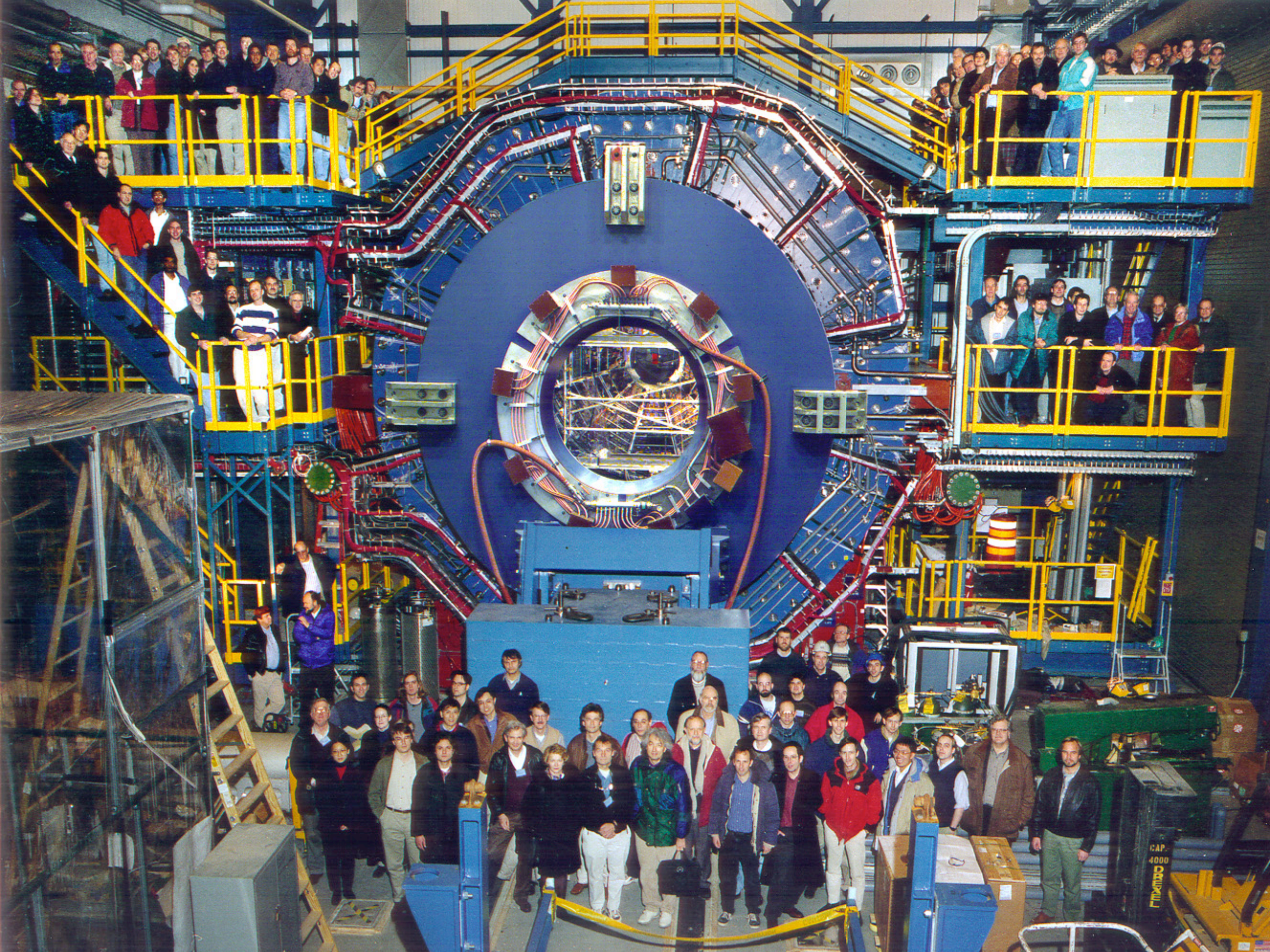
CAP. 4000
DREXEL

ANÁLISE POR FEIXES IÔNICOS
ARTE E ARQUEOLOGIA
PIXE, ERDA, RBS,
PIGE, AMS. . . .
DATAÇÃO
RADIOFÁRMACOS
TERAPIA DE CANCER
γ, N, BNCT, N....
DETERORES DE
IMAGEM : NMR ,PET...
ESTERILIZAÇÃO
ENERGIA NUCLEAR
FISSÃO DE ÍONS PESADOS
TRANSMUTAÇÃO DE
LIXO RADIOATIVO
. . . .
ACELERADORES
MEDICINA
ENERGIA
AMBIENTE
MATERIAIS
T. ESPACIAL
PESQUISA BÁSICA
EM
FÍSICA NUCLEAR
CLIMA
POLUIÇÃO
ANÁLISE DE PARTICULADOS
MOVIMENTO DE ÁGUAS
BURACO DE OZONO
IMPLANTAÇÃO IÔNICA
MICROPOROS
NANOESTRUTURAS
DANOS DE RADIAÇÃO
NOVOS MATERIAIS
ANÁLISE ELEMENTAR
ANÁLISE E x E
CALIBRAÇÃO DE DETETORES
DANOS POR RADIAÇÃO

PELLETRON

Laboratório Aberto de Física Nuclear (LAFN)

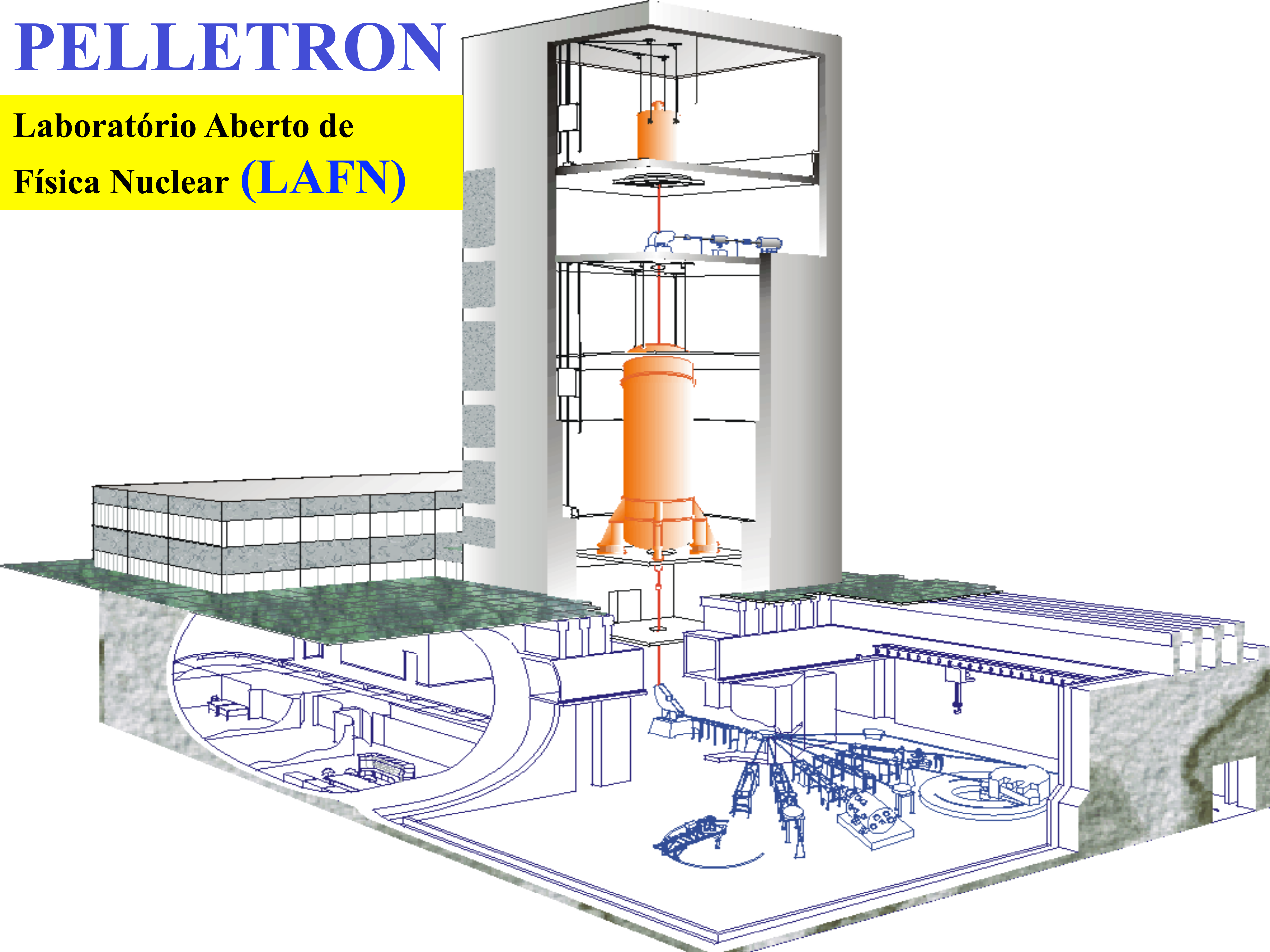

Acelerador Pelletron, tandem, V_{max} = 1.7 MV com *stripper* gasoso de N_2

Fonte de íons tipo RF modelo Alphatross com célula de troca de carga com Rb, para feixes de He e H.

Fonte SNICS (Fonte de íons negativos por *sputtering* de Césio), para feixes de H, C, O, Cl, Si...

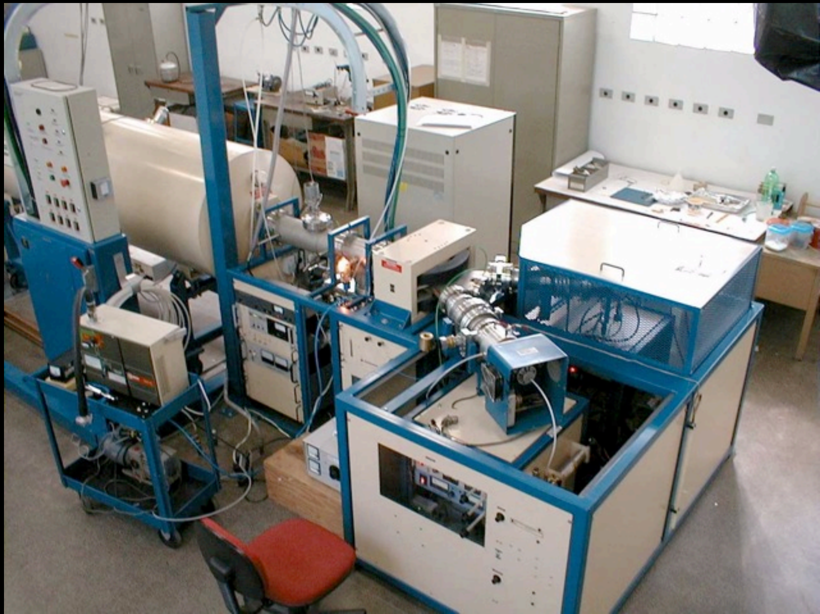

Métodos Analíticos no LAMFI - USP

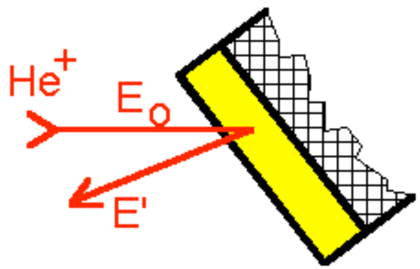

RBS –

Rutherford Backscattering Spectrometry

Concentração e perfil em profundidade

- Medida absoluta em átomos/cm²
- Sensibilidade < 1012 Au/cm²
- Rápido (10 min)
- Sensível à topografia da camada e interface

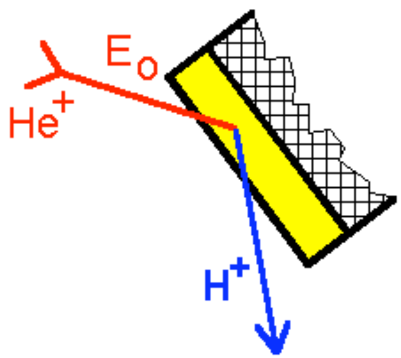

FRS - Forward Recoil Spectometry

ERS - Elastic Recoil Spectometry

ERDA - Elastic Recoil Detection Analysis

- (Concentração e perfil em profundidade
- Medida absoluta em átomos/cm2
- Sensibilidade < 1012 Au/cm2
- Rápido (10 min)
- Sensível à topografia da camada e interface

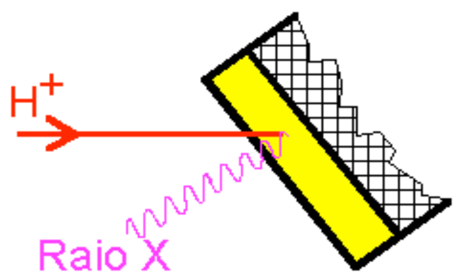

PIXE - Particle Induced X-ray Emission

- Medida absoluta em átomos/cm2
- Alta resolução para elementos vizinhos

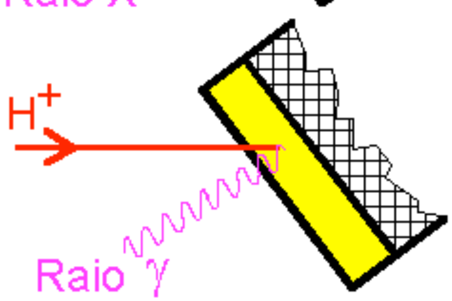

PIXE

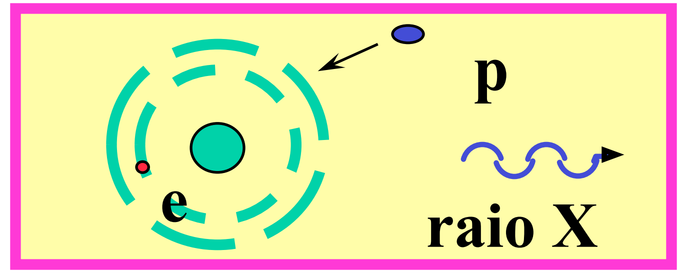

- **Particle Induced X-ray Emission (proton)**

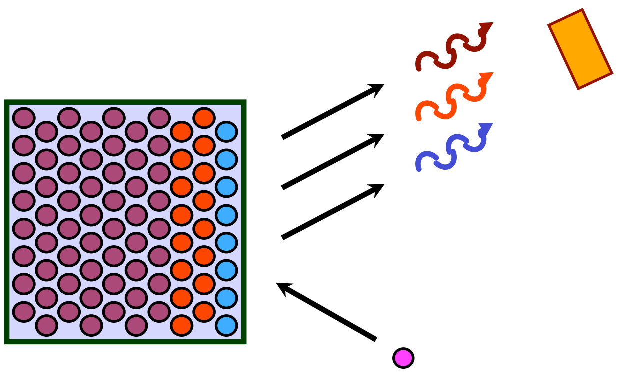

Detetor (SiLi)

Radiação Eletrom
raio X característico (keV)

Partícula

Características

Medidas absolutas em átomos/cm^2

Alta sensibilidade (ppm)

Alta resolução para elementos vizinhos

Eficiente para elementos mais pesados que Si

Rápido (10 min)

RBS

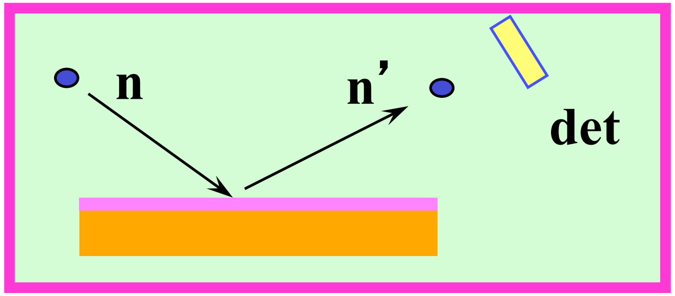

- Rutherford BackScattering

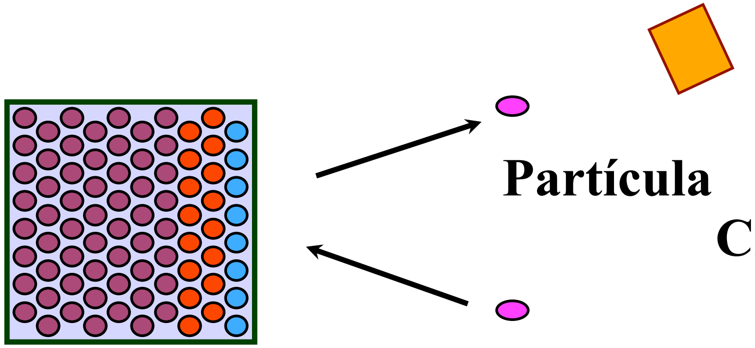

Detetor de Si

Partícula

Cinemática (ângulos traseiros)

Perda de energia

Partícula leve

Características

Concentração e perfil em profundidade

Medida absoluta em átomos/cm^2

Sensibilidade < 10^{12} Au/cm^2

Sensível a topografia da interface

Eficiente para Z acima de Si

ERDA/
FRS

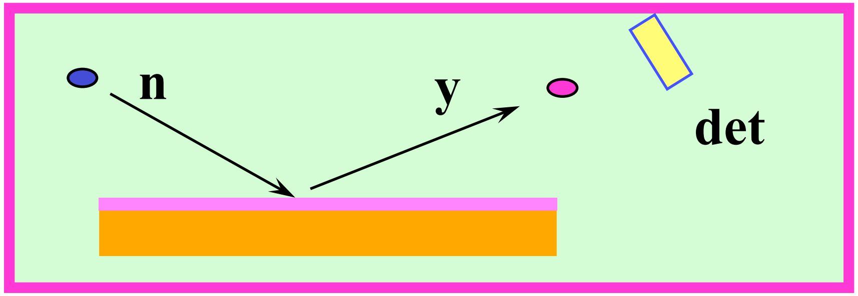

Elastic Recoil Detection Analisys

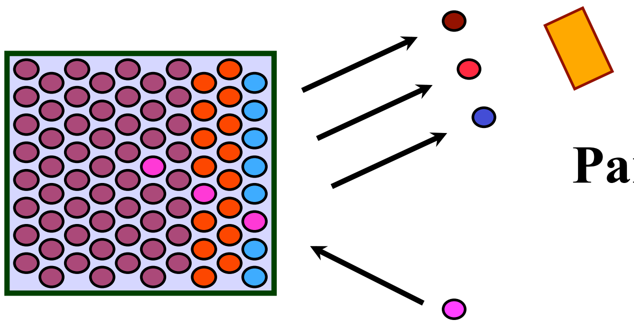

Detetor de Si

Partícula

Cinemática (ângulos dianteiros)

Perda de energia

Partícula pesada(Cl)

Características

Concentração e perfil em profundidade

Medida absoluta em átomos/cm^2

Eficiente para Z abaixo de Si (até H)

Rápido (10 min)

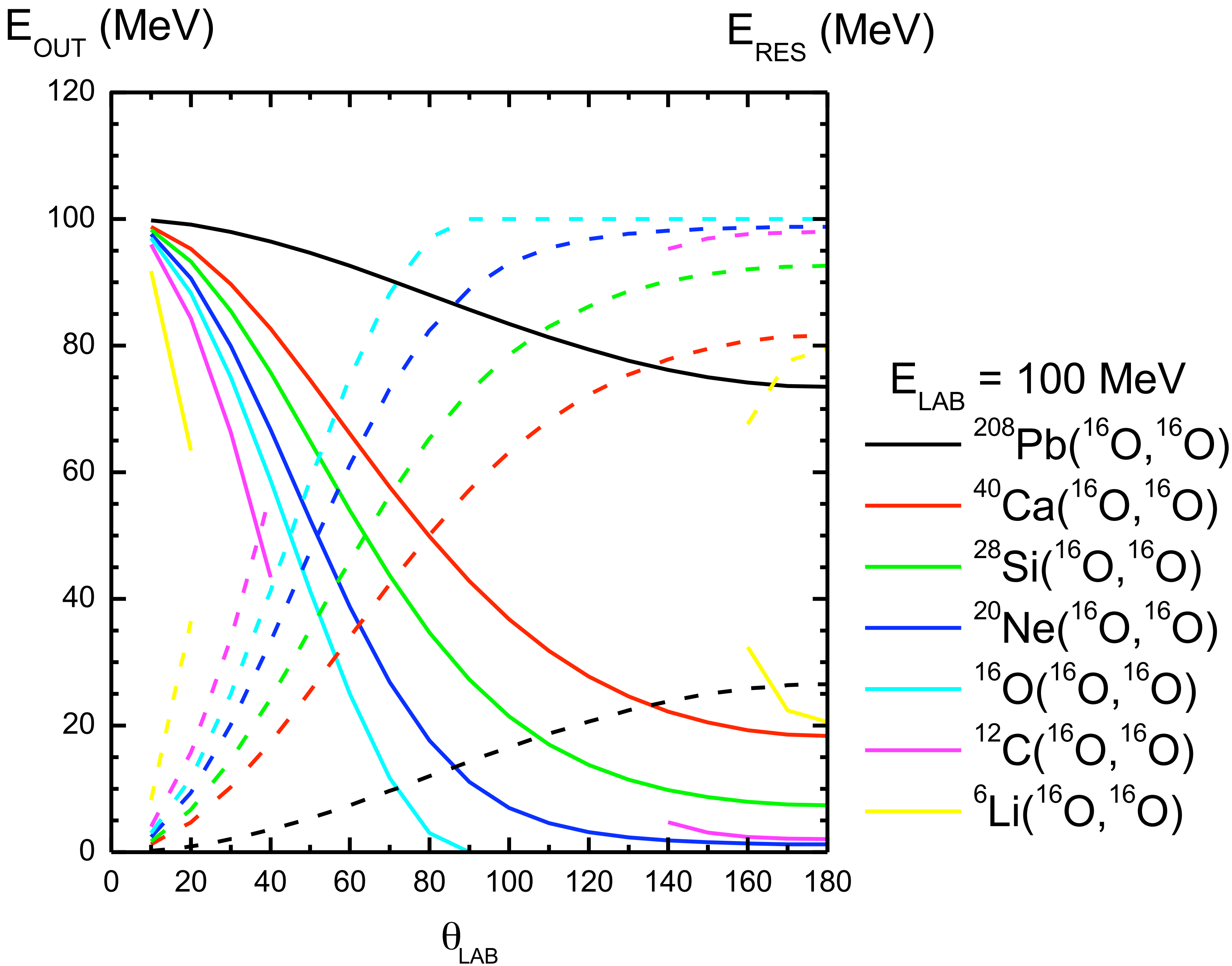

E_OUT (MeV)
E_RES (MeV)
120
100
80
60
40
20
0
0
20
40
60
80
100
120
140
160
180
θ_LAB
E_LAB = 100 MeV
208Pb(16O,16O)
40Ca(16O,16O)
28Si(16O,16O)
20Ne(16O,16O)
16O(16O,16O)
12C(16O,16O)
6Li(16O,16O)

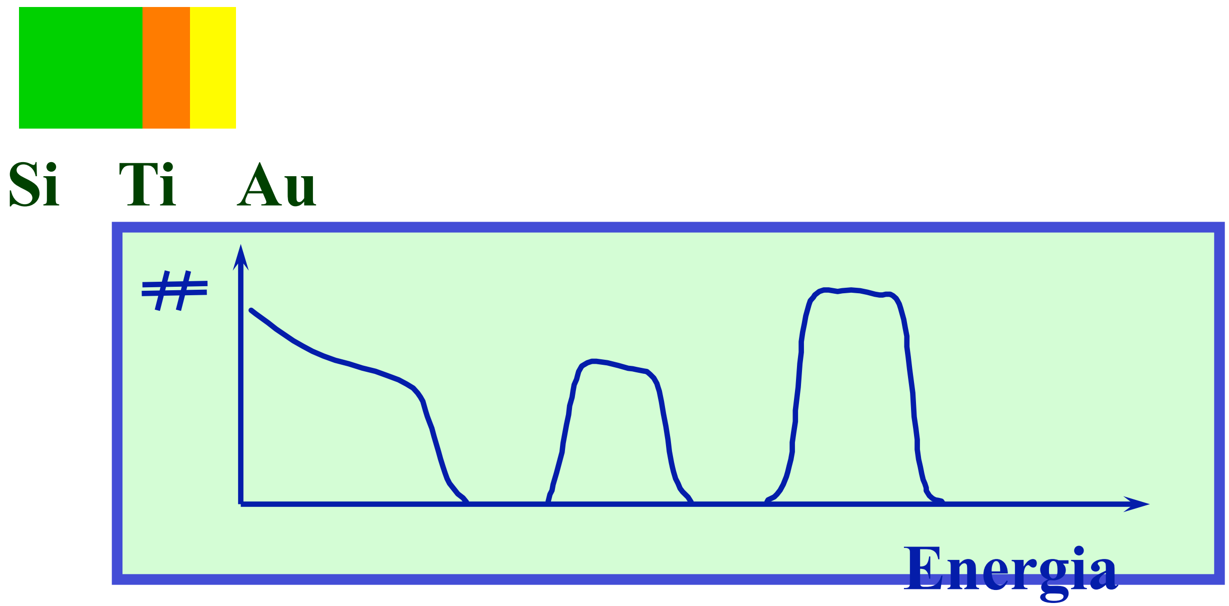
Si
Ti
Au
#
Energia

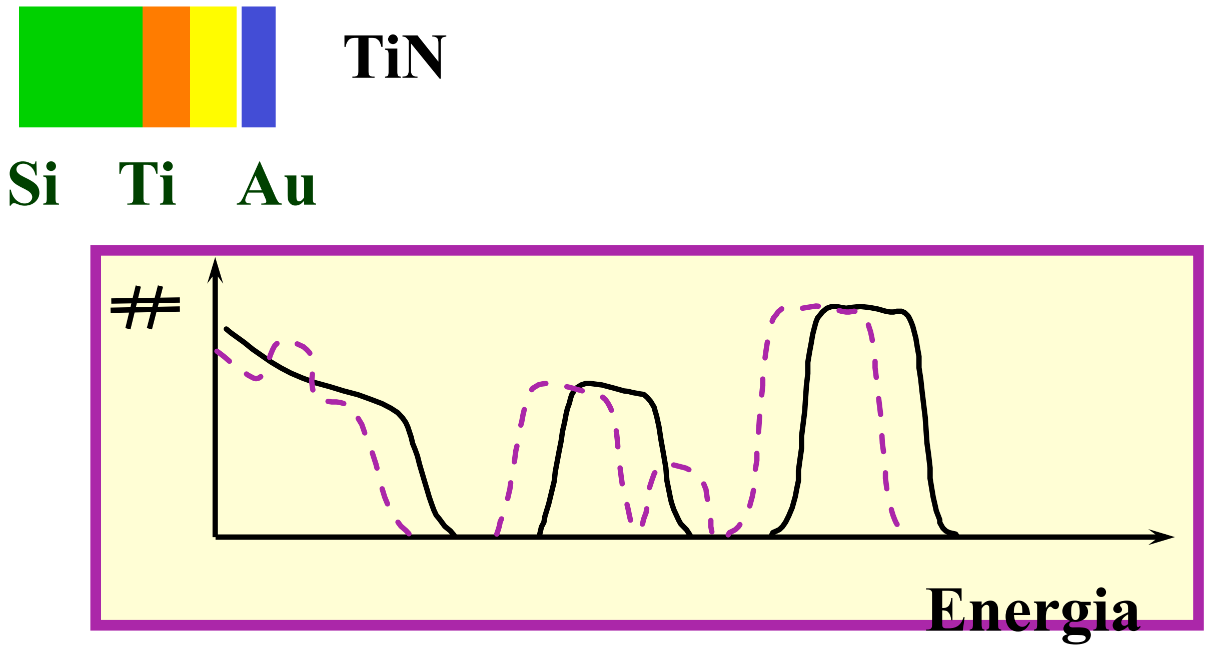
TiN
Si
Ti
Au
#
Energia

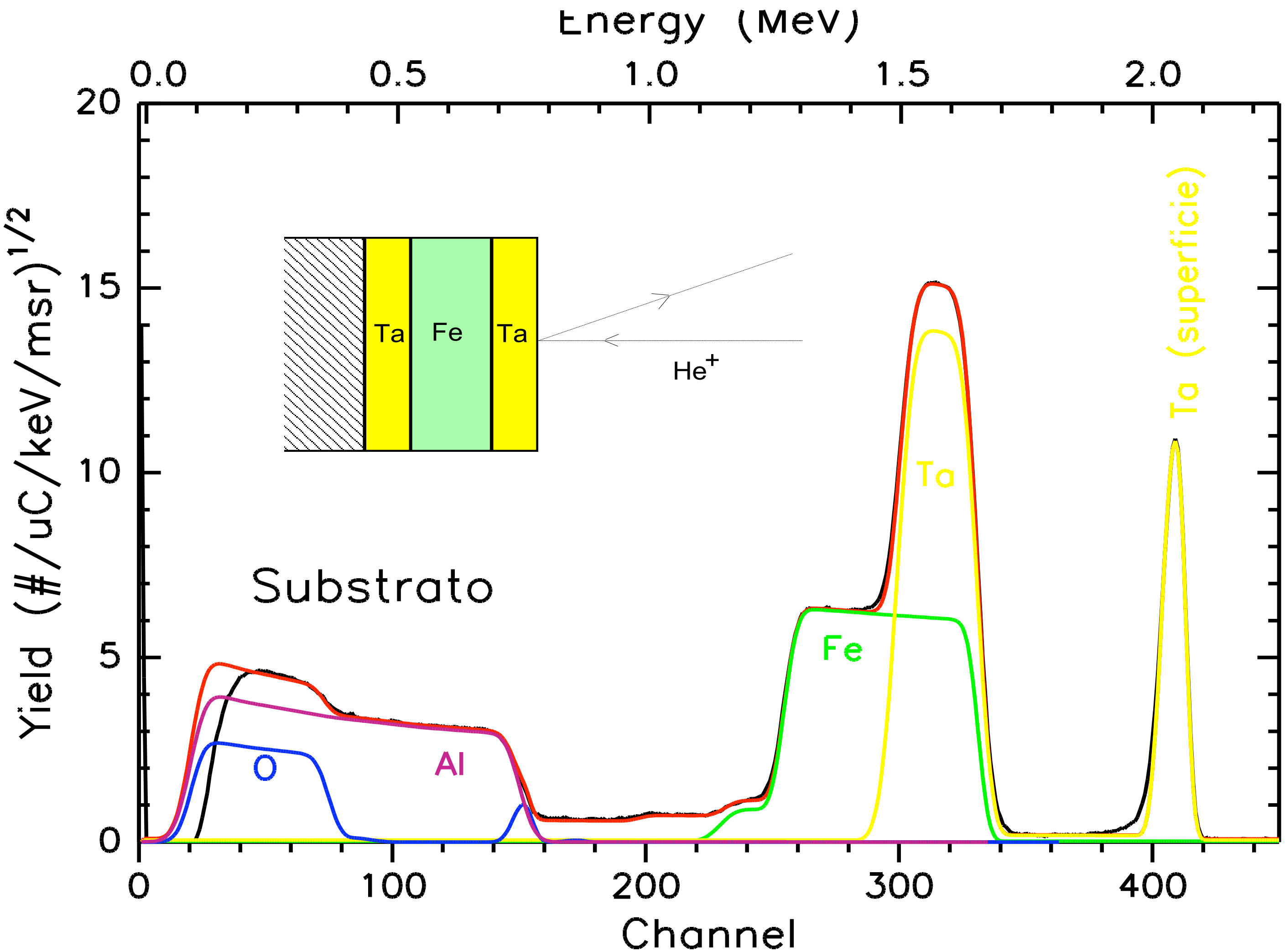

Espectro RBS típico de um filme tri-camada Ta/Fe/Ta sobre Al2O3. As condições experimentais foram: RBS He +, 2.3MeV. Detecção a 170°, filme inclinado de 55°. Dados em linha preta, a simulação teórica com programa RUMP em vermelho e componentes em outras cores.

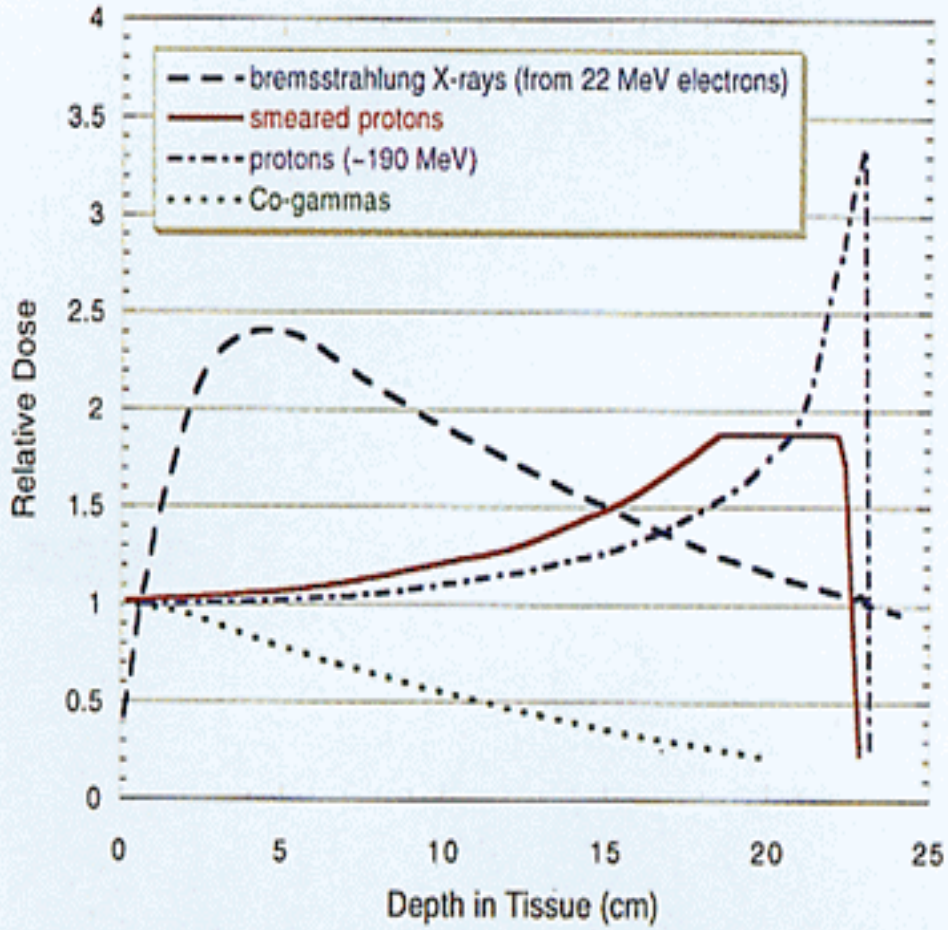

Figure VIII.1: Relative dose at various depths in tissue for bremsstrahlung X-rays generated by 22 MeV electrons (dashed curve), for 190 MeV protons (dot-dashed curve), for protons with smeared energy distribution to provide a plateau dose profile (solid curve), and from γ-rays produced by a cobalt 60 source (dotted curve).

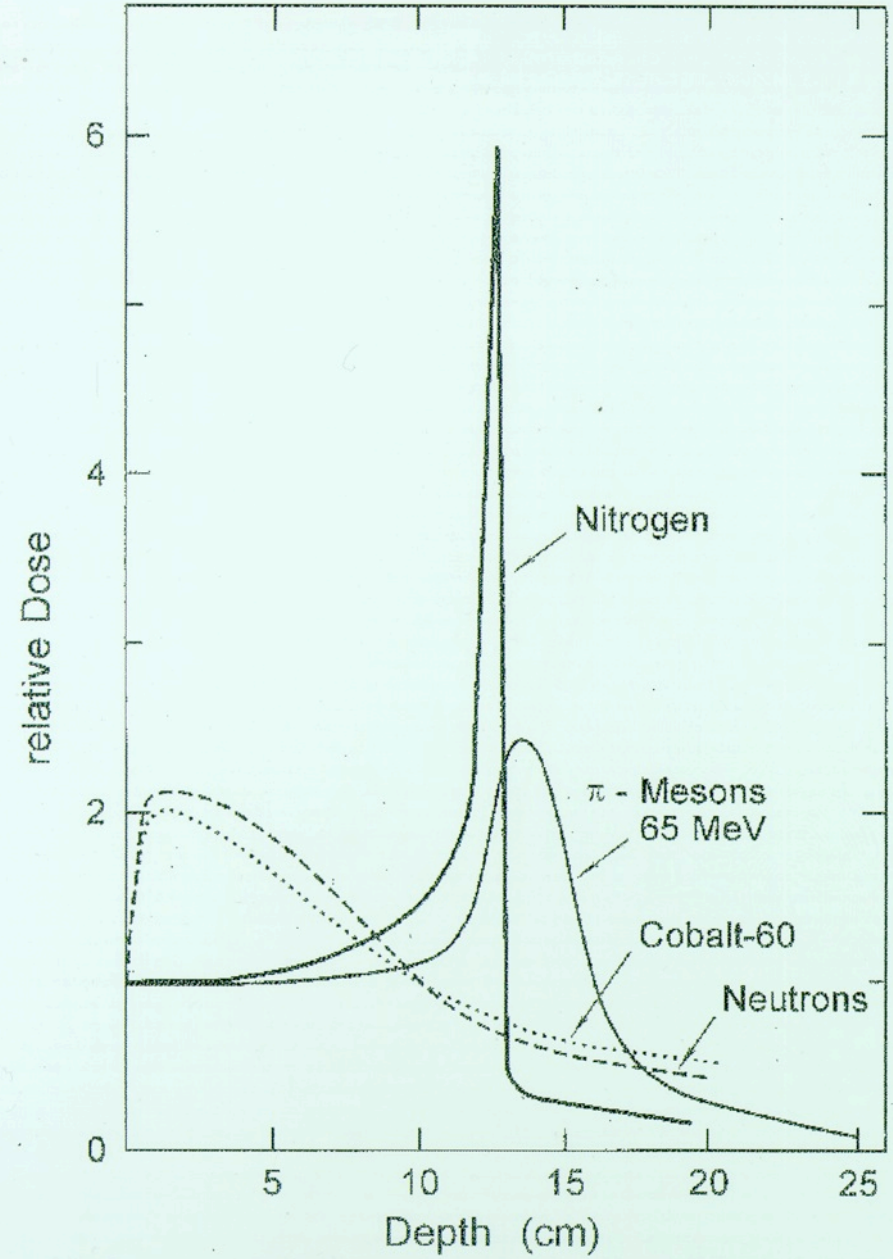

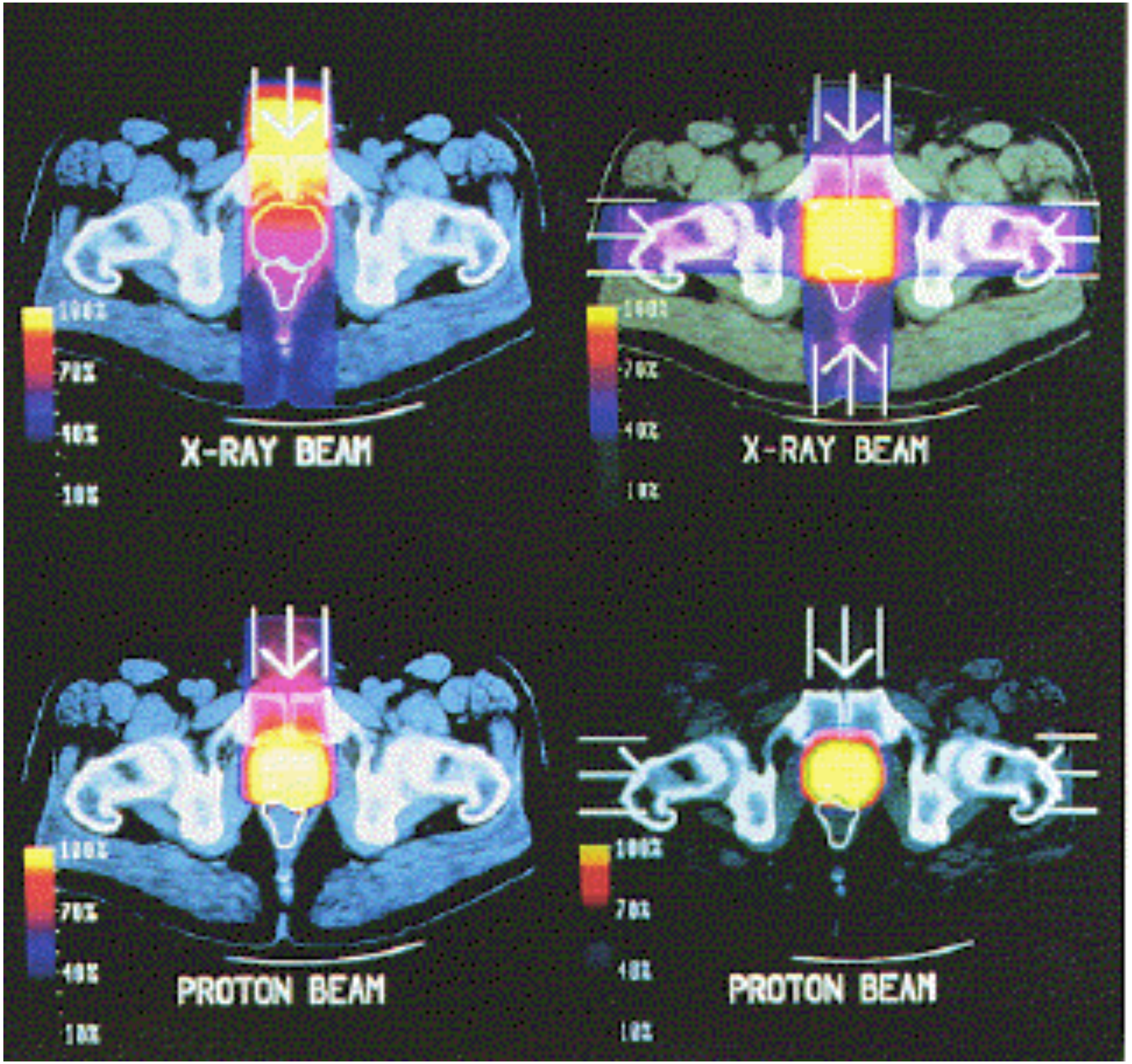
100%
70%
40%
10%
X-RAY BEAM
100%
70%
40%
10%
X-RAY BEAM
100%
70%
40%
10%
PROTON BEAM
100%
70%
40%
10%
PROTON BEAM

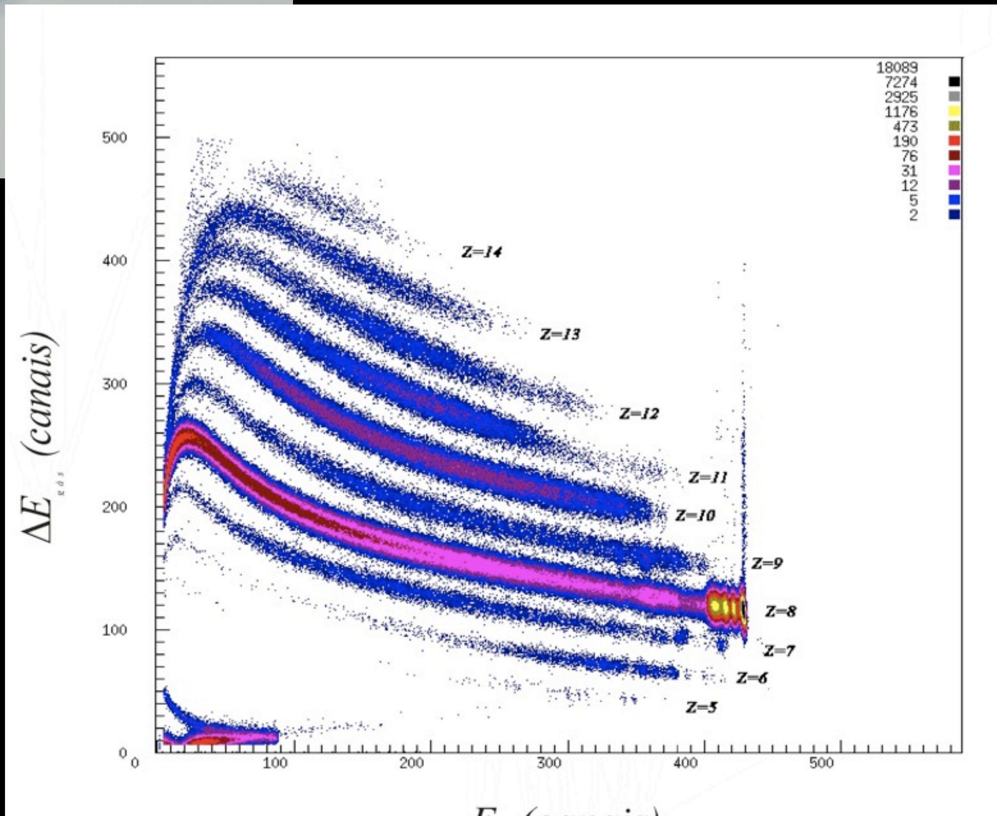

18089
7274
2925
1176
473
190
76
31
12
5
2
Z=14
Z=13
Z=12
Z=11
Z=10
Z=9
Z=8
Z=7
Z=6
Z=5
0
100
200
300
400
500
ΔE (canais)

Perda de energia x Energia

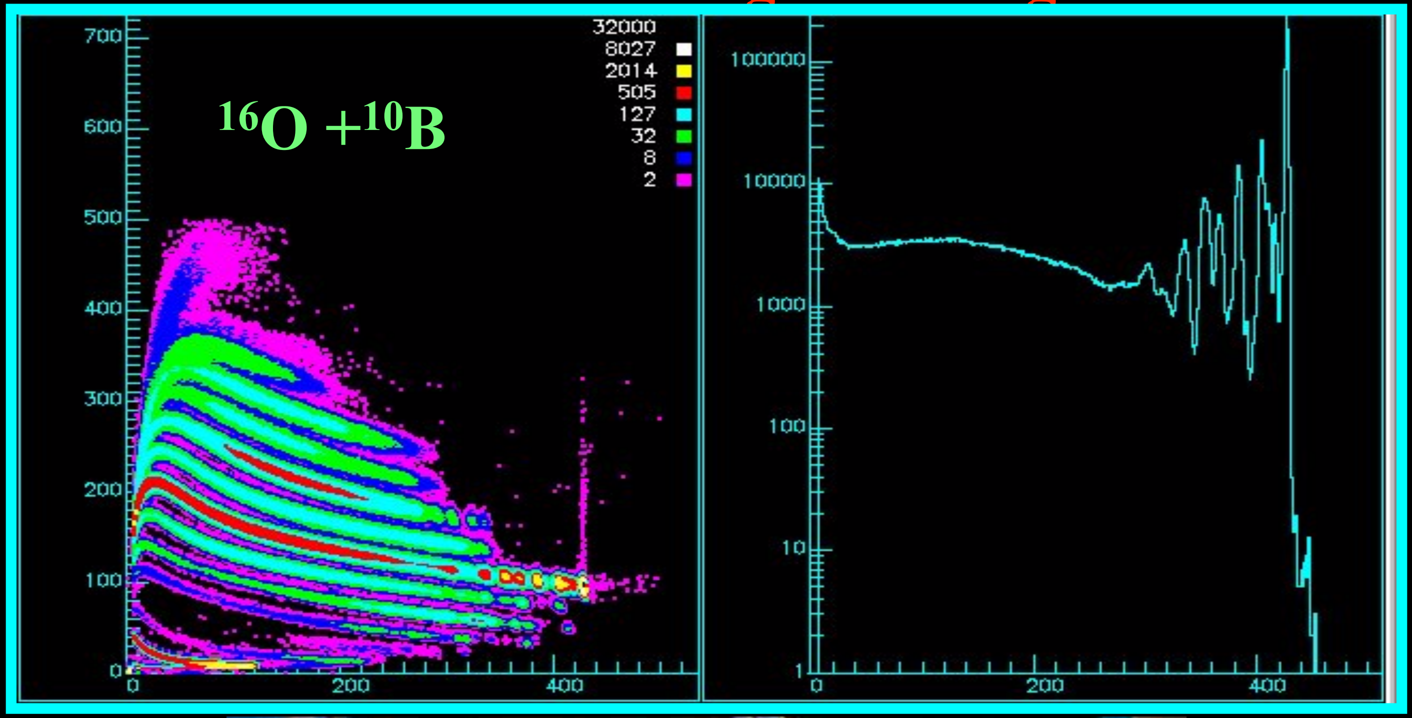

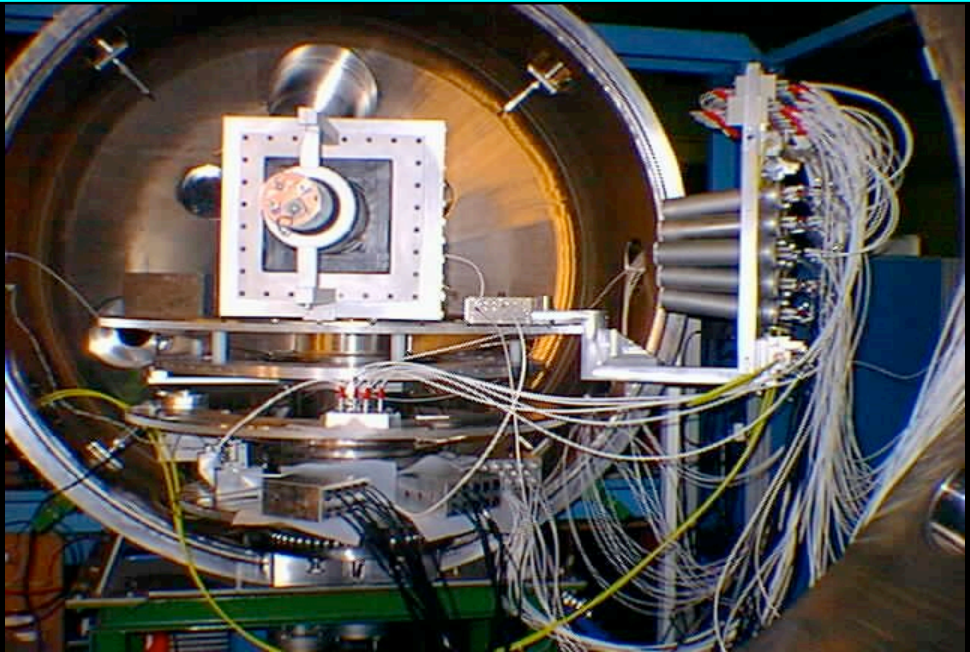

Poluição do Ar em São Paulo

São Paulo em um dia de inverno com baixos niveis de poluicão

São Paulo em um dia de inverno com altos niveis de poluicão

Fotos no topo do edificio da Faculdade de Medicina da USP, na Avenida Doutor Arnaldo.

JPL

Pathfinder Science Payload

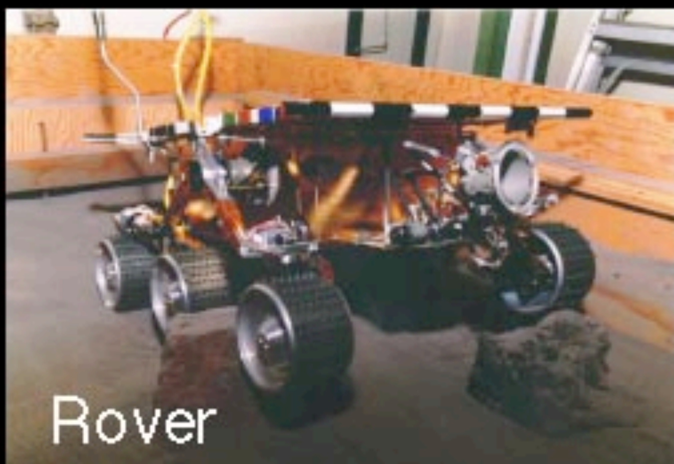

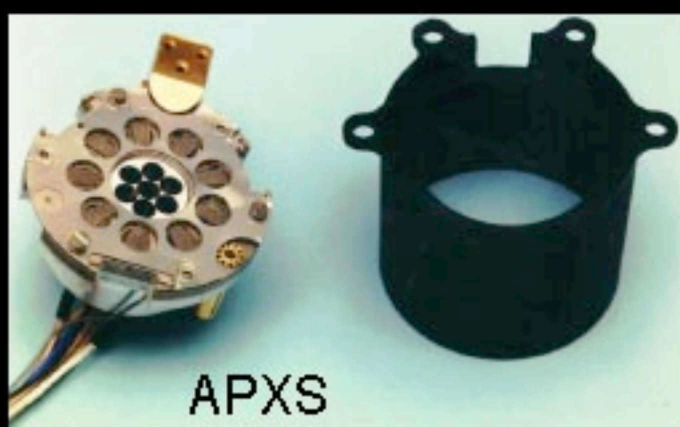

ASI/MET

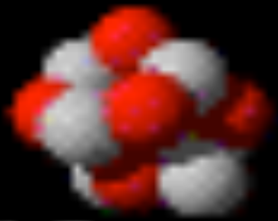

$^{18}_{9}F_{9}$

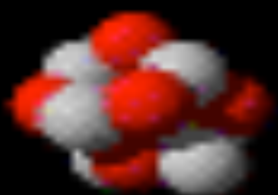

$^{14}_{6}C_{8}$

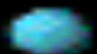

e

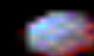

e^{+}

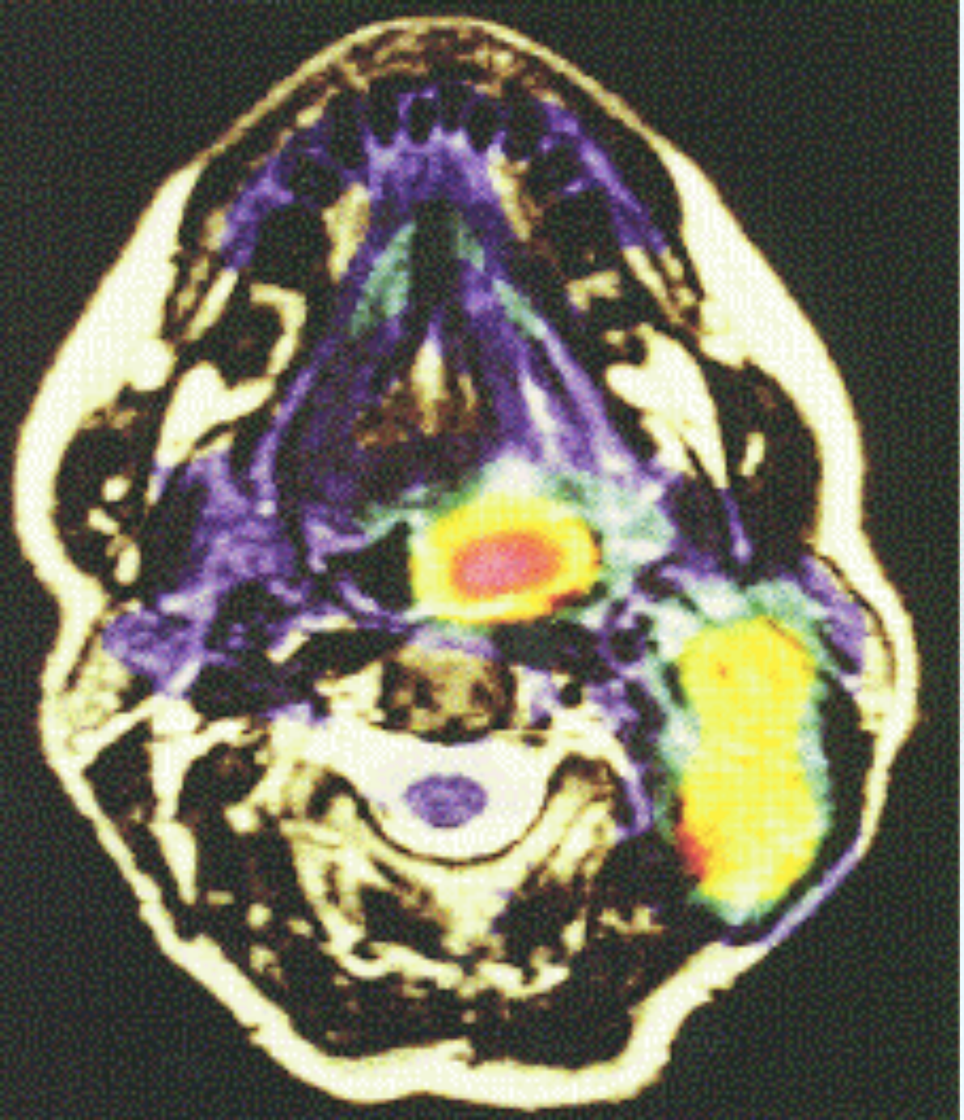

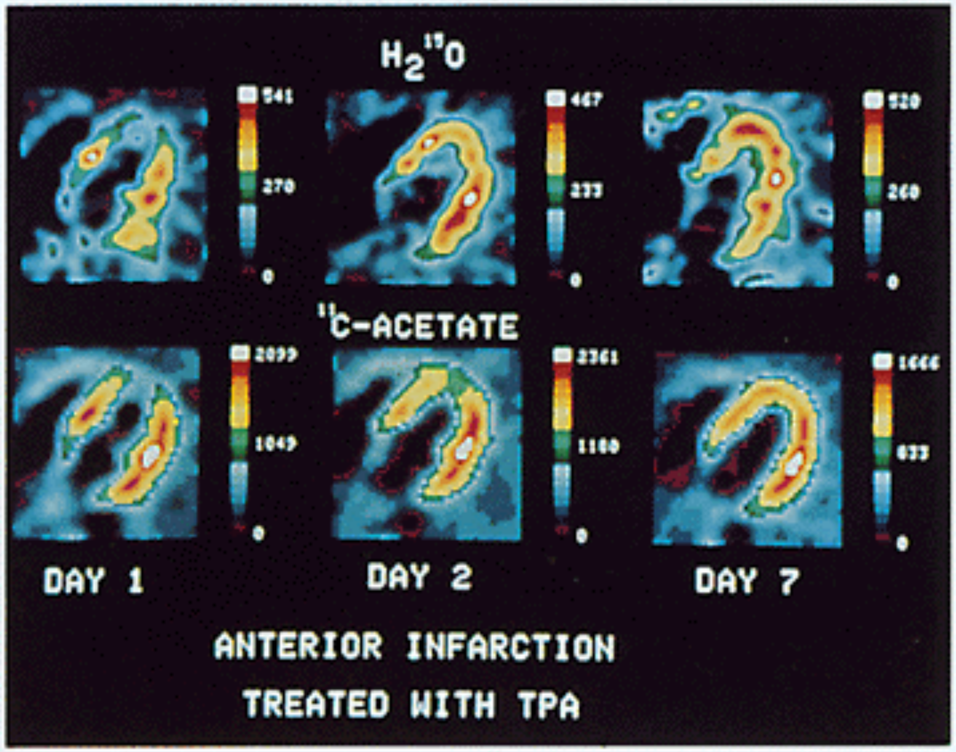

Figure VIII.2: The figure shows PET pictures of the heart of a patient with acute myocardial infarction treated with a thrombolytic agent. The top row shows scans after administration of water containing oxygen-15 nuclei to trace the blood flow. The bottom row shows tomograms obtained after administration of acetate containing carbon-11 nuclei to trace the heart's metabolism, i.e. its rate of oxygen usage. The defects are clearly visible on day 1, both in the impaired blood flow (top left) and the impaired metabolic use of oxygen (bottom left). Recovery of blood circulation has taken place on day 2 (top center) and is maintained through day 7 (top right). Defects in the metabolism are still visible on day 2 (bottom center); full recovery is seen by day 7.

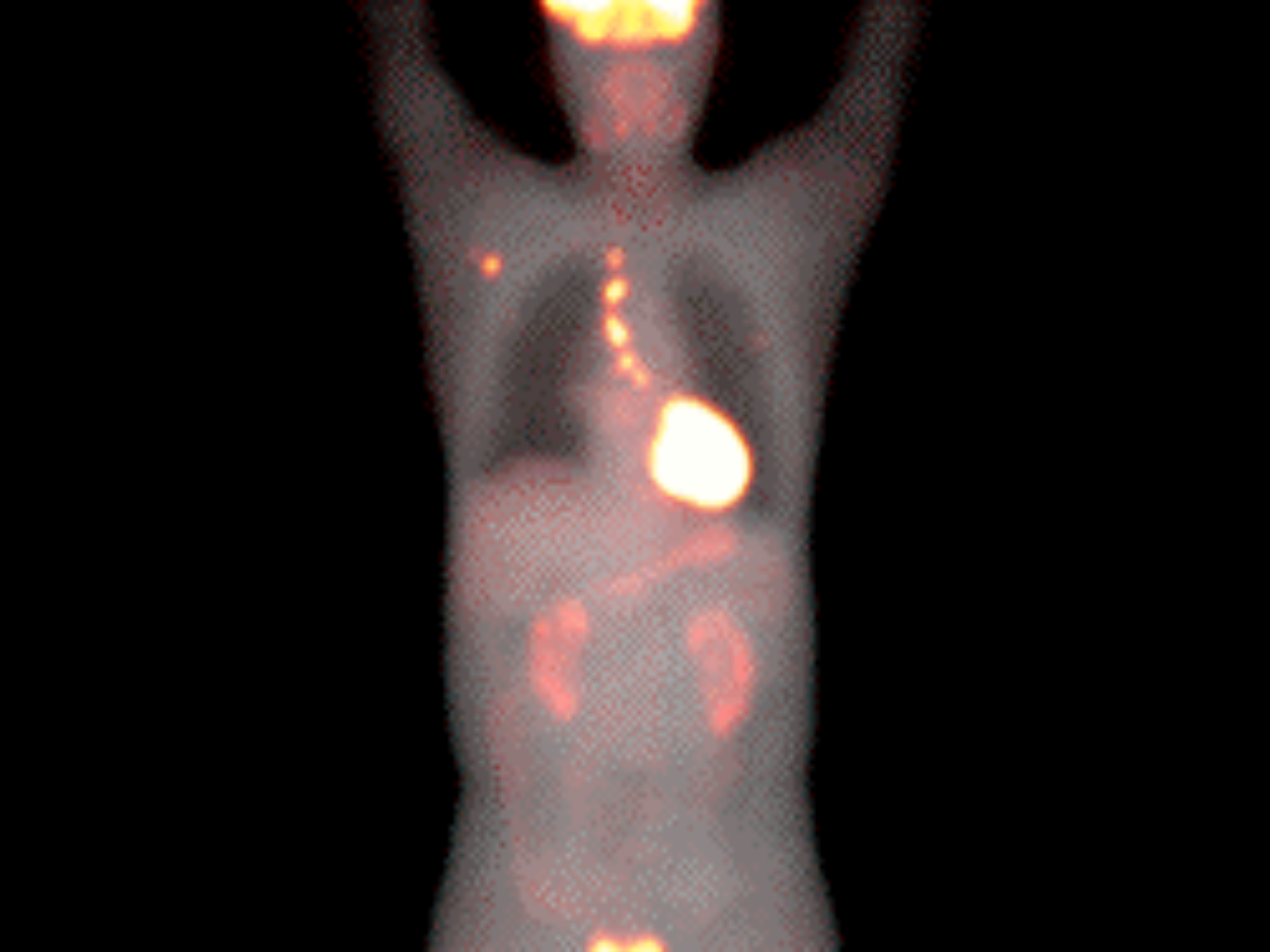

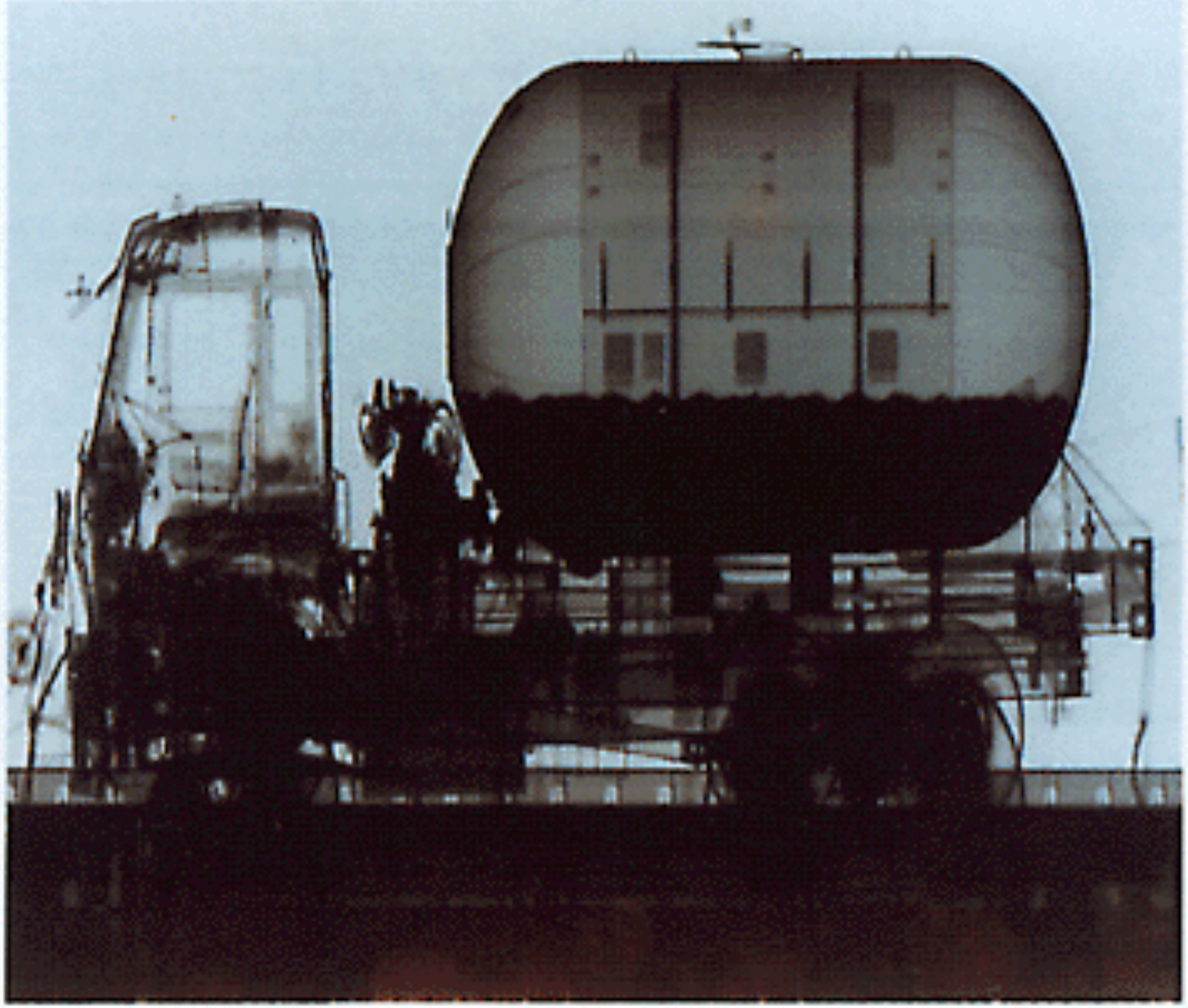

Figure VIII.4: Large-scale X-ray scan of a tanker truck revealing the fill level of the tank. Such systems can be used to detect car-bombs at highly vulnerable transportation centers.

BNCP (“Boron-Neutron Capture Therapy”)

TERAPIA com NEUTRON e I. P. (LET)

MARCADORES MONOCLONAIS e REATIVOS

....

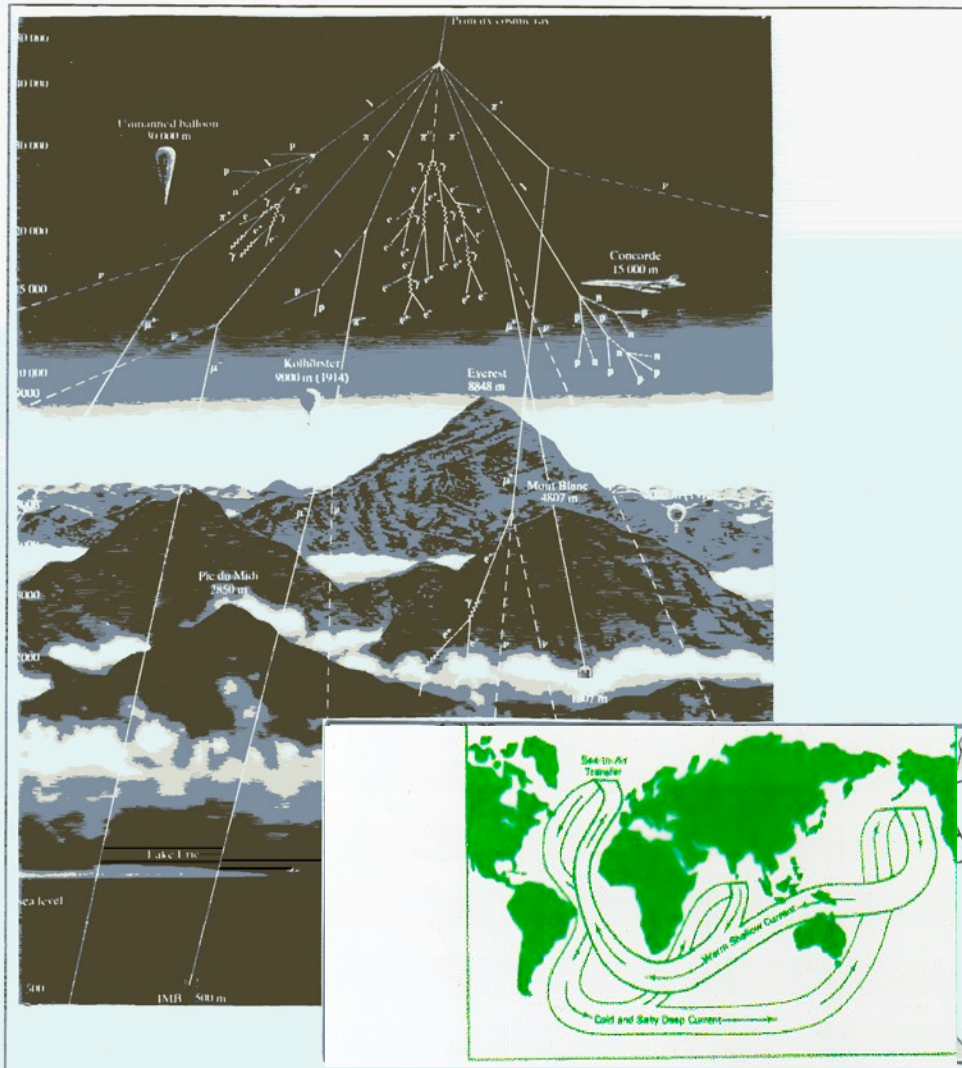

Cosmic-ray induced nuclear reactions in the atmosphere and the earth's crust generate long-lived radioisotopes that serve as wide-spread tracers and dating tools in various studies of geophysical and environmental importance. It is now possible, for example, to use accelerator mass spectrometry (AMS), a technique that was recently developed at nuclear physics accelerators, for highly sensitive carbon-14 dating to measure the age distribution of carbon-dioxide dissolved in oceanwater. This provides important information for understanding oceanic circulation patterns and their influence on the weather, and insights into the phenomenon of global warming.

$^{7,10}Be$

Isótopos de Be criados na estratosfera em colisões de raios cósmicos em átomos de ^{14}N. Átomos de Be são ligados com facilidade em aerosois.

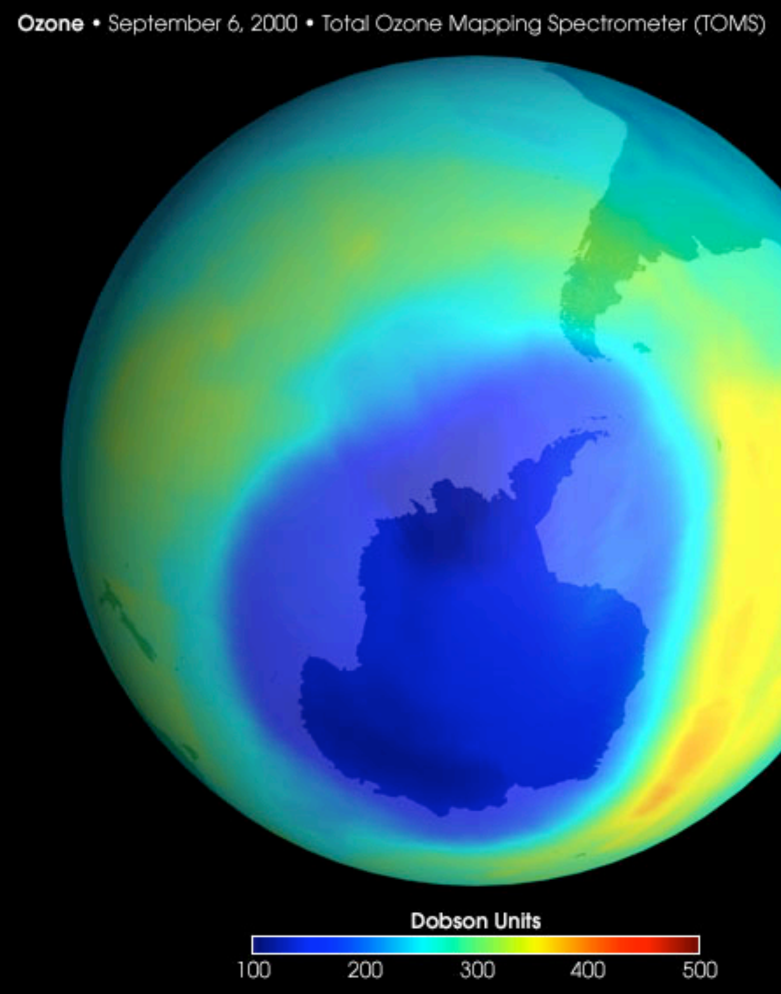

AMS- Accelerator Mass Spectrometry

MÉTODO ANALÍTICO DE IDENTIFICAÇÃO

1) Identificação e contagem de isótopos
(> 10^5 átomos/amostra)

TRAÇADORES

2) Identificação e determinação de razões isotópicas (10^{-15} a 10^{-12})

CRONOLOGIA

ISÓTOPOS DE INTERESSE:

Raros
Radioativos com $T_{1/2}$ longa (10^4 a 10^7a)

^{14}C	5,73Ka	^{36}Cl	301Ka		
^{10}Be	1.5Ma			^{129}I	16Ma
^{26}Al	720Ka				

IRRADIAÇÃO DE ALIMENTOS
γ, e, n, p
Esterilização

Federal University of Rio de Janeiro

COPPE - Department of Nuclear Engineering

Identification of Microorganisms for the Analysis of Images Obtained by Neutron Radiography

J.D.R.Lopes[(a)], V.Crispim[(b)*] and C.Lage[(c)]

ABSTRACT

The main difficulty to identify infectious microorganisms is the required time to obtain a reliable result, a minimum of 72 hours. We propose a reduction to about 5 hours through the technique of neutron radiography. Samples containing the *bacillus Escherichia coli* and the *cocci Staphylococcus epidermidis* were incubated with B^{10}, layered on SSNTD (CR-39) surface and irradiated in the J-9 channel from the Argonauta Reactor (IEN/CNEN) with a flux of thermal neutrons at a rate of 2.2×10^5 n/cm^2.s. Images were observed in an optical microscope after exposure of the plates to chemical development of the latent alpha-tracks. Analysis of the images revealed morphological differences between the species, conferring the technique the perspective to use in microbial diagnosis.

Figure 1- Neutron radiograpic image of bacilli Escherichia coli

Figure 2 - Eletronic micrograph of *E. coli*. Copyright Dennis Kunkel, University of Hawaii

Figure 3 - Neutron radiographic image of *cocci Staphylococcus epidermidis*

Figure 4 - Eletronic micrograph of *S. epidermidis*. Copyright Dennis Kunkel, University of Hawaii

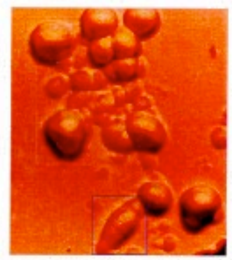

Figure 5 - Neutron radiographic image of both *E. coli* and *S. epidermidis* mixed in the same sample

Figure 6 - Agglomeration of α particles tracks originated from the $^{10}B(n,\alpha)^7Li$ reaction in CR-39

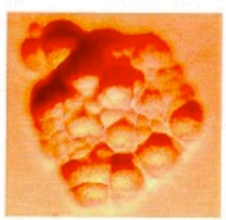

Figure 7 - Neutron radiographic image of an agglomeration of *cocci S. epidermidis*

Figure 8 - Neutron radiographic image of an agglomeration of *bacilli E. coli*

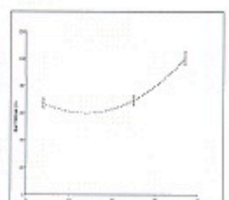

Figure 9 - Percentage of the number of scored in each sample in CR-39 strips as a function of the temperature of incubation with boron.

CONCLUSIONS

In summary, data presented in this paper indicate that the neutron radiography technique has a good perspective in applied Microbiology, serving as a tool for identification of microorganisms. Tests are now being performed to establish protocols for identification of other types of bacteria.

*Corresponding author's
Programa de Engenharia Nuclear/COPPE/UFRJ
Centro de Tecnologia, Bloco G, Sala 206
Caixa Postal 68509 CEP 21945-970
Rio de Janeiro, RJ, BRASIL
FAX: (5521) 290 7144
e-mail: [illegible]

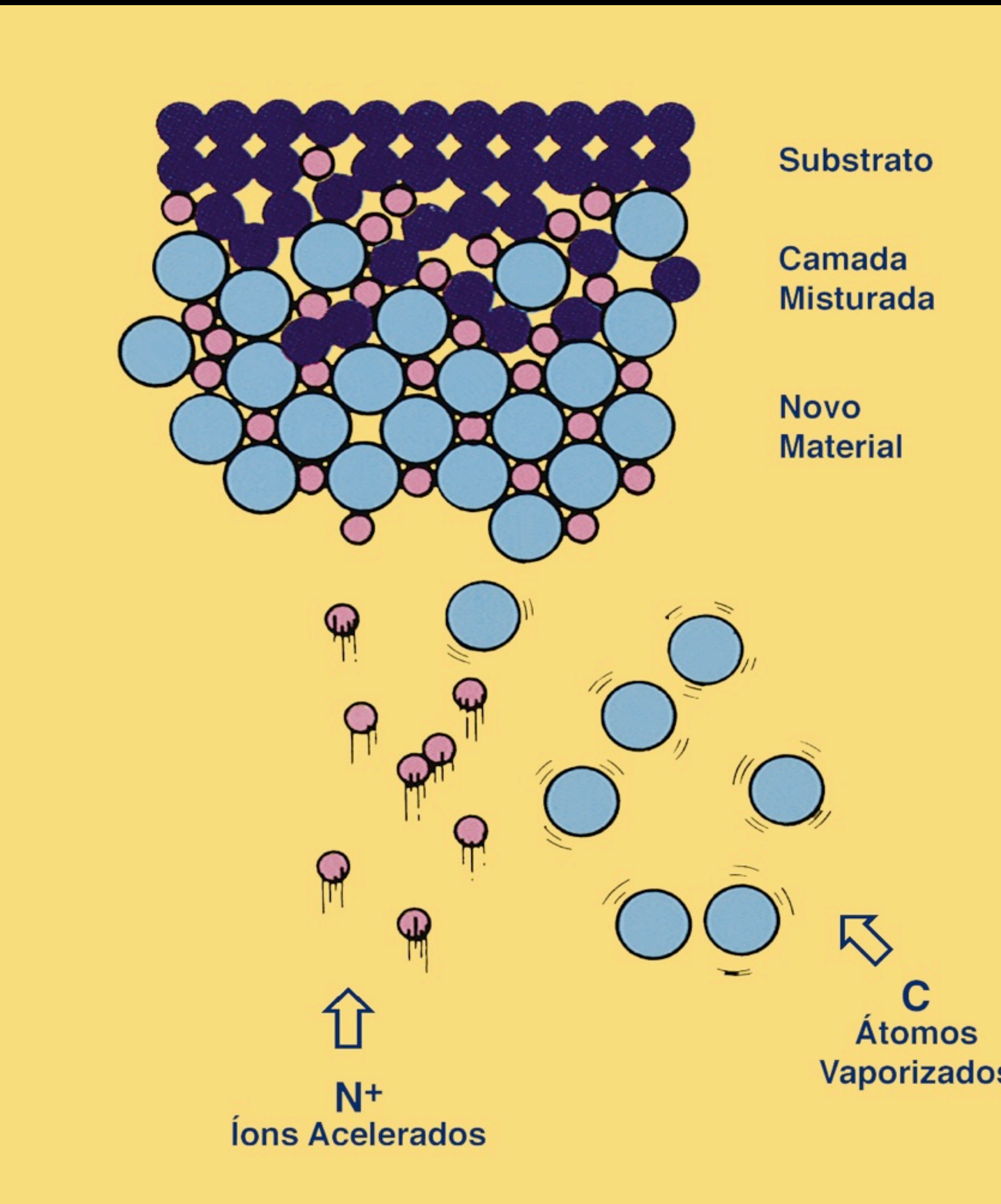
Substrato
Camada
Misturada
Novo
Material
N+
Íons Acelerados
C
Átomos
Vaporizados

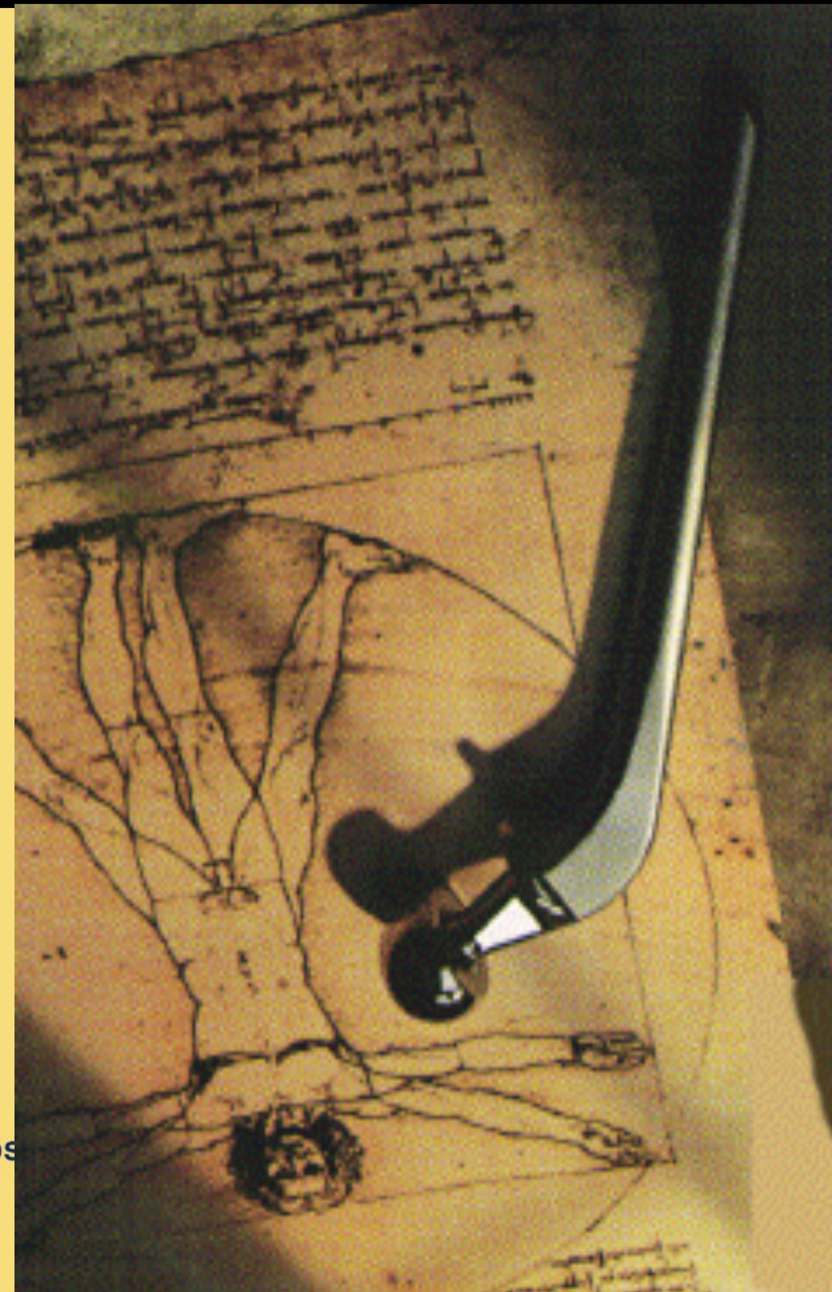

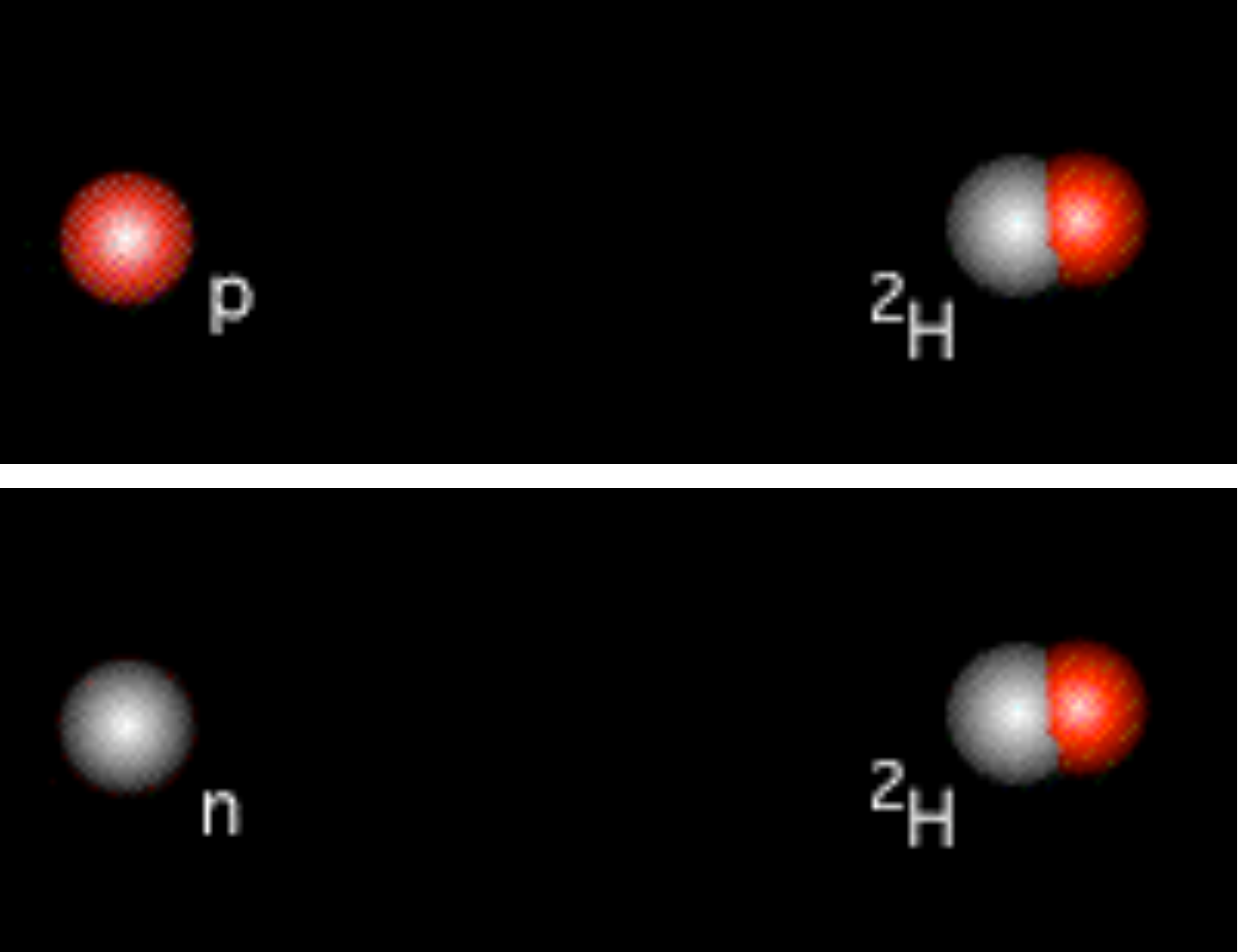
p
2H
n
2H

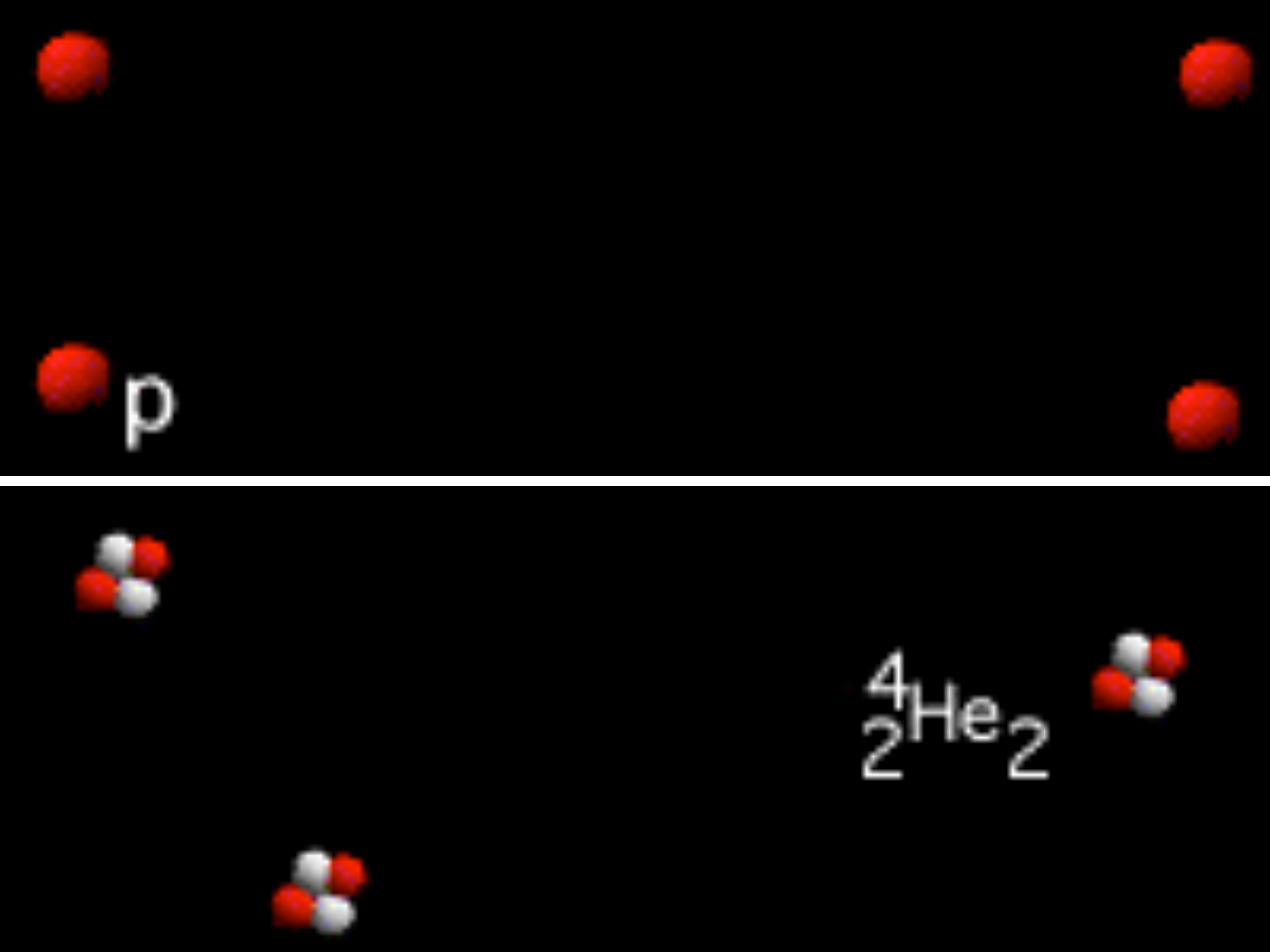
p
$^{4}_{2}He_2$

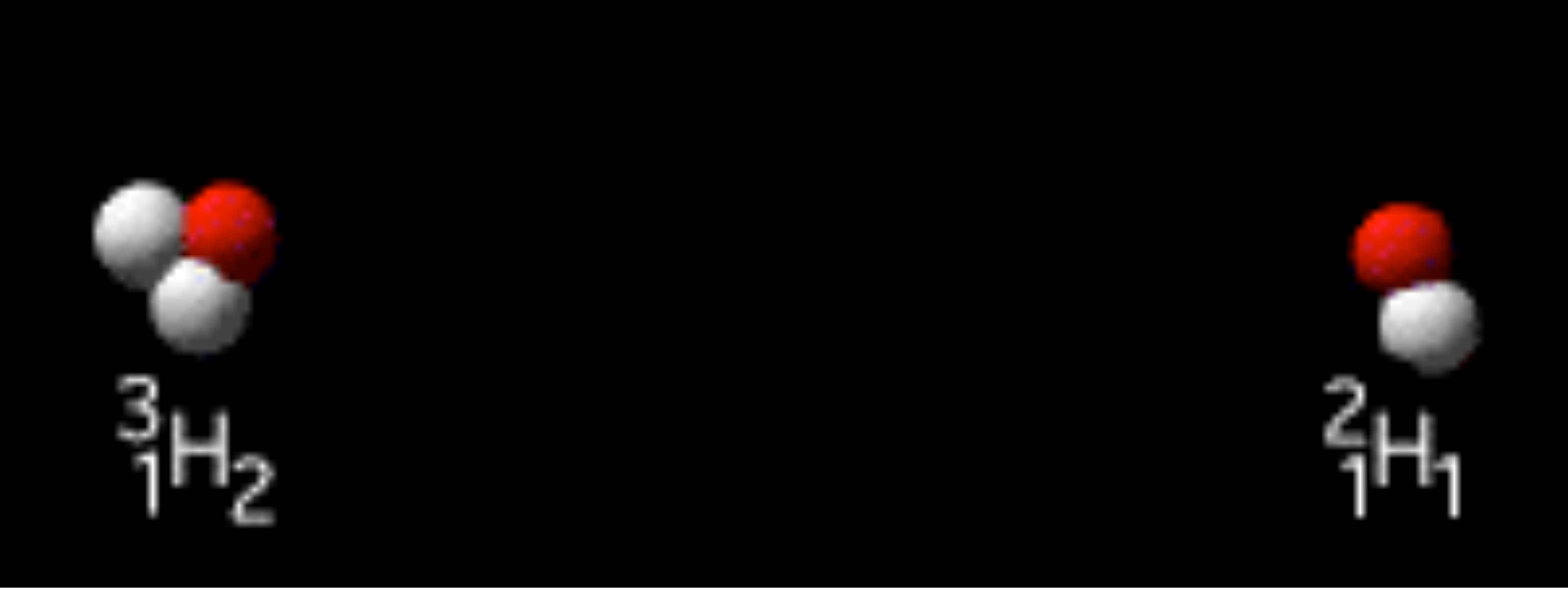
$^{3}_{1}H_2$
$^{2}_{1}H_1$

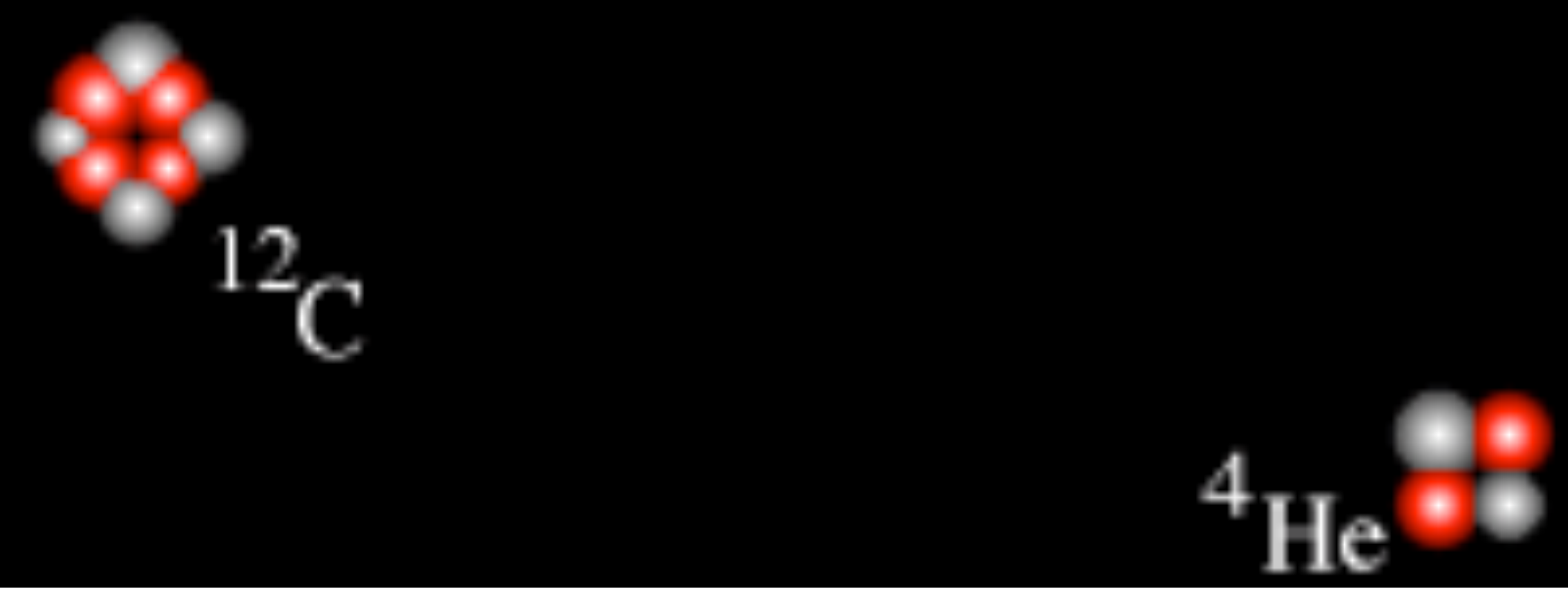

12C
4He

p
12C

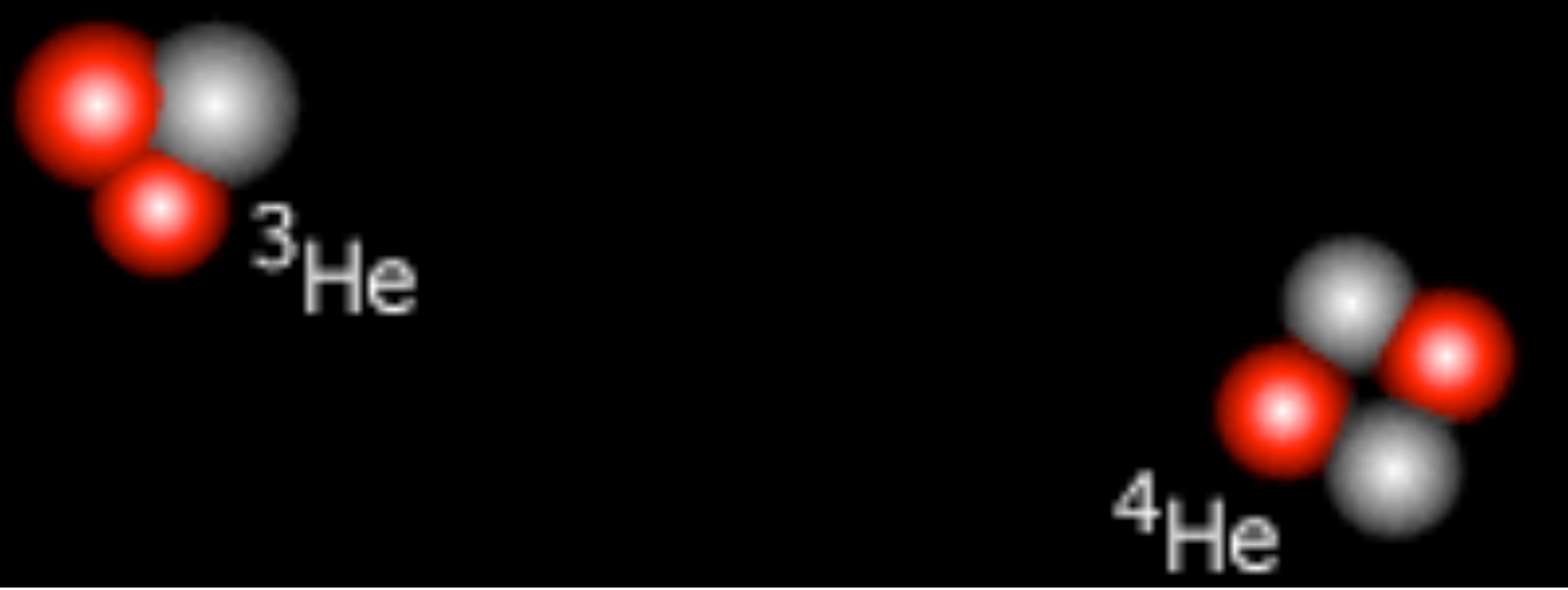
3He
4He


p
12C

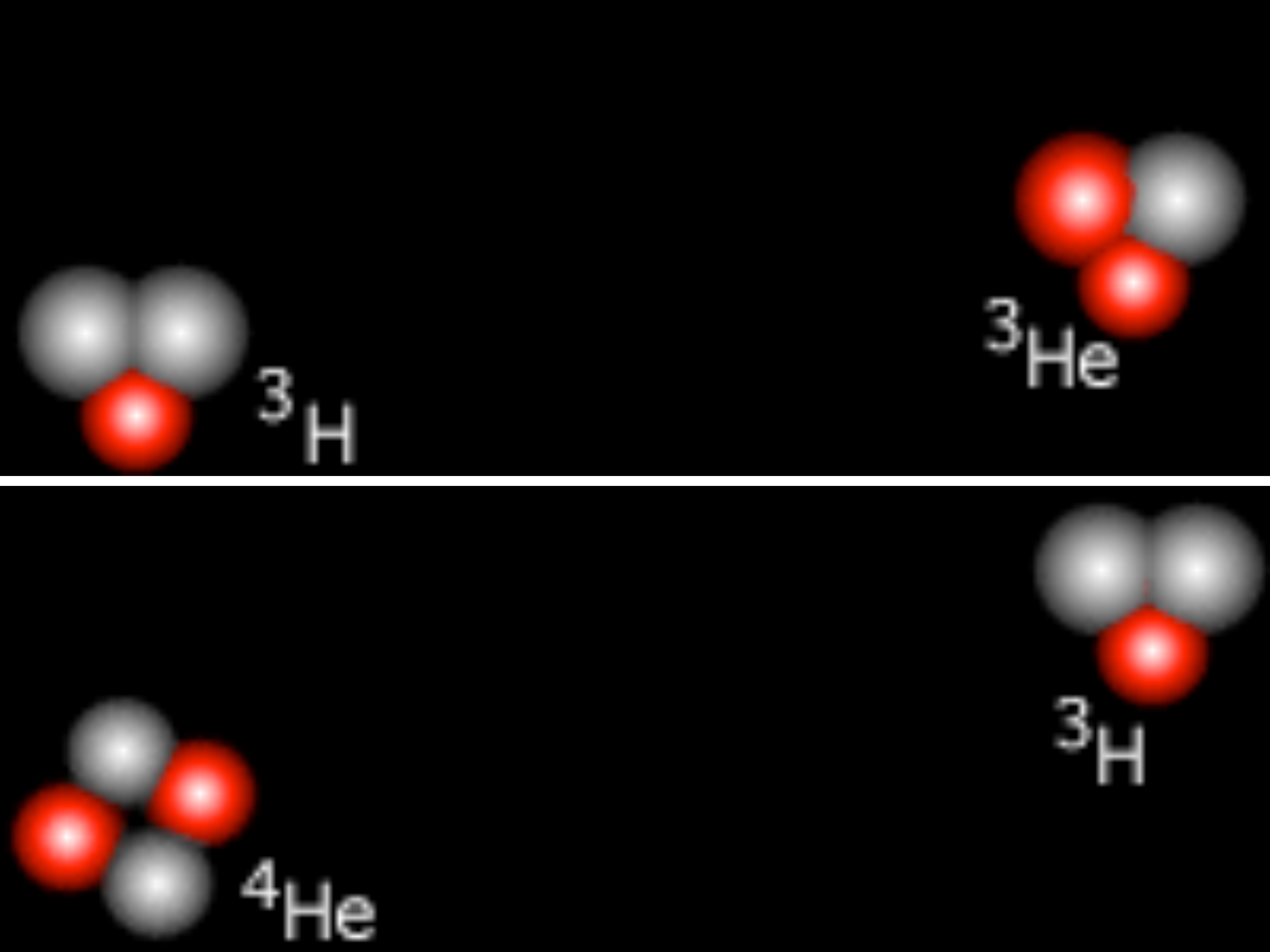

^{3}H
^{3}He
^{4}He
^{3}H

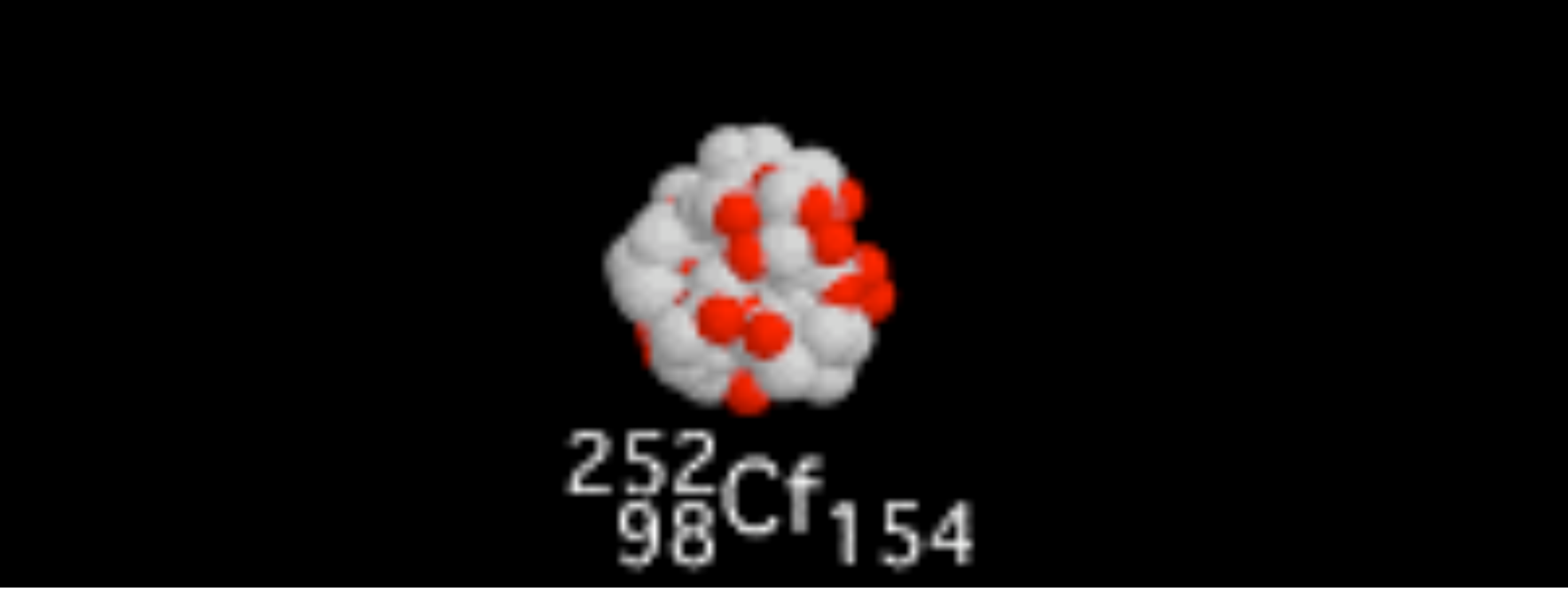
$^{252}_{98}\mathrm{Cf}_{154}$

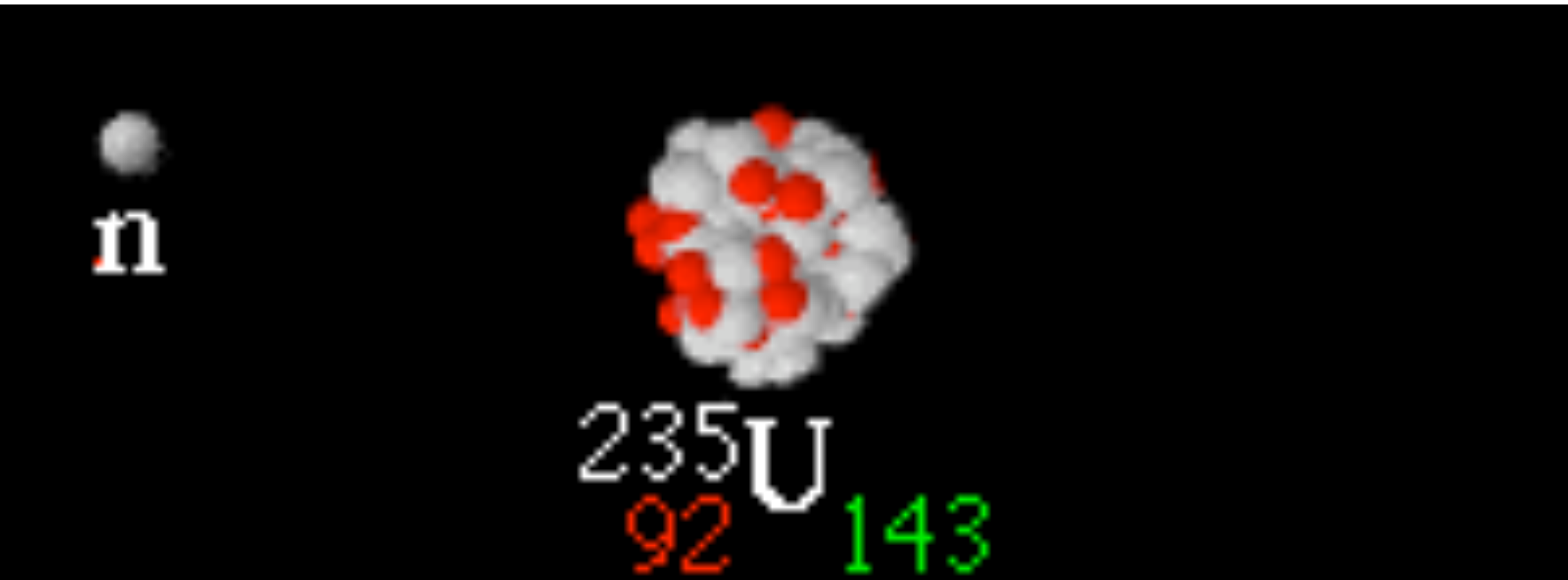
n
$^{235}_{92}\mathrm{U}_{143}$


70Zn 30 40
208Pb 82 126

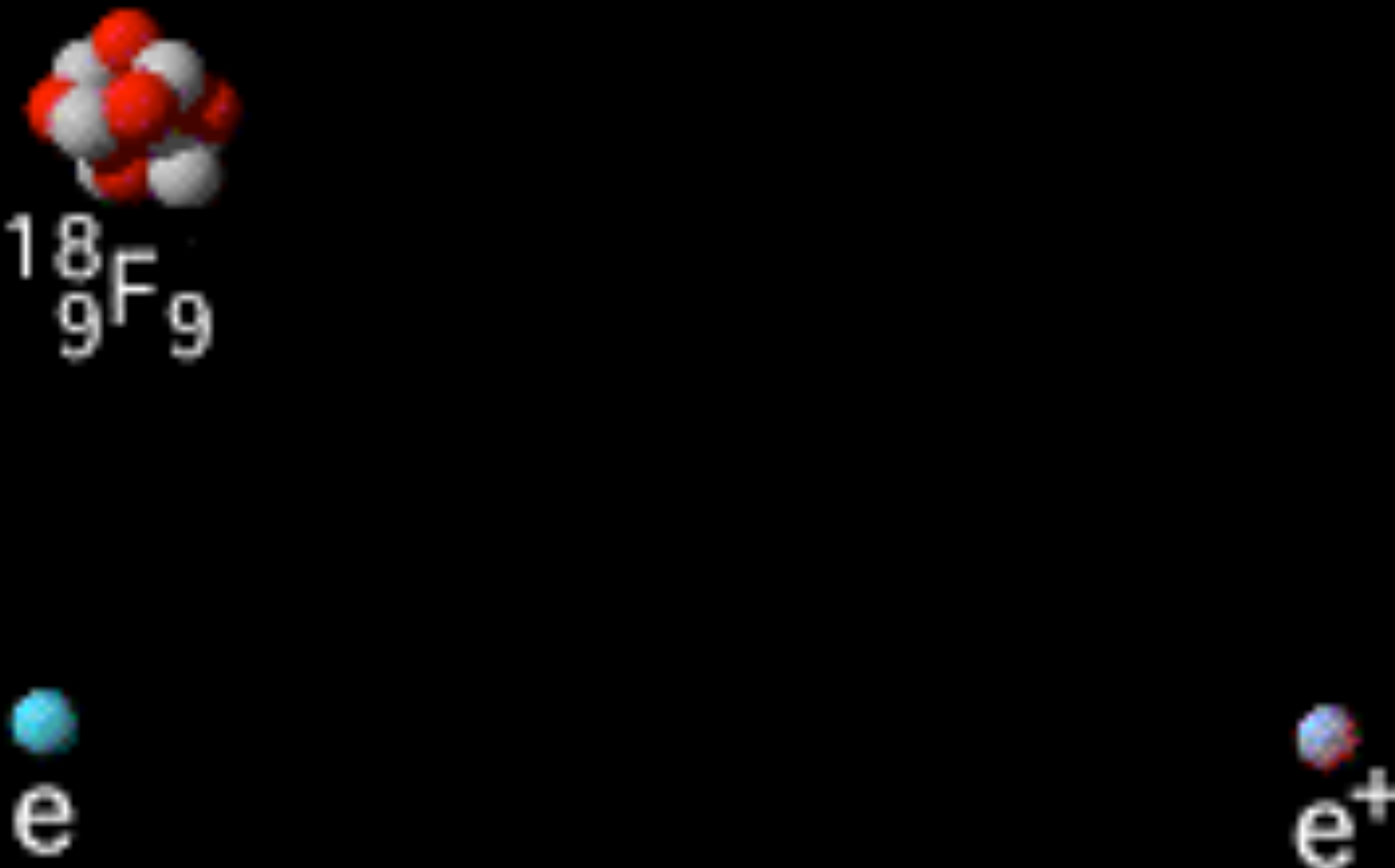

$^{18}_{9}F_{9}$
e
e^{+}

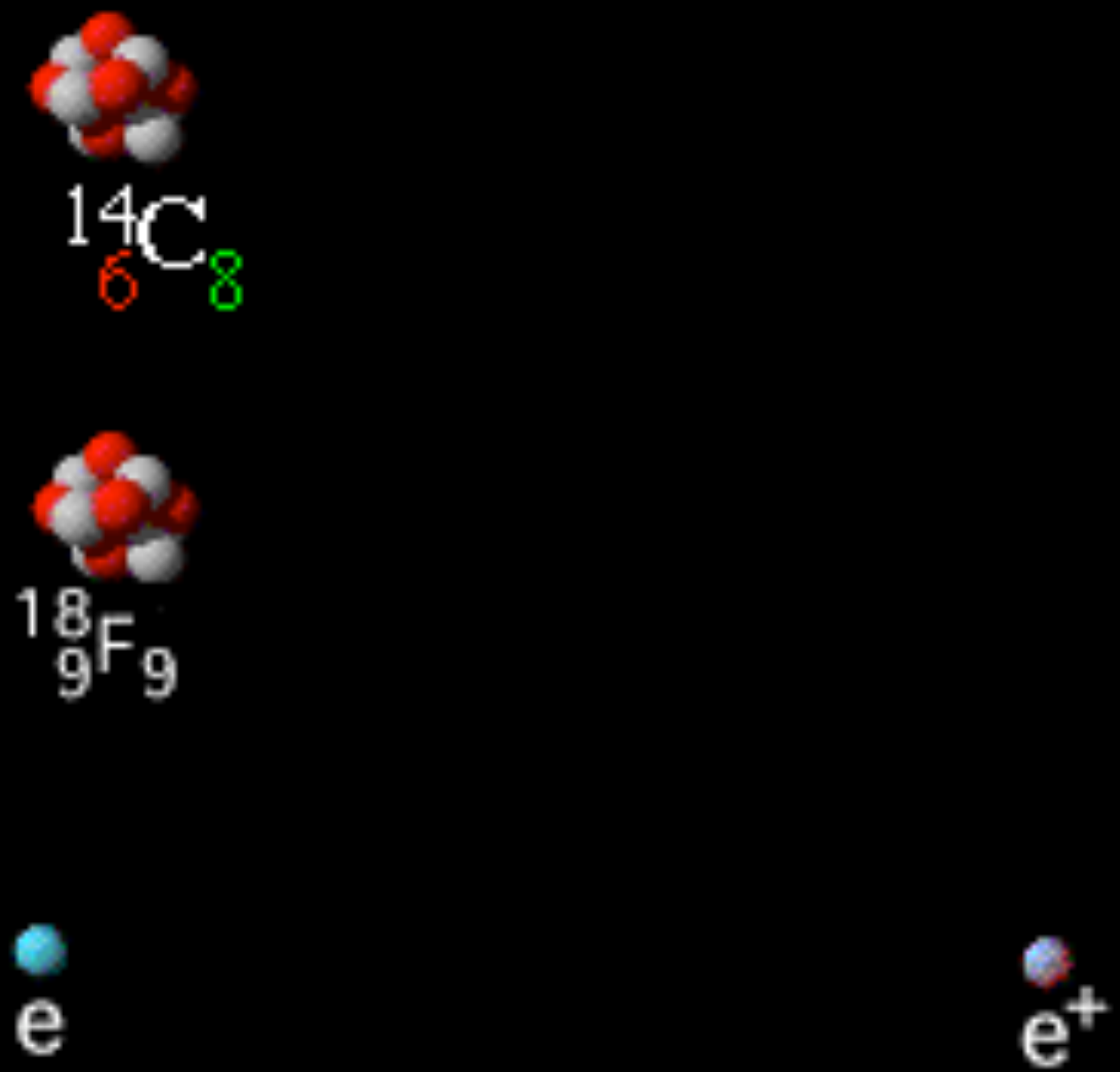

$^{14}_{6}C_{8}$
$^{18}_{9}F_{9}$
e
e^{+}

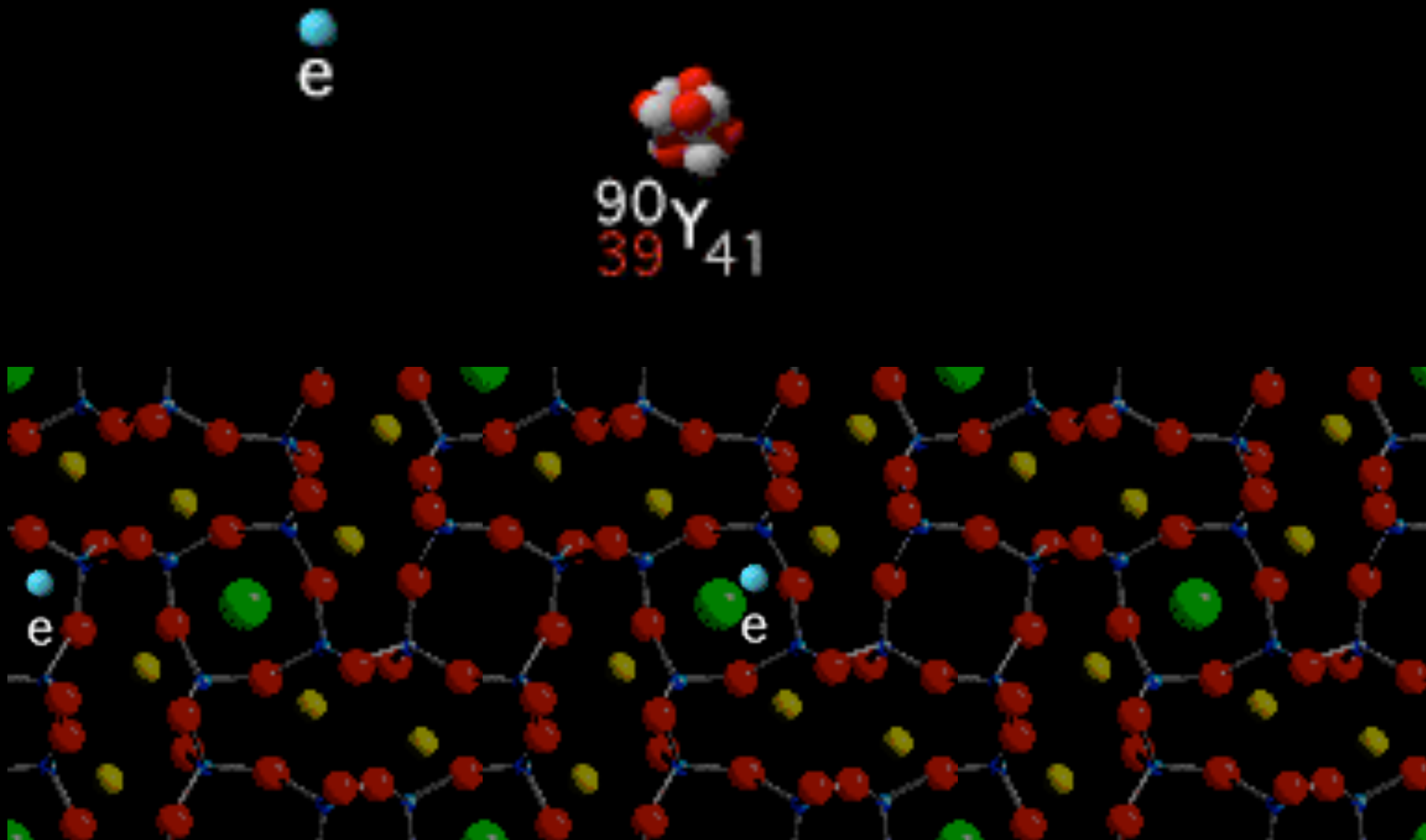
e
90
Y
39
41
e
e

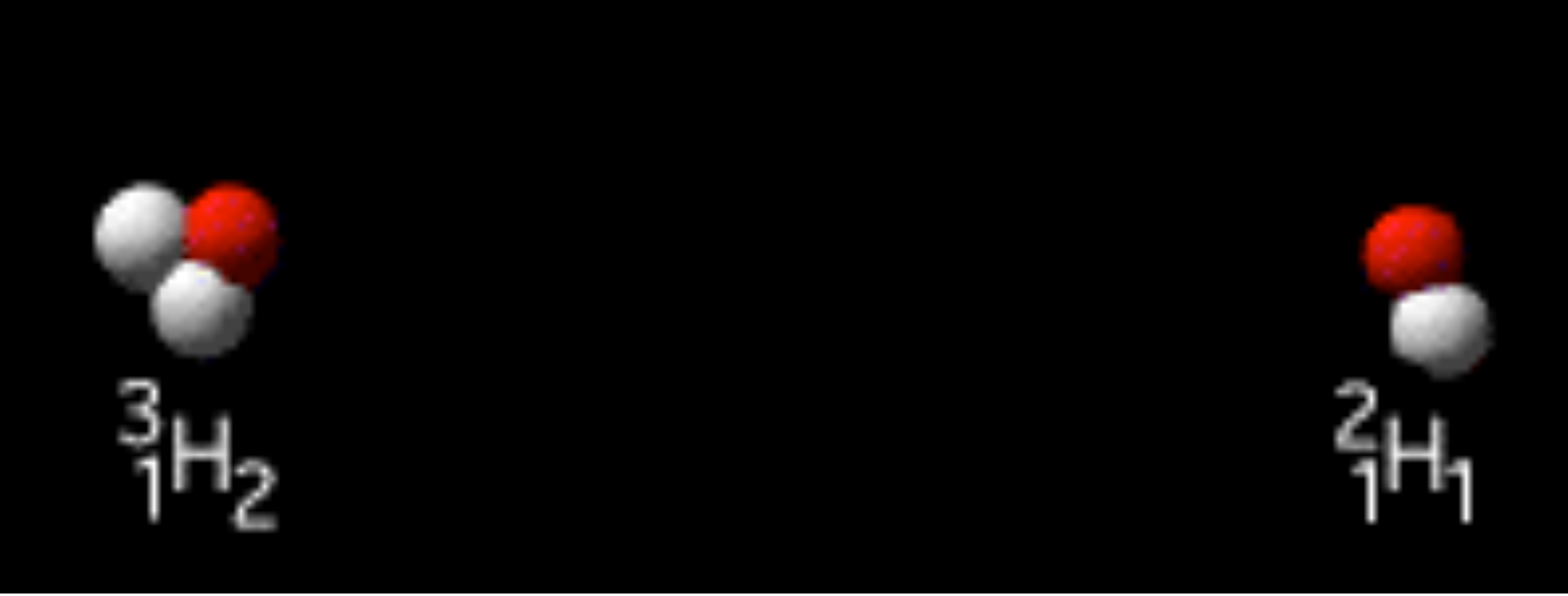
$^{3}_{1}H_{2}$
$^{2}_{1}H_{1}$

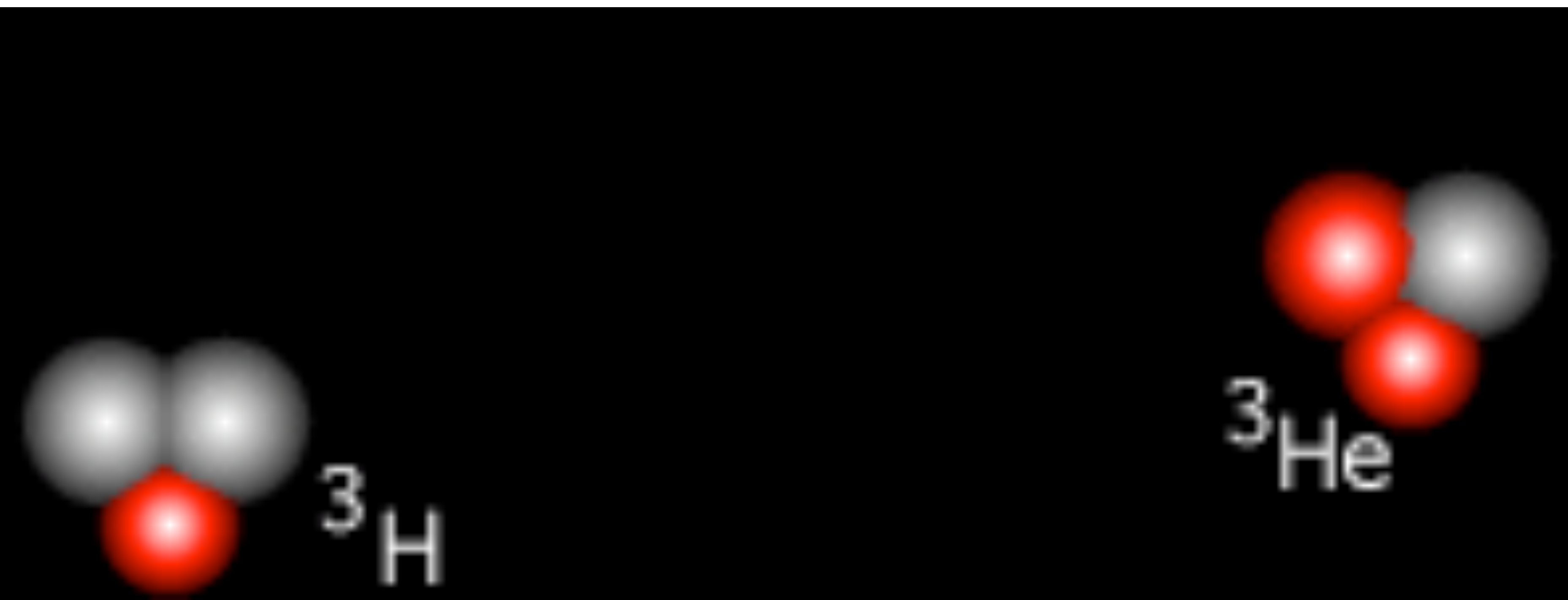
^{3}H
^{3}He

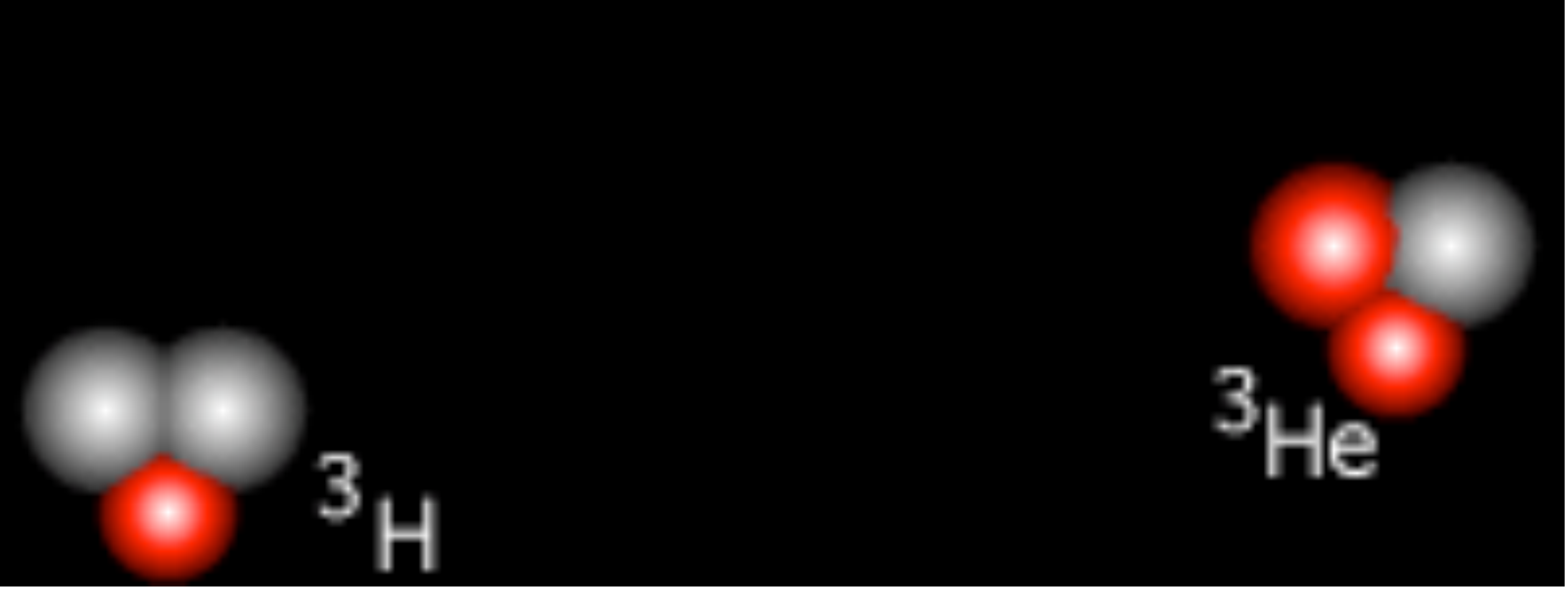
3He
3H

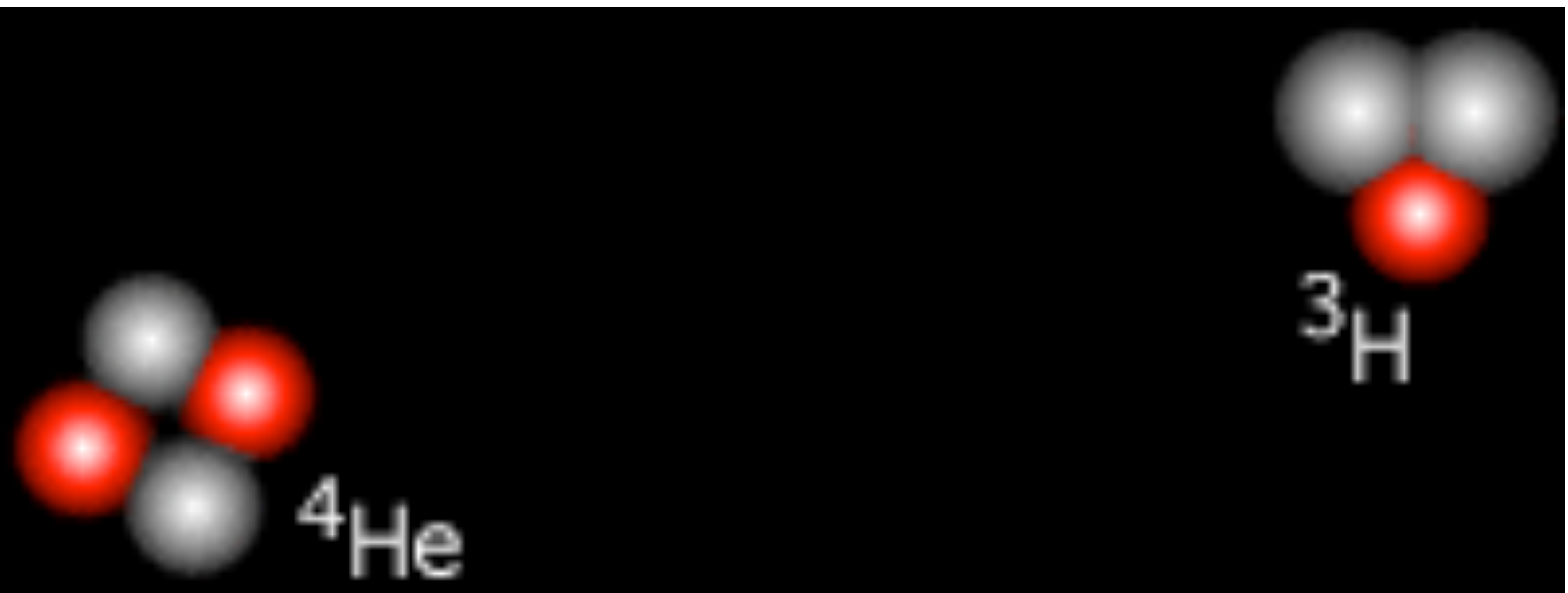
3H
4He